ISTANBUL TECHNICAL UNIVERSITY ★ GRADUATE SCHOOL

MECHANICALLY STRONG HYALURONIC ACID-BASED HYDROGELS

Ph.D. THESIS

Burak TAVŞANLI

Department of Chemistry

Chemistry Programme

APRIL 2021

ISTANBUL TECHNICAL UNIVERSITY ★ GRADUATE SCHOOL

MECHANICALLY STRONG HYALURONIC ACID-BASED HYDROGELS

Ph.D. THESIS

Burak TAVŞANLI
(509142016)

Department of Chemistry

Chemistry Programme

Thesis Advisor: Prof. Dr. Oğuz OKAY

APRIL 2021

İSTANBUL TEKNİK ÜNİVERSİTESİ ★ LİSANSÜSTÜ EĞİTİM ENSTİTÜSÜ

YÜKSEK MEKANİK DAYANIMLI HYALÜRONİK ASİT HİDROJELLERİ

DOKTORA TEZİ

Burak TAVŞANLI
(509142016)

Kimya Anabilim Dalı

Kimya Programı

Tez Danışmanı: Prof. Dr. Oğuz OKAY

NİSAN 2021

Burak TAVŞANLI, a Ph.D. student of ITU Graduate School student ID 509142016, successfully defended the thesis entitled "MECHANICALLY STRONG HYALURONIC ACID-BASED HYDROGELS", which he prepared after fulfilling the requirements specified in the associated legislations, before the jury whose signatures are below.

Thesis Advisor :	**Prof. Dr. Oğuz OKAY** İstanbul Technical University	.....
Jury Members :	**Prof. Dr. Nermin ORAKDÖĞEN** Istanbul Technical University	.....
	Prof. Dr. Mine YURTSEVER Istanbul Technical University	.....
	Assoc. Prof. Dr. Deniz C. TUNCABOYLU Bezmialem Vakif University	.....
	Assoc. Prof. Dr. Murat ÖZMEN Yıldız Technical University	.....

Date of Submission : 15 February 2021
Date of Defense : 04 April 2021

To my family for their support,

and my beloved wife Bensu...

FOREWORD

There are no words to express my gratitude to my advisor Prof. Dr. Oğuz OKAY adequately. He has been the most influential person in my development as a scientist. His support always makes me feel safe while coping with difficulties in my personal life.

I would like to express my thanks to steering committee members Prof. Dr. Nermin ORAKDÖĞEN and Assoc. Prof. Dr. D.Ceylan TUNCABOYLU for their helpful advice and suggestions.

The very first person I came into contact with when I started working in the lab was Dr. Volkan CAN, who quickly became a solid labmate and a friend. Thanks for the kick-start and wonderful days we had in the lab.

Great thanks to Dr. H. Mehmet KAYILI, Dr. Mehmet ATAKAY for being such supportive and honest friends.

Thanks to Prof. Okay's lab members, Dr. Aslıhan Arğun, Dr. Ümit Gülyüz, Berkant Yetişkin, Çağla Erkoç, Ç. Buse Oral, Esra Su, Özge Akça, Sümeyye Özer for a cherished time spent together in the lab. I would like extend my thanks to my collegues from department Dr. Gözde Aktaş Eken, Dr. P. Sinem Omurtag Özgen, Res. Asst. Serter Lüleburgaz, Res. Asst. Ceyda Şimşek. I would also like to thank the security guards of our new laboratory building for keeping doors open at endless experiment nights.

I am extremely grateful to my parents for their love, caring, and sacrifices for my future. Finally, my deepest appreciation belongs to my wife Bensu, for her love, understanding, and unlimited support.

I would also like to thank Istanbul Technical University Research Fund (BAP) (Project No. 39957) and Scientific and Technical Research Council of Turkey (TUBITAK) (Project No. 114Z312 and 218M502) for financial and material support.

February 2020

Burak TAVŞANLI
M.Sc. Chemist

TABLE OF CONTENTS

Page

ABBREVIATIONS

μ-CT : Micro computed tomography
^{1}H NMR : Hydrogen Nuclear Magnetic Resonance Spectroscopy
3D : Three-dimensional
APS : Ammonium persulfate
ATR-FTIR : Attenuated total reflectance-Fourier transform infrared
BAAm : Methylene(bis)acrylamide
BDDE : Butanediol diglycidyl ether
DM : Methacrylation degree
DMA : N,N-dimethylacrylamide
DN : Double-network
DSC : Differantial Scanning Calorimetry
DVS : Divinyl sulfone
EDC : 1-ethyl-3-(3-dimethylaminopropyl) carbodiimide
EGDE : Ethylene glycol diglycidyl ether
GM : Glycidyl methacrylate
GMHA : Methacrylated hyaluronic acid
GTA : Glutaraldehyde
HA : Hyaluronic acid
IPN : Interpenetrating polymer network
MAAc : Methacrylic acid
MCT : Mercury – cadmium − telluride
PAAm : Polyacrylamide
NHS : N-hydroxysuccinimide
PAMPS : Poly(2-acrylamido-2-methylpropane sulfonic acid)
PDMA : Poly(N,N-dimethylacrylamide)
PEG : Poly(ethylene glycol)
PEGDE : Poly(ethylene glycol) diglycidyl ether
PLA : Poly(lactic acid)
PNIPA : Poly(N-isopropylacrylamide)
PVA : Poly(vinyl alcohol)

SD : Standart deviation

SEM : Scanning electron microscope

SF : Silk fibroin

SN : Single-network

TBAB : Tetrabutylammonium bromide

TEA : Triethylamine

TEMED : N,N,N',N'-tetramethylethylenediamine

TN : Triple-network

UV : Ultraviolet

VP : 1-vinyl pyrrolidone

XRD : X-ray Diffraction

SYMBOLS

ΔH_m	: Enthalpy change of melting
C_1	: Monomer concentration in the preparation of the first-network hydrogel
C_2	: Monomer concentration in the preparation of the double-network hydrogel
C_3	: Monomer concentration in the preparation of the triple-network hydrogel
C_{HA}	: HA concentration
C_{NaOH}	: NaOH concentration
C_{nom}	: Nominal concentration
C_{true}	: True concentration
E	: Young's Modulus
E_{norm}	: Normalized Young's Modulus
f_{unf}	: Unfrozen mass fraction of water
f_v	: Fraction of broken bonds
G'	: Elastic modulus
G''	: Viscous modulus
G'_∞	: Limiting modulus
m	: Weight of gels after equilibrium swelling in water
m_{dry}	: Weight of gels in dry state
m_o	: Weight of gels after preparation
m_{rel}	: Equilibrium relative weight swelling ratio
P	: Porosity
q_v	: Equilibrium volume swelling ratio
q_w	: Equilibrium weight swelling ratio in dry state
$q_{w,o}$	: Equilibrium weight swelling ratio in as-prepared state
$\tan \delta$	: Loss factor
U_{hys}	: Hysteresis energy
w_{21}	: Mass ratio of the second to the first network
$w_{32/1}$	: Mass ratio of the second and third to the first network

W_g : Gel fraction

γ_o : Deformation amplitude

$\dot{\gamma}$: Shear rate

ε : Strain

ε_f : Strain at break

η : Viscosity

θ : Half-gelation time

λ : Deformation ratio

λ_{biax} : Biaxial extension ratio

λ_{max} *or* ε_{max} : Maximum strain

v_2 : Volume fraction of gel in equilibrium with water

v_e : Cross-link density

$v_{e,dry}$: Cross-link density of dry polymer

v_2^o : Volume fraction of gel at the preparation

σ_f : Fracture stress

$\sigma_{f,norm}$: Normalized fracture stress

σ_{nom} : Nominal stress

σ_{true} : True stress

ω : Angular frequency

LIST OF TABLES

Page

LIST OF FIGURES

Page

MECHANICALLY STRONG HYALURONIC ACID-BASED HYDROGELS

SUMMARY

Hyaluronan, or hyaluronic acid (HA), is a naturally occurring carbohydrate polymer consists of disaccharide repeating units of β-1,4-D-glucuronic acid - β-1,3-N-acetyl-D-glucosamine. HA is the main component of the extracellular matrix (ECM), and it plays an essential role in the wound-healing processes. HA has become an important building block for creating new biomaterials with utility in tissue engineering and regenerative medicine. Although HA is an attractive biomaterial for soft tissue regeneration due to its distinctive biological functions and lubricating properties, it has limited application areas because of its rapid degradation and poor biomechanical properties. To overcome this drawback, native HA was physically or chemically cross-linked, or alternatively, methacrylate groups were incorporated into HA to generate HA macromers, which are then polymerized to form hydrogels. The resulting hydrogels exhibit poor mechanical properties for use in stress-bearing applications, although the cross-linking of HA decreases its degradation rate and solubility in aqueous media. The lack of mechanical strength in HA hydrogels is primarily due to the lack of viscoelastic dissipation in the chemically cross-linked HA network, resulting in low-stress fracture of the hydrogels. Several techniques including double-network gels (DN), incorporation of additional macromolecules such as silk fibroin (SF), and cryogelation have been developed to enhance the mechanical properties of HA hydrogels.

Double-network (DN) technique allows for the development of high-strength hydrogels via two-step sequential free radical polymerization. DN hydrogels are prepared by swelling a brittle and highly cross-linked first network hydrogel in a second monomer solution. After reaching equilibrium, the second monomer is polymerized to form a ductile and loosely cross-linked second network. In general, the mass ratio of second-network to the first-network is very high, and two networks are strongly entangled with each other. Poly(N,N-dimethylacrylamide) (PDMA) is a biocompatible polymer with associative properties and widely used to produce hydrogels. PDMA hydrogels can easily be prepared by free-radical copolymerization of N,N-dimethylacrylamide (DMA) in bulk or in aqueous solution in the presence of a cross-linker. Recently, a novel triple-network (TN) approach has been developed for preparing mechanically robust nonionic polyacrylamide (PAAm)/PDMA/PDMA hydrogels in our research group. A great variety of hydrogels exhibiting different mechanical properties have been fabricated by tuning the mass ratio of the consecutive networks. The TN approach relies on a second monomer translational entropy loss upon polymerization with the first network.

Silk fibroin (SF) derived from Bombyx mori cocoons is a biopolymer that offers several features comprising biocompatibility, controlled biodegradability, and unique mechanical properties. The primary structure of SF includes repetitive blocks of high molecular weight hydrophobic and low molecular weight hydrophilic chains.

Structural arrangements in the hydrophobic blocks form β-sheet structure, which is responsible for its high strength, whereas hydrophilic blocks provide water solubility and toughness. Hydrogels derived from SF are attractive soft materials in biomedical applications; however, they exhibit poor mechanical properties limiting their load-bearing applications.

In order to fabricate macroporous hydrogels of high toughness and fast responsiveness, there is a facile and versatile technique called cryogelation. During this process, the solvent, mainly water, is used as a porogen in order to form a highly interconnected porous structure. Thus, the cross-linking reactions take place below the freezing point of the reaction medium. As water freezes, frozen solvent crystals and unfrozen liquid system containing concentrated monomer or polymer solution form. After cryogelation, a polymer network with a porous structure is obtained.

The aim of this thesis is to produce HA hydrogels exhibiting extraordinary mechanical performances. Firstly, sequential polymerization reactions were conducted to produce HA/PDMA double- and HA/PDMA/PDMA triple-network hydrogels starting from native and methacrylated HA (GMHA). Next, one-pot synthesis of HA hydrogels was introduced to shorten the reaction time and to reduce the amount of reagents used. For this purpose, DMA or methacrylic acid (MAAc), and DMA and SF were incorporated separately into a reaction solution containing GMHA and then polymerized to produce HA hydrogels. Lastly, to produce robust macroporous HA hydrogels, the cryogelation technique was conducted at sub-zero temperatures starting from GMHA in the presence of DMA monomer.

The thesis presented here resulted in five publications, mainly based on fabricating mechanically strong HA hydrogels. Within each following section, the mechanical properties of HA hydrogels and cryogels were investigated in detail and their internal structures were clarified by various techniques.

In the first part of the thesis, HA hydrogels were prepared by utilizing a two-step process. Primarily, HA was chemically cross-linked in aqueous solutions using ethylene glycol diglycidyl ether (EDGE) under different experimental conditions. EGDE cross-linked HA hydrogels containing 97-99% water were fragile and ruptured when compressed to 25-51% strain under 0.02-0.15 MPa stresses. By applying the double-network (DN) approach in the second step, high strength DN hydrogels containing 84-94% water were generated. Shortly, single-network brittle HA hydrogels were first swollen in aqueous N,N-dimethylacrylamide (DMA) solutions containing a small amount of BAAm cross-linker, and then photopolymerized to form a loosely cross-linked poly(N,N-dimethylacrylamide) (PDMA) second network. Adjusting the first and second network components ratio resulted in hydrogels exhibiting a compressive modulus of 0.9 MPa that sustain 19.4 MPa compressive stresses. Cyclic mechanical tests show irreversible stress-strain curves with a large hysteresis, indicating that the elastically effective cross-links of HA first-network are irreversibly destroyed under load by dissipating energy.

In the second part of the thesis, triple-network (TN) hydrogels based on GMHA and DMA were prepared by sequential free radical photopolymerizations. Multifunctional GMHA macromers, used as the first network component, were prepared with various metacrylation degrees and characterized by H-NMR technique. DN hydrogels were prepared by swelling SN hydrogels in DMA solutions containing a small amount of BAAm cross-linker, following by photopolymerization. This leads to the formation of GMHA/PDMA hydrogels with a compressive modulus and fracture stress of up to 0.4

MPa and 12 MPa, respectively. Due to the reduction of the second monomer's translational entropy after photopolymerization, an additional monomer solution could be introduced to DN hydrogels to obtain GMHA/PDMA/PDMA TN hydrogels that sustain compressive stresses above 20 MPa. Cyclic mechanical tests showed that, although TN hydrogels internally fracture even under small strain, the ductile components hinder macroscopic crack propagation by keeping the macroscopic gel samples together.

In the third part of this study, a simple one-pot synthesis of HA hydrogels via free-radical copolymerization of GMHA and DMA in aqueous solutions were introduced. It was found that GMHA acts as a multifunctional cross-linker during its copolymerization with DMA leading to the formation of interpenetrated and interconnected polymer networks. The effective functionality of GMHA increases with its degree of methacrylation as well as with the DMA concentration. The viscoelastic and mechanical properties of HA hydrogels could be tuned by varying the degree of methacrylation of GMHA and DMA concentration. A significant improvement in the mechanical performance of the hydrogels was observed when DMA is replaced with methacrylic acid monomer. By adjusting the synthesis parameters, hydrogels with a Young's modulus of around 200 kPa could be prepared that sustain up to 20 MPa stresses at 96% compression.

In the fourth part, mechanically robust and stretchable SF/HA hydrogels were prepared from GMHA and SF in aqueous solutions in the presence of a radical initiator. DMA monomer was also included in the reaction solution as a spacer to connect GMHA's through their pendant vinyl groups. After incorporating SF into the gel network, Young's modulus and fracture stress of the as-prepared hydrogels increased markedly from 5 to 54 kPa and from 0.6 to 4.9 MPa, respectively. Additionally, and most importantly they sustain up to 400% stretch ratio under a stress of 80 kPa. The presence of SF significantly enhances the mechanical strength of HA hydrogels due to its β-sheet domains, which was confirmed by XRD measurements, acting as physical cross-links. The damage in the SF network under large strain leads to a significant energy dissipation, which is responsible for the improved mechanical properties of SF/HA hydrogels.

In the last part of this study, the preparation of HA cryogels via free-radical copolymerization of methacrylated HA and DMA in aqueous solutions was presented. By adjusting both the methacrylation degree of HA and DMA concentration, we were able to produce cryogels exhibiting Young's modulus up to around 350 kPa and compressive fracture stress of above 3 MPa. HA cryogels have an interconnected pore structure with pores of >90 μm in diameter and exhibit a high porosity (>97%), as observed by scanning electron microscopy (SEM) and micro-computed tomography analysis (μ-CT). HA cryogels are squeezable, and no crack propagation occurred when compressed up to 99% strain. They also exhibit a very fast swelling-deswelling behavior in good and poor solvents, respectively. Increasing the degree of methacrylation of HA or DMA concentration reduces the swelling ratio, porosity and pore size of the cryogels. Moreover, the fracture stress of dried cryogels increases with increasing DMA concentration, whereas in their swollen states, an opposite behavior was observed. This unusual behavior could be explained with the water content of the cryogels under large strain conditions.

YÜKSEK MEKANİK DAYANIMLI HYALÜRONİK ASİT HİDROJELLERİ

ÖZET

Hyalüronan veya hyalüronik asit (HA), β-1,4-D-glukuronik asit- β-1,3-N-asetil-D-glukozamin disakkarit tekrarlayan birimlerinden oluşan doğal bir karbonhidrat polimeridir. HA, hücre dışı matrisin (ECM) ana bileşenidir ve yara iyileşme sürecinde önemli bir rol oynamaktadır. HA, doku mühendisliği ve rejeneratif tıpta kullanılmak üzere yeni biyomalzemeler oluşturmak için önemli bir yapı taşı haline gelmiştir. Ayırt edici biyolojik fonksiyonları ve kayganlaştırıcı özellikleri sayesinde yumuşak doku rejenerasyonu için çekici bir biyomateryal olmasına rağmen, hızlı bozunması ve zayıf biyomekanik özellikleri nedeniyle sınırlı uygulama alanına sahiptir. Bu dezavantajların üstesinden gelmek amacıyla HA fiziksel veya kimyasal olarak çapraz bağlanabilmekte veya çok fonksiyonlu makromerler oluşturmak amacıyla metakrilat grupları ile modifiye edilerek hidrojel oluşumu için çapraz bağlanmaktadır. Bu yöntemler HA'nın sulu ortamda bozunma hızını ve çözünürlüğünü azaltsa bile, yük dayanımı gerektiren uygulamalarda kullanımı için zayıf mekanik özellikler sergilemektedir. Mekaniksel mukavemet eksikliği, temel olarak kimyasal olarak çapraz bağlı HA ağındaki enerji dağılım mekanizması olmamasından kaynaklanmakta ve sonuç olarak hidrojellerin düşük yük altında parçalanmalarına neden olmaktadır. Hidrojellerin mekanik özelliklerini geliştirmek için çift-ağyapılı jeller (DN), ipek fibroin (SF) gibi ek makromoleküllerin dahil edilmesi ve kriyojelasyon gibi çeşitli teknikler geliştirilmiştir.

Çift-ağyapılı jel sentez tekniği, iki aşamalı sıralı serbest radikal polimerizasyonu yoluyla yüksek mukavemetli hidrojellerin geliştirilmesine olanak sağlamaktadır. İlk olarak, yüksek oranda çapraz bağlanmış birinci ağ yapı ikinci bir monomer çözeltisi içinde şişirilmektedir. Dengeye ulaştıktan sonra, ikinci monomer, gevşek bir şekilde çapraz bağlı ikinci bir ağ oluşturmak için polimerleştirilmektedir. Genel olarak, ikinci ağın birinci ağa kütle oranı çok yüksek olmakta ve iki ağ birbirleriyle güçlü bir etkileşim halinde bulunmaktadır. N, N-dimetilakrilamid'in (DMA) serbest radikal kopolimerizasyonu ile elde edilen Poli(N, N-dimetilakrilamid) (PDMA), asosiyatif özelliklere sahip biyo-uyumlu bir polimerdir ve hidrojel sentezlerinde yaygın olarak kullanılmaktadır. Araştırma grubumuz tarafından yakın zamanda mekanik olarak kuvvetli iyonik olmayan poliakrilamid (PAAm)/PDMA/PDMA hidrojelleri hazırlanarak yeni bir üç-ağyapılı (TN) sentez yaklaşımı geliştirilmiştir. Ardışık ağların kütle oranlarının ayarlanmasıyla yüksek mekanik özellikler sergileyen çok çeşitli hidrojeller oluşturulmuştur. TN yaklaşımıyla, DN monomerinin polimere dönüşümü ile jel içindeki entropi azalması sonucu jel dışındaki çözeltiden DN hidrojeline daha fazla monomer çözeltisinin girmesi sağlanmıştır..

Bombyx mori ipek böceğinin kozalarından üretilen ipek fibroin (SF), biyouyumluluk, kontrollü biyolojik bozunabilirlik ve eşsiz mekanik özellikler sunan bir biyopolimerdir. SF'nin birincil yapısı, yüksek molekül ağırlıklı hidrofobik ve düşük molekül ağırlıklı hidrofilik zincirlerin tekrarlayan bloklarını içermektedir. Hidrofobik

bloklardaki yapısal düzenlemeler, yüksek mukavemet sağlayan β-tabaka yapısını oluştururken, hidrofilik bloklar ise suda çözünürlük ve tokluk sağlamaktadır. İpek fibroin ile üretilen hidrojeller, biyomedikal uygulamalarda ilgi çekici malzemeler olmasına rağmen yük dayınımı gerektiren uygulamalarda zayıf mekanik özellik göstermektedirler.

Yüksek tokluk ve hızlı yanıt verme özelliğine sahip makrogözenekli hidrojelleri elde etmek amacıyla kriyojelasyon adı verilen basit ve çok yönlü bir teknik kullanılmaktadır. Bu işlem sırasında, yüksek oranda birbirine bağlı gözenekli bir yapı oluşturmak amacıyla porojen olarak özellikle su ve diğer çözücüler kullanılmaktadır. Polimerizasyon ve çapraz bağlanma reaksiyonları, reaksiyon ortamının donma noktasının altında gerçekleşmektedir. Su donarken, donmuş çözücü kristalleri ve donmamış mikrobölgeler içeren bir sistem oluşmakta, kriyojelasyondan sonra gözenekli bir yapıya sahip polimer ağı elde edilmektedir.

Bu tez çalışmasında, olağanüstü mekanik performans gösteren HA hidrojelleri üretmek amaçlanmıştır. İlk olarak, sırasıyla doğal ve metakrile edilmiş HA (GMHA) kullanılarak; HA/PDMA çift- ve HA/PDMA/PDMA üçlü-ağyapılı hidrojeller ardışık polimerizasyon reaksiyonları kullanılarak elde edilmiştir. İkinci aşamada, reaksiyon süresi ve kullanılan reaktif miktarını azaltmak amacıyla HA hidrojelleri tek basamakta (one-pot) sentezlenmiştir. DMA veya metakrilik asit (MAAc), ve DMA ve SF olmak üzere iki ayrı reaksiyon sistemi GMHA ile aynı anda polimerize edilmiştir. Son olarak, makrogözenekli malzemeler üretmek amacıyla DMA varlığında GMHA'dan başlayarak kriyojelleşme reaksiyonları gerçekleştirilmiştir.

Burada sunulan tez, mekaniksel dayanıma sahip HA hidrojellerinin farklı yöntemlerle üretilmesine dayanan ve tez çalışmaları sırasında yayınlanan beş makaleden oluşmaktadır. Her bir bölümde hidrojellerin mekanik özellikleri incelenerek iç yapıları çeşitli tekniklerle aydınlatılmıştır.

Tezin ilk bölümünde HA hidrojelleri iki aşamalı ardışık polimerizayon tekniği uygulanarak hazırlanmıştır. Öncelikle HA, farklı deneysel koşullar altında etilen glikol diglisidil eter (EDGE) kullanılarak sulu çözeltilerde kimyasal olarak çapraz bağlanmıştır. % 97-99 su içeren EGDE çapraz bağlı HA hidrojelleri oldukça kırılgan olup 0.02-0.15 MPa gerilim değerlerinde ve %25-51 gerinim aralığında parçalanmaktadır. İkinci adımda DN yaklaşımı uygulanarak, %84-94 su içeren yüksek dayanımlı DN hidrojeller üretilmiştir. Kısaca, kırılgan ve tek ağyapılı HA hidrojelleri az miktarda BAAm çapraz bağlayıcı içeren sulu DMA çözeltilerinde şişirilmiş ve fotopolimerize edilmiştir. Bu şekilde düşük çapraz bağlı bir PDMA ikinci ağyapı oluşturulmuştur. Birinci ve ikinci ağyapıların bileşen oranının ayarlanması ile 0.9 MPa modüle sahip ve 19.4 MPa sıkıştırma gerilimine dayanabilen hidrojeller sentezlenmiştir. Çevrimsel mekanik testler sonucunda jellerin yüksek tersinmez histeresis enerjisine sahip olması birinci ağyapının elastik olarak etkili çapraz bağlantılarının yük altında enerji dağıtarak tersinmez bir şekilde parçalandığını göstermektedir.

Tezin ikinci bölümünde, ardışık serbest radikal fotopolimerizasyonları ile GMHA ve DMA esaslı üç-ağyapılı (TN) hidrojeller elde edilmiştir. Tek-ağyapılı jel sentezinde kullanılan çok fonksiyonlu GMHA makromeri farklı metakrilasyon derecelerinde hazırlanarak ^{1}H-NMR tekniği ile karakterize edilmiştir. Çift-ağyapılı (DN) hidrojeller, SN jellerinin az miktarda BAAm çapraz bağlayıcısı içeren DMA çözeltisinde önce şişirilmeleri ve ardından fotopolimerizasyonu sonucunda elde edilmiştir. Bu şekilde 0.4 MPa modüle sahip 12 MPa parçalanma gerilimine dayanan GMHA/DMA

hidrojelleri elde edilmiştir. İkinci ağyapıdaki monomerin polimere dönüşmesi sonucunda jel içindeki entropi azalmakta ve ek bir monomer çözeltisinin DN hidrojeline girmesine olanak vermektedir. Bu sayede 20 MPa'nın üzerinde parçalanma gerilimine dayanan GMHA/PDMA/PDMA TN hidrojelleri elde edilmiştir. Çevrimsel mekanik testler sonucunda, tok ağyapılı ikincil ve üçüncül bileşenlerin makroskopik parçalanmayı engellediği belirlenmiştir.

Çalışmanın üçüncü bölümünde, HA hidrojelleri sulu çözelti içerisinde GMHA ve DMA'nın serbest radikal kopolimerizasyonu ile tek basamakta sentezlenmiştir. GMHA'nın, DMA ile kopolimerizasyonu sırasında çok işlevli bir çapraz bağlayıcı olarak hareket ettiği ve bunun iç içe geçmiş ve birbirine bağlı polimer ağyapıların oluşumunu sağladığı anlaşılmıştır. GMHA'nın etkin çapraz bağ işlevselliği; gerek onun metakrilasyon derecesi ve gerekse DMA konsantrasyonu ile artmaktadır. GMHA'nın metakrilasyon derecesi ve DMA derişimi değiştirilerek HA hidrojellerinin viskoelastik ve mekanik özellikleri ayarlanabilmektedir. DMA yerine metakrilik asit (MAAc) kullanıldığında ise mekanik özelliklerde önemli bir gelişme gözlenmiştir. Sentez parametreleri ayarlanarak, Young modülü yaklaşık 200 kPa olan ve %96 sıkıştırmada 20 MPa parçalanma gerilimine kadar dayanabilen hidrojeller başarıyla sentezlenmiştir.

Dördüncü bölümde, bir radikal başlatıcı varlığında sulu çözelti içerisinde GMHA ve SF esaslı, mekanik olarak kuvvetli ve çekilebilir SF/HA hidrojelleri hazırlanmıştır. DMA monomeri GMHA'daki vinil grupları üzerinden birbirine bağlanması için bir ayırıcı grup (spacer) olarak reaksiyon çözeltisine ayrıca eklenmiştir. İpek fibroin'in (SF) jel ağına dahil edilmesinden sonra hidrojellerin Young modül ve parçalanma gerilim değerleri, sırasıyla 5'den 54 kPa'ya ve 0.6'dan 4.9 MPa'ya artmıştır. Ek olarak, 80 kPa'lık bir gerilim altında %400 uzama oranına kadar çekilebilen hidrojeller elde edilmiştir. Fiziksel çapraz bağ olarak işlev gören β-tabakaların, HA hidrojellerinin mekanik özelliklerini önemli bir ölçüde iyileştirdiği gözlenmiştir. Ayrıca β-tabakaların varlığı X-ışını kırınımı ölçümleriyle doğrulanmıştır. Yüksek gerinim altında ipek fibroin ağ yapısı içerisinde oluşan hasar önemli bir enerji dağılımı sağlamaktadır ve bu durum HA/SF hidrojellerinin üstün mekanik özelliklerinin nedeni olarak görülmektedir.

Çalışmanın son bölümünde, görünür olarak donmuş GMHA ve DMA sulu çözeltilerinde uygulanan serbest radikal kopolimerizasyonu ile HA kriyojellerinin hazırlanışı sunulmuştur. Metakrilasyon derecesi ve DMA derişimleri ayarlanarak Young modülü 350 kPa'a ulaşan, 3 MPa ve üzerindeki gerilim değerlerine kadar dayanabilen kriyojeller üretilmiştir. HA kriyojellerinin taramalı elektron mikroskobu ve bilgisayarlı mikro tomografi analizleri sonucunda birbirine bağlı %97'in üzerinde gözenekliliğe sahip olduğu ve gözenek açıklıklarının 90 μm den büyük olduğu belirlenmiştir. Kriyojel örnekleri herhangi bir parçalanma olmadan %97'nin üzerinde bir deformasyona kadar sıkıştırılabilmektedir. Aynı zamanda, sırasıyla iyi ve kötü çözücülerde çok hızlı bir şişme-büzülme davranışı sergilemektedirler. Metakrilasyon derecesinin ve DMA derişiminin arttırılmasıyla, kriyojellerin şişme oranı, gözenekliliği ve gözenek boyutunun azaldığı belirlenmiştir. Ayrıca, kuru durumdaki kriyojellerin kırılma gerilimi, artan DMA derişimi ile artarken, şişmiş durumlarında ise tam tersi bir davranış gözlemlenmektedir. Bu olağandışı davranış, büyük gerinim altında kriyojel içindeki serbest halde bulunan suyun plastikleştirici etkisi olarak açıklanmıştır.

1. INTRODUCTION

Hydrogels are insoluble three-dimensional hydrophilic polymer networks that swell in aqueous solutions without dissolving. As a result of their soft, flexible nature and high water content, hydrogels have been widely investigated for biomedical applications such as drug delivery systems, wound dressings, cancer research, pharmaceuticals, tissue engineering, and regenerative medicine. Hydrogels for biomedical applications mainly consist of synthetic polymers such as, poly(ethylene glycol) (PEG), poly(lactic acid) (PLA), poly(vinyl alcohol) (PVA) or natural biopolymers, such as alginate, chitosan, collagen, silk fibroin (SF) or hyaluronic acid (HA). Biocompatible, biofunctional, biodegradable, non-immunogenic, and versatile hydrogels are essential for medical applications. Hyaluronic acid (HA) is one of the most used biopolymers in this field. It is a naturally occurring carbohydrate polymer that consists of alternating disaccharide repeating units of β-1,4-D-glucuronic acid - β-1,3-N-acetyl-D-glucosamine. Despite its simple chemical structure, HA plays extraordinary physiological and biological roles in the human body. Because of its hydrodynamic characteristics such as viscosity and water retention ability, hyaluronan plays a major role in biomechanical integrity of extracellular matrix and tissue homeostasis. Viscoelasticity and lubrication became acquainted through hyaluronan's high molecular weight and its capacity to absorb high amounts of water. HA also plays an important role in intracellular functions such as adhesion, differentiation, metastasis, migration, proliferation, and tumor progression. These extraordinary properties make HA an ideal candidate for the preparation of hydrogel scaffolds. However, poor biomechanical properties and rapid enzymatic degradation limit the broadening of HA application to biomedical fields and emphasise the need for some property improvement. HA has hydroxyl- (-OH) and carboxyl- (-COOH) functional groups, available for cross-linking. To overcome the mechanical property limitations, HA hydrogels have been prepared using crosslinkers such as divinyl sulfone, formaldehyde, glutaraldehyde, or they are chemical modified prior to the cross-linking by incorporating functional groups to HA, such as methacrylation by glycidyl methacrylate, thiol-functionalization, and Michael-addition. However, these hydrogels

are generally still brittle in nature, limiting their uses in biomedical applications requiring high mechanical properties because of the lack of an effective energy dissipation in covalently cross-linked HA network.

Several techniques for toughening of gels have been proposed to overcome these drawbacks, including double network gels, topological gels, sliding-ring hydrogels, nanocomposite hydrogels, cryogels, and supramolecular polymer network hydrogels. The double-network (DN) technique is a special class of interpenetrating polymer networks (IPN) and it allows for the development of high-strength hydrogels via a two-step sequential free radical polymerization. DN technique was firstly reported by Gong and co-workers in 2003 and has been intensively researched. DN hydrogels prepared from a highly cross-linked poly(2-acrylamido-2-methylpropane sulfonic acid) (PAMPS) polyelectrolyte first network and linear or loosely cross-linked polyacrylamide (PAAm) second network exhibit exceptional compressive strengths of about 20 MPa and fracture energies of up to 300 J m^{-2}. Poly(N,N-dimethylacrylamide) (PDMA) is a biocompatible polymer with associative properties and widely used to produce hydrogels. PDMA hydrogels are generally prepared by free-radical copolymerization of N,N-dimethylacrylamide (DMA) in bulk or in aqueous solutions in the presence of a cross-linker. Recently in our research group, a novel triple-network (TN) approach has been developed for preparing mechanically robust nonionic PAAm/PDMA/PDMA hydrogels exhibiting high compressive fracture stresses up to 19 MPa and compressive moduli up to 1.9 MPa. The TN approach relies on a second monomer translational entropy loss upon polymerization with the first network.

In addition to sequential polymerization, various macromolecules such as silk fibroin (SF) have been incorporated by one-pot synthesis to obtain mechanically robust hydrogels. SF, derived from Bombyx mori cocoons, is a biopolymer that offers several features comprising biocompatibility, controlled biodegradability, and unique mechanical properties. The primary structure of SF includes repetitive blocks of high molecular weight hydrophobic and low molecular weight hydrophilic chains. Structural arrangements in the hydrophobic blocks form β-sheet structure, which is responsible for its high strength, whereas hydrophilic blocks provide water solubility and toughness. Hydrogels derived from SF are attractive soft materials in biomedical applications; however, they exhibit poor mechanical properties, limiting their load-bearing applications. SF/HA scaffolds, hydrogels, patches, and films have been

prepared in the past years using several techniques including ultrasonication, cross-linking using enzymes, or chemical cross-linking agents such as genipin and carbodiimides. The resulting composites exhibit, however, poor mechanical properties and have no stretchability limiting their applications.

Cryogelation is an environmental friendly method to produce hydrogels with a high macroporosity. This technique comprises an apparently frozen aqueous solution below its freezing temperature, in which the polymerization and cross-linking reactions of a monomer-cross-linker or linear polymer-cross-linker pair take place in the unfrozen reaction domains. As water freezes, linear polymers or monomers rejected from the ice phase make up a highly dense solution phase, which is called cryoconcentration. After the reaction system is in thermally equilibrium with the external cooling bath, it consists of unfrozen solution phases containing a high concentration of polymer and cross-linker that are interconnected by ice crystals forming a template for the porous structure. As the cryoconcentration effect usually predominates over the reduced cross-linking reaction rates at a low temperature, cross-linked polymerization can be achieved even at very low temperatures. After cryogelation following by thawing the ice crystals, a polymer network with a 3D structure containing μm-sized pores are obtained.

1.1 Purpose of The Thesis

The aim of this thesis is to produce HA hydrogels exhibiting extraordinary mechanical performances. The main purpose of using HA for the production of functional materials is due to its distinct properties that are suitable for preparation of advanced biocompatible materials. Firstly, sequential polymerization reactions were conducted to produce HA/PDMA double and HA/PDMA/PDMA triple-network hydrogels, starting from native and methacrylated HA (GMHA), respectively. Next, one-pot synthesis of HA hydrogels was introduced to shorten the reaction time and to reduce the amount of reactants used. For this purpose, DMA or MAAc, and DMA and SF were incorporated separately into a reaction solution containing GMHA and then polymerized to produce HA hydrogels. Lastly, to produce robust macroporous HA hydrogels, the cryogelation technique was conducted at sub-zero temperatures starting from GMHA in the presence of DMA.

The thesis presented here resulted in five publications, mainly based on fabricating mechanically strong HA hydrogels. Within each following section, the mechanical properties of HA hydrogels were investigated in detail, and their internal structures were clarified by various techniques.

In the first part of the thesis, we used pure native HA for the preparation of mechanically strong double-network HA hydrogels. HA hydrogels were prepared in aqueous HA solutions in the presence of EGDE cross-linker under various conditions. Since the hydroxyl groups on HA molecules react with the EGDE, intermolecular cross-links form during gelation resulting in the formation of a three-dimensional HA network. The cross-linking reactions of HA with EGDE cross-linker in alkaline solutions was monitored by rheometry using oscillatory deformation tests. HA hydrogels formed were subjected to rheological and mechanical measurements to evaluate their viscoelastic and mechanical properties as a function of the cross-linker content. By applying DN approach, it became possible to generate HA/PDMA hydrogels containing 84-94% water. The hydrogels sustain 0.8-19.4 MPa compressive stresses and exhibit compressive moduli up to 0.9 MPa.

In the second part of the thesis, TN hydrogels were prepared consisting of a highly cross-linked first HA network and loosely cross-linked PDMA second and third networks. Because the equilibrium degree of swelling and the elasticity of the first network significantly affect the mechanical strength of the resulting DN and TN hydrogels, we first investigated the properties of the first network (or, single network) hydrogels derived from methacrylated HA macromers of various methacrylation degrees. By tuning the methacrylation degree, we were able to generate DN hydrogels exhibiting a fracture stress of around 10 MPa. Swelling these double networks in DMA solutions following polymerization of DMA in the gel phase further increased the ratio of ductile-to-brittle components and thus produces HA/PDMA/PDMA TN hydrogels capable of sustaining above 20 MPa of compressive stress.

In the third part of this study, one-pot synthesis of single-network HA hydrogels via free-radical copolymerization of GMHA and DMA in aqueous solutions was described. GMHA at various levels of methacrylation between 4 and 25% was prepared by methacrylation of native HA using glycidyl methacrylate. GMHA acts as a multifunctional cross-linker during its copolymerization with DMA leading to the formation of interpenetrated and interconnected polymer network hydrogels. The

effective functionality of GMHA increases with its degree of methacrylation as well as with the DMA concentration. The viscoelastic and mechanical properties of the hydrogels could be tuned by varying the degree of methacrylation of GMHA and DMA concentration. A significant improvement in the mechanical performance of the hydrogels was observed when DMA is replaced with methacrylic acid (MAAc) monomer. By adjusting the synthesis parameters, hydrogels with a Young's modulus of around 200 kPa could be prepared that sustain up to 20 MPa stresses at 96% compression.

In the fourth part, a novel strategy for the preparation of mechanically robust SF/HA hydrogels with a high stretchability (up to around 400%) was introduced. GMHA of various methacrylation degrees between 4 and 25% and SF isolated from Bombyx mori cocoons were the starting materials of the composite hydrogels. Due to the presence of pendant vinyl groups on GMHA molecules, they act both as a macromer and multifunctional chemical cross-linker during the radical polymerization in aqueous solutions. By conducting polymerization of GMHA in the presence of SF at an elevated temperature, we intend to induce β-sheet domains between SF molecules and hence, to produce additional cross-links of physical nature. DMA monomer was also included into the reaction system as a spacer to connect GMHA's through their pendant vinyl groups. The presence of SF significantly enhances the mechanical strength and toughness of GMHA hydrogels by creating an energy dissipation mechanism under load. Further, a wide range of tunable mechanical and swelling properties could be achieved by varying the methacrylation degree of GMHA.

In the last part of the thesis, a new cryogelation approach for the fabrication of macroporous HA cryogels with a wide variety of properties, flow-dependent viscoelasticity (poroelasticity), complete squeezability, and a high mechanical strength was presented. HA cryogels were synthesized from aqueous solutions of methacrylated HA of varying methacrylation degree at -18 °C by free-radical mechanism using a redox initiator system. A small amount of DMA was also included in the reaction system as a spacer. HA cryogels in swollen state sustain up to 2.6 ± 0.2 MPa compressive stress. HA cryogels confined between parallel plates also exhibit reversible strain-dependent apparent gel-to-sol transition behavior due to the flowing-out and flowing-in water through the pores, similar to water squeezing out of a sponge. HA cryogels are squeezable and no crack propagation occurred when compressed up

to 99% strain. They also exhibit a very fast swelling-deswelling behavior in good and poor solvents, respectively.

2. PREPARATION AND FRACTURE PROCESS OF HIGH STRENGTH HYALURONIC ACID HYDROGELS CROSS-LINKED BY ETHYLENE GLYCOL DIGLYCIDYL ETHER[1]

Hyaluronic acid (HA) is a natural anionic polyelectrolyte consisting of disaccharide repeat units of β-1,4-D-glucuronic acid - β-1,3-N-acetyl-D-glucosamine [1]. HA is the main component of extracellular matrix, and it plays an important role in wound-healing processes [2]. Because of the distinctive biological functions and lubricating properties, HA is an effective biomaterial for soft tissue regeneration [3–6]. However, rapid in vivo degradation and poor biomechanical performance of pure native HA limit its clinical applications. To generate a less degradable HA with improved mechanical properties, HA was chemically cross-linked to form HA hydrogels [7,8]. The functional groups in HA as potential cross-link points are the one carboxyl group and four hydroxyl groups on its repeat unit, which can be cross-linked via ester and ether linkages, respectively (Figure 2.1).

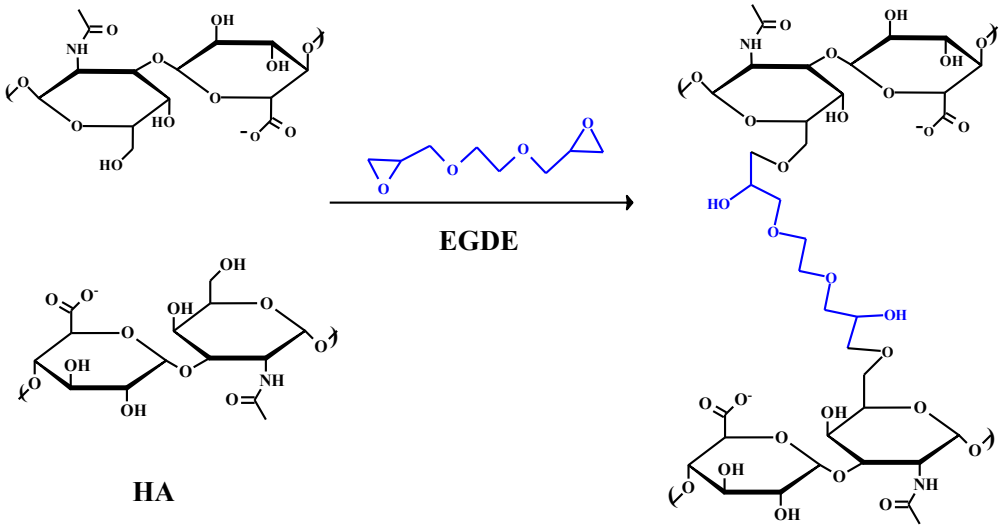

Figure 2.1 : Cross-linking of hyaluronic acid (HA) using ethylene glycol diglycidyl ether (EGDE).

[1] This chapter is based on the paper "Tavsanli, B. and Okay, O. (2016). Preparation and fracture process of high strength hyaluronic acid hydrogels cross-linked by ethylene glycol diglycidyl ether. *Reactive and Functional Polymers*, 109, 42-51."

Cross-linking of HA has been reported using several cross-linkers [9–15], including divinyl sulfone (DVS), glutaraldehyde (GTA), 1-ethyl-3-(3-dimethylaminopropyl) carbodiimide (EDC), ethylene glycol diglycidyl ether (EGDE), butanediol diglycidyl ether (BDDE) and poly(ethylene glycol) diglycidyl ether (PEGDE). Although the cross-linking of HA reduces its degradation rate and solubility in aqueous media, the resulting hydrogels exhibit poor mechanical properties to be used in stress-bearing applications. The lack of mechanical strength in HA hydrogels is mainly due to the absence of a viscoelastic dissipation in the chemically cross-linked HA network leading to the fracture of the hydrogels under low stresses [16,17]. Recently, high-toughness HA hydrogels with a macroporous structure have been prepared using cryogelation of aqueous HA solutions at subzero temperatures in the presence of EGDE cross-linker [18,19]. Due to the cryoconcentration of the reactants in the unfrozen micro-domains of the cryogelation system [20], HA cryogels are very tough and can completely be squeezed without any crack propagation. However, the toughness of HA cryogels is due to water flowing out of their macropores under stress and, they are very soft materials exhibiting an elastic modulus of below 2 kPa [18].

An alternative two-step approach to produce HA hydrogels is the chemical modification of HA prior to the cross-linking reactions to incorporate additional functional groups. The widely used strategy is to introduce photopolymerizable methacrylate groups on HA molecules using glycidyl methacrylate, which are subsequently photopolymerized to form HA-based hydrogels [21–23]. Another strategy is the synthesis of thiol-functionalized HA which spontaneously forms intermolecular disulfide bonds upon exposure to air [24,25]. To increase the rate of cross-linking, Michael-type addition reaction was also employed by the addition of poly(ethylene glycol) diacrylate cross-linker [24]. However, the hydrogels derived from the chemically modified HA also exhibit poor mechanical properties [26,27]. To achieve a high mechanical strength, they can be reinforced with other macromolecules [28–30], or energy dissipation mechanisms can be created to slow crack propagation within the gel network [31,32]. By using the double-network (DN) concept [33–37], Weng et al. prepared mechanically strong HA hydrogels consisting of a highly cross-linked methacrylated HA (GMHA) first-network and a lightly cross-linked ductile poly(N,N-dimethylacrylamide) (PDMA) second-network [31]. DN hydrogels exhibit a compressive modulus of 0.5 MPa and a fracture stress of 5.2 MPa. A similar

procedure was recently applied by Tavsanli et al. for the synthesis of triple-network hydrogels [32]. The hydrogels consisting of GMHA/PDMA/PDMA interconnected interpenetrated network components exhibit compressive fracture stresses up to 20 MPa.

However, the chemical modification procedures of HA summarized above to prepare DN hydrogels involve macromonomer synthesis and purification steps with many chemicals including dihydrazides, trimethylamine and phase transfer catalysts. Alternatively, a simple way to produce DN hydrogels is to use native HA to create the first-network hydrogels instead of GMHA. Moreover, because GMHA is more hydrophobic than HA due to its methacrylate groups, one may expect that the single-network HA hydrogels will exhibit a higher degree of swelling in aqueous solutions as compared to GMHA hydrogels. This means that a larger amount of the second ductile PDMA network component could be introduced in HA hydrogels during double networking leading to better mechanical properties [33]. This is the main motivation of this study.

Here, we use pure native HA for the preparation of mechanically strong double-network HA hydrogels. To our knowledge, such hydrogels have not been reported before. HA hydrogels were prepared in aqueous HA solutions in the presence of EGDE cross-linker under various experimental conditions. EGDE contains epoxide groups on both ends and, has been widely used for cross-linking of biopolymers carrying hydroxyl, amino, and sulfhydryl groups [38–40]. Since the hydroxyl groups on HA molecules react with the EGDE [18,19], intermolecular cross-links form during gelation, resulting in the formation of a three-dimensional HA network (Figure 2.1). We monitored the cross-linking reactions of HA with EGDE cross-linker in alkaline solutions by rheometry using oscillatory deformation tests. HA hydrogels formed were subjected to rheological and mechanical measurements to evaluate their viscoelastic and mechanical properties as a function of the cross-linker content. By applying DN approach, we were able to generate HA/PDMA hydrogels containing 84-94% water. The hydrogels sustain 0.8-19.4 MPa compressive stresses and exhibit compressive moduli up to 0.9 MPa. These values are much larger than those reported before for DN hydrogels derived from GMHA macromers [31,32]. Thus, HA hydrogels described here are promising materials for stress-bearing biomedical applications. As will be discussed below, high mechanical strength of the present hydrogels is due to the

internal fracture of HA network by dissipating energy as well as due to the larger swelling capacity of the first-network hydrogels based on HA as compared to GMHA, increasing the ratio of the second-to-first network components in DN hydrogels.

2.1 Experimental Part

2.1.1 Materials

Hyaluronic acid sodium salt (HA) from Streptococcus equi was obtained from Sigma-Aldrich (impurities: ≤1 protein), and its viscosity averaged molecular weight is $1.2x10^6$ $g.mol^{-1}$ [18]. Ethylene glycol diglycidyl ether (EGDE, Polysciences, Inc., total chlorine content: 0.6 %), NaOH (Merck, ≥ 99%), N,N-dimethylacrylamide (DMA, Sigma-Aldrich, 99%, contains 500 ppm monomethyl ether hydroquinone as inhibitor), 2-oxoglutaric acid (Fluka, ≥ 99%), and N,N -methylene(bis)acrylamide (BAAm, Merck, ≥ 99%), were used as received.

2.1.2 Hydrogel preparation

HA solutions were prepared by dissolving HA in 1 w/v% NaOH solution by gently stirring at 25 °C for 1 h. To ensure a complete dissolution, HA solutions were kept at 4 °C for 24 h. After adding EGDE cross-linker, the solution was stirred for 15 min before being transferred into plastic syringes (inner diameter = 6 mm, length = 70 mm) to conduct the cross-linking reactions. The reactions were carried out both at 25 °C and 50 °C for 4 days and 4 h, respectively. DN hydrogels were synthesized by immersing HA hydrogels in as-prepared states in aqueous solutions containing the monomer DMA (30 w/v%), the second-network cross-linker BAAm (0.05 and 0.10 mol% of DMA), and the photo-initiator 2-oxoglutaric acid (0.1 mol% of DMA). The volume of the aqueous solution was much larger than the gel volume (around 120 mL solution per gram of hydrogel sample), so that the concentration of the solution was practically unchanged. After the swelling equilibrium was established within 4 days, the solution containing the hydrogel was transferred into syringes of 10 mL in volume and the polymerization was carried out 25 °C under UV light at 365 nm for 24 h.

2.1.3 Swelling and gel fraction measurements

Hydrogel samples in as-prepared states were immersed in a large excess of water at 25 °C for at least 4 days whereby the water was replaced every day to extract any soluble species. The swelling equilibrium was tested by weighing the gel specimens. The hydrogels in both as-prepared and equilibrium swollen states were transparent indicating that macrophase separation did not occur. The equilibrium relative weight swelling ratio m_{rel} was calculated as $m_{rel} = m/m_o$, where m is the mass of the equilibrium swollen gel sample, and m_o is its mass after preparation. To determine the gel fraction, the equilibrium swollen gel samples were taken out of water and immersed into excess acetone for 1 day. After drying at 80 °C under vacuum to constant mass, the gel fraction W_g was calculated from the masses of dry polymer network and from the comonomer feed.

2.1.4 Rheological experiments

The cross-linking reactions of HA with EGDE cross-linker were monitored at 50 °C within the rheometer (Gemini 150 Rheometer system, Bohlin Instruments) equipped with a cone-and-plate geometry (cone angle = 4°, diameter = 40 mm). The instrument was equipped with a Peltier device for temperature control. During the rheological measurements, a solvent trap was used and the outside of the upper plate was covered with a thin layer of low-viscosity silicone oil to prevent the evaporation of water. An angular frequency ω of 6.3 rad s^{-1} and a deformation amplitude γ_o of 0.01 were selected to ensure that the oscillatory deformation is within the linear regime. After a reaction time of 3 h, the elastic moduli G' of the reaction solutions approached limiting values. Then, frequency-sweep tests were carried out at 25 °C.

2.1.5 Mechanical tests

Uniaxial compression measurements were conducted on equilibrium swollen hydrogels at 25 °C on a Zwick Roell Z0.5 TH test machine using a 500 N load cell. The gel samples were cut into cubic samples with dimensions 3x3x3 mm. Before the test, an initial compressive contact of 0.01 N was applied to ensure a complete contact between the gel and the plates. The tests were performed at a constant cross-head speed of 0.3 and 1 mm min^{-1} below and above 15% compression, respectively. Compressive stress was presented by its nominal N and true values σ_{true} (= λ σ_{nom}), which are the forces per cross-sectional area of the undeformed and deformed gel specimen,

respectively, and λ is the deformation ratio (deformed length/initial length). The compressive strain ε is defined as the change in the length relative to the initial length of the gel specimen, i.e., $\varepsilon = 1 - \lambda$. Cyclic compression tests were conducted at a constant cross-head speed of 1 $mm.min^{-1}$. The gel samples were first compressed up to a maximum strain λ_{max}, followed by retraction to zero relaxation force. After waiting for 1 min at zero relaxation force, the test was repeated four times with a fixed maximum strain as well as with increasing this strain. For reproducibility, at least five samples were measured for each gel and the results were averaged.

2.2 Results and Discussion

2.2.1 HA hydrogels

HA hydrogels were prepared in aqueous NaOH solutions at 50 ^{o}C in the presence of EGDE cross-linker. The selection of NaOH solutions as the solvent to conduct the cross-linking reactions is due to the fact that the intramolecular hydrogen bonds in HA molecules are easily disrupted at high pH values [41], thereby providing a more flexible HA chain conformation and easier solubility in water. Increasing chain flexibility of HA in alkaline solutions will also promote the cross-linking reactions between its functional groups via the epoxy groups of EGDE. Preliminary experiments were carried out to optimize the concentrations of NaOH (C_{NaOH}) and HA (C_{HA}) during the gel formation. At $C_{NaOH} < 1$ w/v%, HA could not be completely dissolved in aqueous solutions while at higher NaOH concentrations ($\geq$ 2 w/v%), the solution viscosity of HA and the elastic modulus *G'* of the resulting hydrogels drastically decreased indicating hydrolytic degradation of HA [41]. Moreover, at $C_{HA} < 8$ w/v%, weak hydrogels with an elastic modulus below 1 kPa were obtained in 1 w/v% NaOH solutions, while, at or above 10 w/v% HA, the preparation of a homogeneous HA solution was difficult due to the high solution viscosity. In the following, we present our results obtained in a 1 w/v% NaOH solution containing 8 w/v% HA and various amounts of the cross-linker EGDE. Rheological measurements conducted on 8 w/v% HA solution in 1 w/v% NaOH before the addition of the cross-linker showed a decrease in the solution viscosity and elastic modulus *G'* with increasing time or with increasing temperature (Figs. 2.2, 2.3).

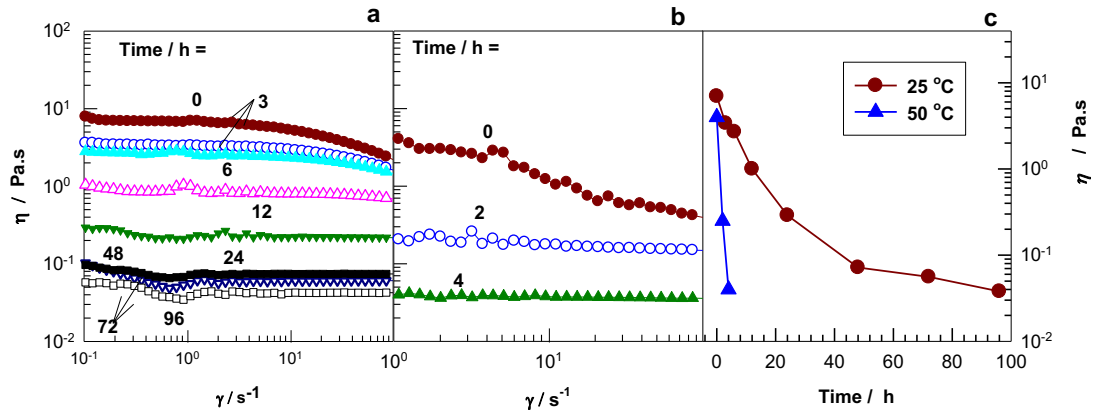

Figure 2.2 : (a, b): Shear rate $\dot{\gamma}$ dependence of the viscosities η of 8 w/v% HA solution in 1 w/v% NaOH at various times after preparation of the solutions. Temperature = 25 (a) and 50 °C (b). Measurement times are indicated. (c): Viscosities η measured at $\dot{\gamma}$ = 1 s^{-1} plotted against the measurement time. Temperatures are indicated.

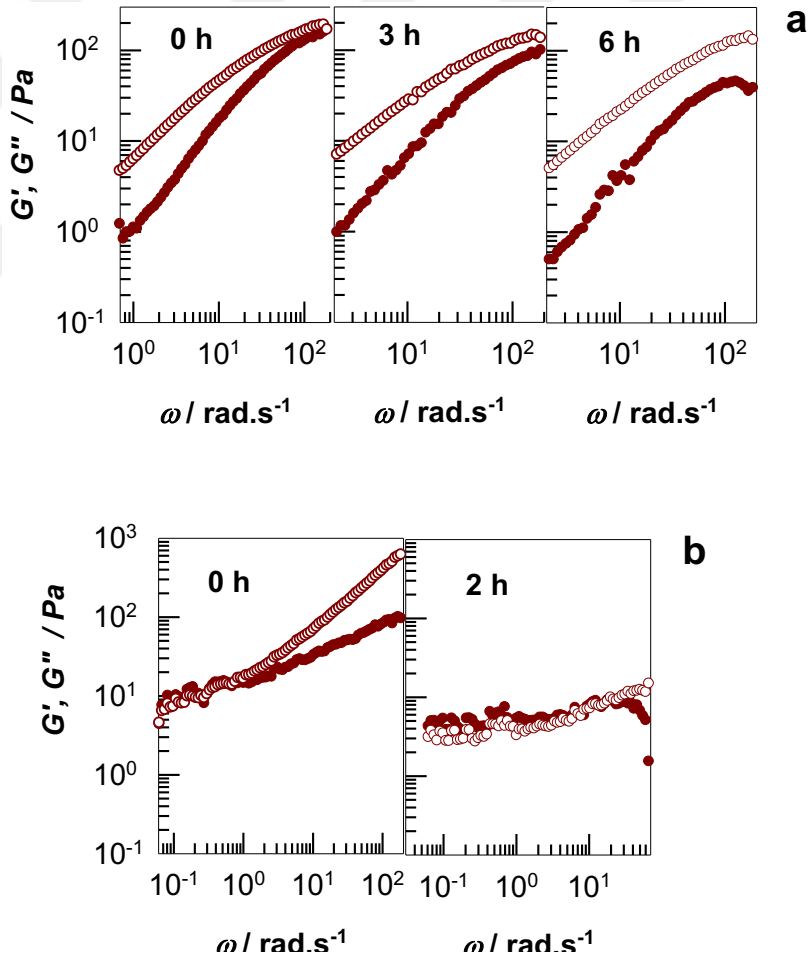

Figure 2.3 : Frequency dependencies of *G'* (filled symbols) and *G''* (open symbols) of 8 w/v% HA solutions in 1 w/v% NaOH at various times after preparation of the solutions. Temperature = 25 (a) and 50 °C (b). γ_o = 0.01.

This behavior of alkaline HA solutions has been reported before [41], and it originates from the decrease of the size of HA molecules due to the disruption of intermolecular hydrogen bonds and/or from the degradation of HA backbone resulting in a decrease of the molecular weight.

We first monitored the gelation reactions by dynamic rheological measurements in order to follow the gradual formation of the three-dimensional HA network. Typical gelation profiles of 8 w/v% HA solutions at 50 ºC and at four different cross-linker contents are shown in Fig. 2.4a where the elastic modulus *G'* and the loss factor *tan δ* are plotted against the reaction time. During the reactions, the elastic modulus *G'* increases rapidly while *tan δ* decreases and then, they approach plateau values after about 3 h. The higher the EGDE content, the higher the elastic modulus *G'*, and the lower the loss factor *tan δ* indicating that increasing cross-linker content decreases the viscous, energy dissipating properties of HA hydrogels. To estimate the limiting modulus $G_{\infty}^{'}$ of the hydrogels, the experimental *G'* vs gelation time data were fitted to the equation [42–44]:

$$G'(t) = G'_{\infty} \frac{t^n}{t^n + \theta^n} \tag{2.1}$$

where θ is the half-gelation time at which the modulus *G'* becomes equal to $G'_{\infty}/2$, and the exponent *n* relates to the slope *P* at θ by:

$$P = \frac{n G'_{\infty}}{4\theta} \tag{2.1a}$$

The solid red curves in Fig. 2.4a showing the best fits to the experimental data indicate that eq 2.1 well simulates the gelation process of HA solutions. Gelation reactions conducted at eight different cross-linker concentrations between 0.95 and 22.4 w/v% EGDE revealed that both the half-gelation time θ and the coefficient *n* are almost independent on the EGDE content and they remain at 143±38 min and 1.6±0.3, respectively. This indicates that the cross-linking reactions are not accelerated with increasing EGDE concentration. In contrast, the slope *P* at the half-gelation time θ increased from 2 to 140 kPa.min^{-1} indicating formation of a larger number of intermolecular cross-links as the EGDE content is increased. The limiting values of $G_{\infty}^{'}$ obtained from the fits are shown in Fig. 2.4b together with the loss factor *tan δ* after

a reaction time of 3 h both plotted against the EGDE concentration. HA hydrogels with an elastic modulus between 10^{-1} and 10^{1} kPa could be obtained by tuning the cross-linker concentration. Moreover, the hydrogels exhibit a loss factor between 0.07 and 0.7, i.e., they belong to the category of weak gels [45].

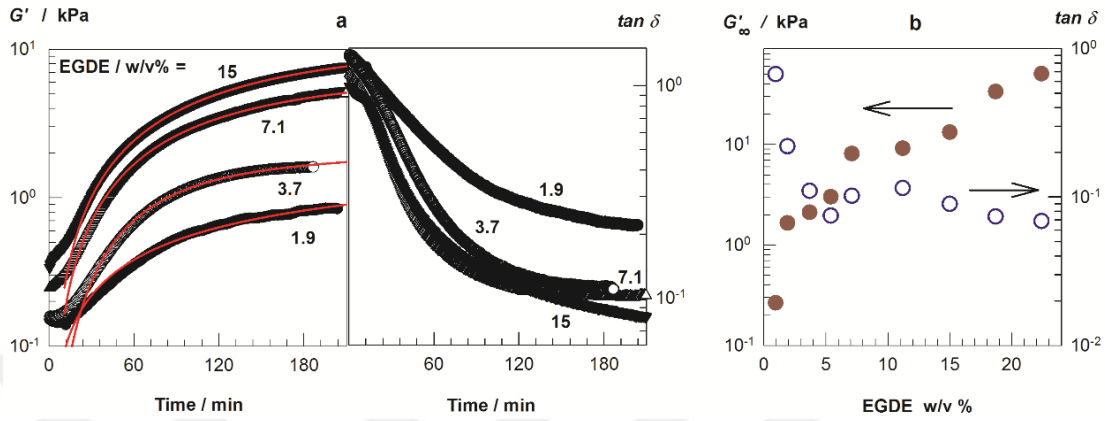

Figure 2.4 : Rheological monitoring of HA gelation. (a) Elastic modulus *G'* (left) and the loss factor *tan δ* (right) of the reaction system shown as a function of the reaction time. $\omega = 6.3$ rad.s^{-1}. $\gamma_o = 0.01$. Temperature = 50 °C. EGDE concentrations are indicated. The solid curves were calculated using eq 2.1. (b) The limiting elastic modulus G'_∞ (filled symbols) and *tan δ* after a reaction time of 3 h (open symbols) plotted against EGDE %.

After a reaction time of 4 h, dynamic frequency-sweep tests were carried out to explore the internal dynamics of HA hydrogels. Fig. 2.5a-e show the frequency dependencies of *G'* (filled symbols) and the viscous modulus *G''* (open symbols) at a strain amplitude $\gamma_o = 0.01$ for the hydrogels formed at various EGDE contents. At the lowest cross-linker content of 0.95 w/v% EGDE (Fig. 2a), both *G'* and *G''* increase with frequency similar to the semi-dilute polymer solutions. However, unlike these solutions, the present system exhibits an elastic character (*G'* > *G''*) at low frequencies and a predominantly viscous character above the crossover frequency of 20 rad.$^{-1}$ at which *G'* and *G''* intersect. This unusual behavior was observed before in aqueous solutions of sodium alginate - poly(N-isopropylacrylamide) (PNIPA) [46], HA-graft-PNIPA [47], and methyl cellulose [48]. We attribute this feature to the intermolecular hydrogen bonds between HA molecules acting as physical cross-links and thus, contributing to the elasticity of the hydrogel at a low frequency. Increasing frequency gradually breaks H-bonds so that the weak gel transforms to a viscous solution. As the cross-linker content is increased, the crossover frequency shifts outside of the experimental window indicating that the effect of chemical EGDE links dominate over

the physical cross-links (Fig. 2.5a→e). However, the viscous modulus *G''* still rises with frequency implying increasing extent of energy dissipation due to the rearrangement of HA molecules leading to their sliding past each other at short experimental time scales. Fig. 2.5 also shows that, at 3.7 w/v% EGDE, a plateau-like behavior appears in the low-frequency range, whereas the height of the plateau increases and its width expands as EGDE concentration is further increased. For instance, the plateau elastic modulus increases from 1.6 to 24.5 kPa with increasing EGDE content from 3.7 to 22.4 w/v% indicating increasing elastic response of the hydrogels.

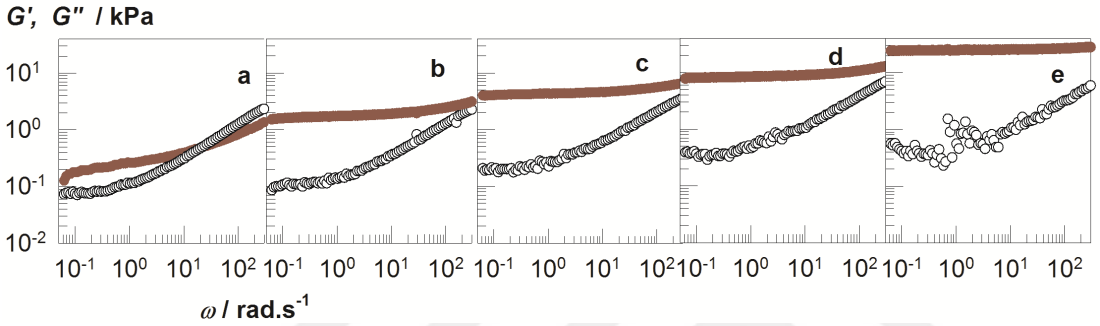

Figure 2.5 : *G'* (filled symbols) and *G''* (open symbols) of HA hydrogels at 25°C shown as a function of the frequency ω measured after a gelation time of 4 h. γ_o = 0.01. EGDE = 0.95 (a), 3.7 (b), 7.1 (c), 15.0 (d), and 22.4 w/v% (e).

After a gelation time of 4 h, HA hydrogels were subjected to swelling and mechanical measurements. The hydrogels formed below 2 w/v% EGDE were soluble in water while those formed at or above 3.7 w/v% EGDE were insoluble with a gel fraction W_g above 0.90 and contained 97-99% water (Table 2.1 and 2.2). Since the molecular weights of the cross-linker EGDE and the disaccharide repeat units of HA are 174.2 and 416 g.mol^{-1}, respectively, and HA concentration at gelation was fixed at 8 w/v%, a conversion factor of 0.15 converts the EGDE concentration (in w/v%) to the molar ratio of epoxide and hydroxide groups. Thus, the threshold concentration of 3.7 w/v% EGDE corresponds to the presence of about 0.56 epoxides per OH group, or 2.2 moles of epoxide groups per disaccharide repeat unit of HA molecules. Assuming that each epoxide group forms elastically effective cross-links, this molar ratio would lead to a ladder-like highly cross-linked HA structure with a modulus in the MPa range. Thus, a large fraction of EGDE in the gelation solution seems to be wasted in side reactions, such as the reaction of the epoxides with water, and/or is attached to HA only with its one end while the other end reacts with water.

Table 2.1 : Preparation conditions and mechanical data of the hydrogels. Single-network (SN) HA hydrogels were prepared at 25 °C at 8 w/v% HA concentration. DN hydrogels were prepared in 30 w/v% DMA solutions containing 0.05 and 0.10 mol% BAAm cross-linker. Standard deviations are in parentheses.

Type	EDGE w/v%	BAAm mol%	W_g [a]	m_{rel} [b]	w_{21} [c]	σ_f [d] / kPa	E [e] / kPa	ε_f % [f]	Water %[g]
SN	1.9	0	0.91	123 (7)	0	18 (2)	7 (1)	51	99
DN	1.9	0.05	0.97	27 (2)	102	3700 (80)	36 (7)	93	94
DN	1.9	0.10	0.98	26 (1)	97	2600 (90)	54 (4)	90	93
SN	3.7	0	0.94	43 (4)	0	47 (3)	11 (1)	49	99
DN	3.7	0.05	0.99	20 (1)	70	8300 (700)	154 (17)	94	90
DN	3.7	0.10	0.96	21 (1)	75	5200 (400)	82 (9)	92	90
SN	7.1	0	0.93	10 (1)	0	61 (10)	42 (8)	42	97
DN	7.1	0.05	0.99	14 (2)	49	19400 (900)	534 (36)	95	85
DN	7.1	0.10	0.97	14 (1)	48	13300 (1100)	366 (26)	93	83
SN	11.2	0	0.98	6 (0)	0	77 (9)	115 (12)	32	91
DN	11.2	0.05	0.98	5 (0)	14	8700 (1100)	773 (108)	85	84
DN	11.2	0.10	0.97	5 (0)	14	11100 (1300)	548 (105)	86	85
SN	15	0	0.98	3 (0)	0	151 (10)	296 (11)	32	92
DN	15	0.05	0.96	3 (0)	8	800 (25)	246 (10)	39	87
DN	15	0.10	0.95	3 (0)	7	3400 (300)	329 (20)	55	87
SN	22.4	0	0.91	2 (0)	0	103 (30)	585 (62)	25	63
DN	22.4	0.05	-						
DN	22.4	0.10	-			Fracture during double networking			

[a] Gel fraction, [b] relative swelling ratio, [c] the mass ratio of the second to the first network units, [d] fracture stress, [e] Young's moludus, [f] strain at break, [g] water content. Standard deviations in parentheses.

Table 2.2 : Preparation conditions and mechanical data of the hydrogels. Single-network (SN) HA hydrogels were prepared at 50 °C at 8 w/v% HA concentration. DN hydrogels were prepared in 30 w/v% DMA solutions containing 0.05 and 0.10 mol% BAAm cross-linker. Standard deviations are in parentheses.

Type	EDGE w/v%	BAAm mol%	W_g [a]	m_{rel} [b]	w_{21} [c]	σ_f [d] / kPa	E [e] / kPa	ε_f % [f]	Water %[g]
SN	3.7	0	0.93	76 (5)	0	19 (4)	3 (1)	46	99
DN	3.7	0.05	0.98	35 (2)	126	2400 (400)	27 (4)	89	94
DN	3.7	0.10	0.95	34 (2)	124	1200 (200)	51 (1)	84	93
SN	7.1	0	0.96	21 (2)	0	40 (1)	14 (4)	46	99
DN	7.1	0.05	0.94	14 (1)	49	15300 (300)	318 (17)	95	92
DN	7.1	0.10	0.94	14 (2)	49	12100 (800)	200 (37)	94	91
SN	11.2	0	0.97	13 (1)	0	65 (5)	29 (5)	45	98
DN	11.2	0.05	0.92	10 (1)	34	10000 (600)	546 (56)	91	86
DN	11.2	0.10	0.92	10 (1)	35	11300 (900)	319 (20)	91	87
SN	15	0	0.93	7 (0)	0	88 (4)	63 (10)	47	97
DN	15	0.05	0.94	8 (0)	25	7500 (300)	942 (128)	86	85
DN	15	0.10	0.95	7 (0)	24	2340 (400)	459 (44)	89	86
SN	22.4	0	0.92	3 (0)	0	43 (7)	98 (6)	26	97
DN	22.4	0.05	-	-	-	-	-	-	-
DN	22.4	0.10	-	-	-	-	-	-	-

[a] Gel fraction, [b] relative swelling ratio, [c] the mass ratio of the second to the first network units, [d] fracture stress, [e] Young's moludus, [f] strain at break, [g] water content. Standard deviations in parentheses.

All HA hydrogels described above were prepared by conducting the cross-linking reactions at 50 °C. Because HA may degrade at an elevated temperature, we repeated the gelation reactions at 25 °C. However, the reactions were too slow to monitor the gelation process by dynamic rheological measurements. Gravimetric tests conducted at or above 1.9 w/v% EGDE revealed that a gel fraction W_g above 0.90 could only be obtained by increasing the gelation time to 4 days (Table 2.1-2.2). The hydrogels formed both at 50 and 25 °C were subjected to swelling measurements in water. Filled circles in Fig. 2.6a & b show the relative swelling ratio m_{rel} (with respect to the as-prepared state) of HA hydrogels formed at 50 and 25 °C, respectively, plotted against their EGDE contents. For comparison, m_{rel} values of GMHA hydrogels reported before are also shown in Fig. 2.6a by the open symbols plotted against the methacrylation degree (DM) of GMHA [32]. m_{rel} of HA hydrogels is a decreasing function of the cross-linker content and varies between 2-123, corresponding to the equilibrium swelling ratio with respect to dry state of 25-1540. This high degree of swelling is a consequence of the osmotic pressure exerted by the counterions of cross-linked HA molecules, similar to the synthetic polyelectrolyte hydrogels [11]. The hydrogels formed at 25 °C exhibit a slightly lesser degree of swelling in water as compared to those formed at 50 °C. Another point is that HA hydrogels swell much more than those prepared from GMHA exhibiting relative swelling ratios m_{rel} between 3 and 4.5. This reveals a reduction in the hydrophilicity of native HA upon its modification with methacrylate groups.

Mechanical properties of HA hydrogels equilibrium swollen in water were investigated by uniaxial compression tests. Fig. 2.6c represents compressive stress-strain curves of the gel samples formed at 50 °C and at various EGDE contents, where the nominal stress σ_{nom} is plotted against the strain ε. In Fig. 2.6d & e, the Young's modulus E, fracture stress σ_f and fracture strain ε_f of the hydrogels formed at 50 °C and 25 °C, respectively, are plotted against the EGDE content. Depending on the cross-linker content and gelation temperature, Young's modulus E of the hydrogels varies one to two orders of magnitude, i.e., between 3 and 590 kPa. For a tetrafunctional phantom network of Gaussian chains, the Young's modulus E is related to the elastically effective cross-link density ν_e (number of network chains per unit volume of swollen gel) by [49,50]:

$$E = 1.5 \nu_e RT \left(m_{rel} \right)^{2/3} \tag{2.2}$$

where R is the gas constant and T is the absolute temperature. Note that eq (2.2) assumes that the weight swelling ratio m_{rel} is equal to the volume swelling ratio. In Fig. 2.6f, the cross-link density ν_e of HA hydrogels is shown as a function of the EGDE content. For comparison, ν_e of GMHA hydrogels is also plotted against DM% [32]. In accord with the lower swelling capacity of HA hydrogels formed at 25 °C, their modulus E and cross-link density ν_e are larger than those formed at 50 °C indicating increasing cross-linking efficiency by reducing the gelation temperature.

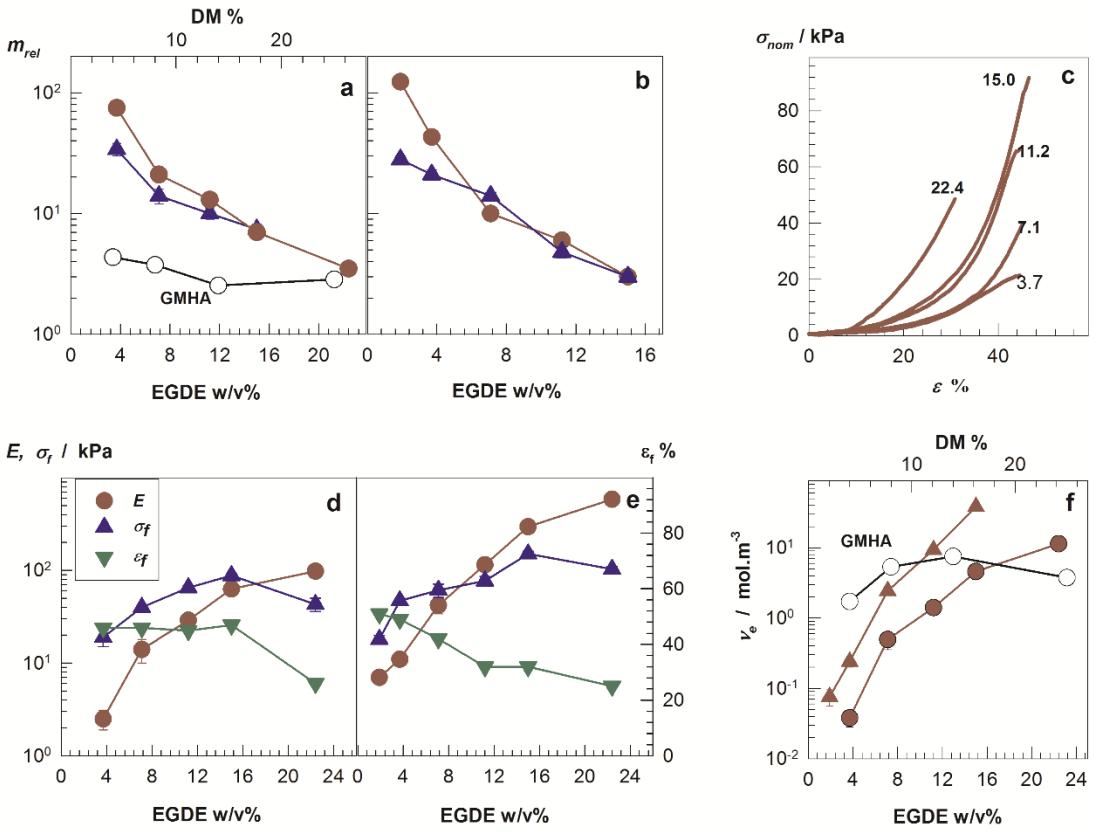

Figure 2.6 : Swelling behavior and mechanical properties of HA hydrogels. (a, b) Relative swelling ratio m_{rel} of HA hydrogels formed at 50 °C (a) and 25 °C (b) in water (filled circles) and in aqueous 30% DMA solution (filled triangles) plotted against EGDE%. For comparison, m_{rel} values of GMHA hydrogels reported before are also shown in Fig. 2.6a by the open symbols plotted against the methacrylation degree (DM) of GMHA [32]. (c) Typical stress-strain curves of HA hydrogels formed at 50 °C under compression as the dependences of nominal stress σ_{nom} on the strain ε. EGDE contents (in w/v%) are indicated. (d, e) Young's modulus E, fracture stress σ_f and fracture strain ε_f plotted against the EGDE content for the hydrogels formed at 50 °C (d) and 25 °C (e). (f) The cross-link density ν_e of HA hydrogels formed at 50 °C (filled circles) and 25 °C (filled triangles) plotted against EGDE %. Open symbols represent υ_e of GMHA hydrogels plotted against DM% of GMHA [32].

The decrease of the cross-linking efficiency with rising temperature is attributed to the partial degradation of HA molecules producing shorter primary chains. Moreover, when comparing the swelling ratios of GMHA and HA hydrogels having similar cross-link densities, the former hydrogels exhibit a lower degree of swelling in water supporting the fact that the methacrylation makes HA less hydrophilic as compared to native HA. We have to note that because the cross-link density v_e of the hydrogels calculated using eq (2.2) bases on the swollen gel volume, its value is affected by the swelling degree of the hydrogels. However, calculation of the cross-link densities based on dry polymer lead to the similar trends as mentioned above (Fig. 2.7).

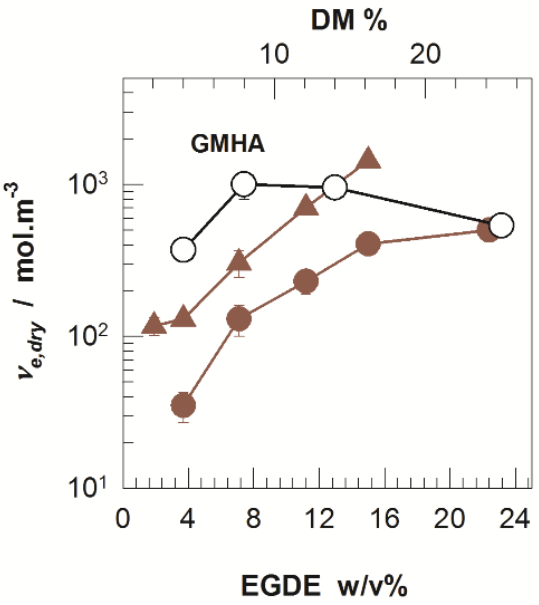

Figure 2.7 : The crosslink density $v_{e,dry}$ of HA hydrogels based on dry polymer plotted against EGDE %. The hydrogels were prepared at 50 °C (filled circles) and 25 °C (filled triangles) Open symbols represent the crosslink density $v_{e,dry}$ of GMHA hydrogels plotted against DM% of GMHA. Note that $v_{e,dry}$ was calculated from v_e using the equation $v_{e,dry} = (v_e\ m_{rel})/v_2^o$ where v_2^o is the volume fraction of HA at the gel preparation ($\cong 0.08$).

The results in Fig. 2.6d & e also show that all HA hydrogels rupture when compressed to 25-51% strain under 20-150 kPa stresses. Thus, they are brittle hydrogels similar to the chemically cross-linked synthetic hydrogels [51], indicating that the viscoelastic energy dissipation of HA molecules under stress does not contribute much to their mechanical performances.

2.2.2 Double-network HA hydrogels

As mentioned in the previous section, HA hydrogels exhibit a larger degree of swelling as compared to those obtained from GMHA macromers. This suggests that a larger amount of a ductile component could be introduced during double-networking of HA hydrogels leading to double-network (DN) hydrogels with better mechanical properties as compared to those produced from GMHA macromers [33,52]. We prepared DN hydrogels by swelling HA hydrogels, taken as the first-network, in N,N-dimethylacrylamide (DMA) solutions containing a small amount of BAAm cross-linker, and then photopolymerizing DMA to form a loosely cross-linked poly(N,N-dimethylacrylamide) (PDMA) second network. The filled triangles in Fig. 2.6a & b show the swelling ratio m_{rel} of HA hydrogels formed at 50 and 25 ^{o}C, respectively, in aqueous 30 w/v% DMA solutions plotted against the EGDE content. Although a slight reduction in the swelling degree m_{rel} of the hydrogels in the DMA solution is observable as compared to their m_{rel} values in water, they still exhibit a high swelling ratio up to 40, which is one of the requirements for obtaining high strength DN hydrogels.

HA hydrogels swollen in 30 w/v% DMA solutions containing 0.05 and 0.10 mol% BAAm as the second-network cross-linker were subjected to photopolymerization using 2-oxoglutaric acid initiator. In this way, double-network hydrogels with a gel fraction W_g above 0.90 were obtained (Table 2.1-2.2). In equilibrium swollen state, they contained 84-94% water which decreased with increasing cross-linker content of the first-network hydrogel (Table 2.2). In the following DN hydrogels are denoted by DN-*x* where *x* is the mole percent of BAAm in the second monomer solution. Fig. 2.8 represents typical compressive stress-strain curves of SN hydrogels formed at 50 ^{o}C (dashed bold curves) and DN hydrogels (dash-dot-dot and solid curves) formed in 30 w/v% DMA solutions containing 0.05 and 0.10 mol% BAAm. EGDE content of the first network HA hydrogel is 3.7, 7.1, and 11.2 w/v% in Fig. 2.8a, b, and c, respectively. General trend is that the compressive stress required to deform the hydrogels increases from kPa to MPa scales after the double-networking process (Fig. 2.6c vs Fig. 2.8). Simultaneously, compression ratio at rupture increases from 26-47% to above 80% indicating toughening effect of the second PDMA network. It is also obvious that the EGDE content of the first HA network, that is, its cross-link density has a significant effect on the mechanical performance of DN hydrogels. We have to

note that DN hydrogels were rather brittle in tensile tests with very low elongation at break. As a consequence, tensile tests could not be performed in a meaningful way.

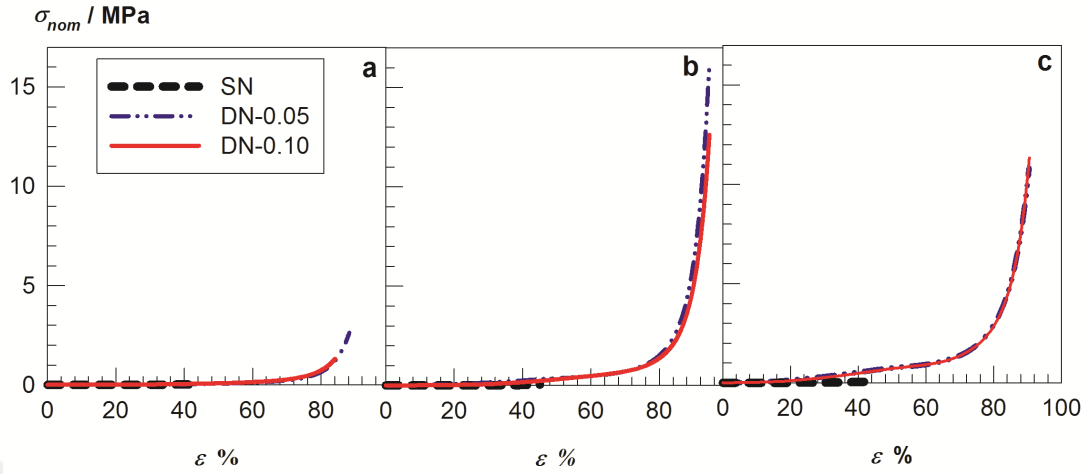

Figure 2.8 : Compressive stress-strain curves of SN hydrogels formed at 50 °C (dashed bold curves) and DN hydrogels (dash-dot-dot and solid curves). EGDE of the first-network HA hydrogel = 3.7 (a), 7.1 (b), and 11.2 w/v% (c). DN hydrogels were prepared in 30 w/v% DMA solutions containing 0.05 (dash-dot-dot curves) and 0.10 mol% BAAm cross-linker (solid curves).

In Fig. 2.9a & b, Young's modulus E, the fracture stress σ_f and strain at break ε_f of single-network HA (open symbols) and DN hydrogels (filled symbols) are plotted against EGDE concentration. The first-network HA hydrogels were prepared at 50 °C and 25°C in (a) and (b), respectively. The modulus E of DN hydrogels is more than one order of magnitude greater than that of SN hydrogels and approaches to 1 MPa at high EGDE concentrations (Table 2.1-2.2). This increase in the modulus suggests the existence of physical and chemical cross-links between the first- and second-network components contributing to the rubber elasticity of DN hydrogels. The fracture stress σ_f and strain at break ε_f exhibit slight maxima at around 7 w/v% EGDE. The largest modulus and fracture stress of DN hydrogels thus obtained are 0.94 ± 0.13 MPa and 19.4 ± 0.9 MPa, respectively. These values are higher than those of DN hydrogels prepared from GMHA macromer exhibiting fracture stresses up to 5.2 and 12 MPa for 10 and 4% methacrylation degrees of HA, respectively [31,32]. Moreover, comparison of the mechanical characteristics of DN-0.05 and DN-0.10 hydrogels also indicates that the amount of the second-network cross-linker in this range does not have an effect on the mechanical properties of DN hydrogels.

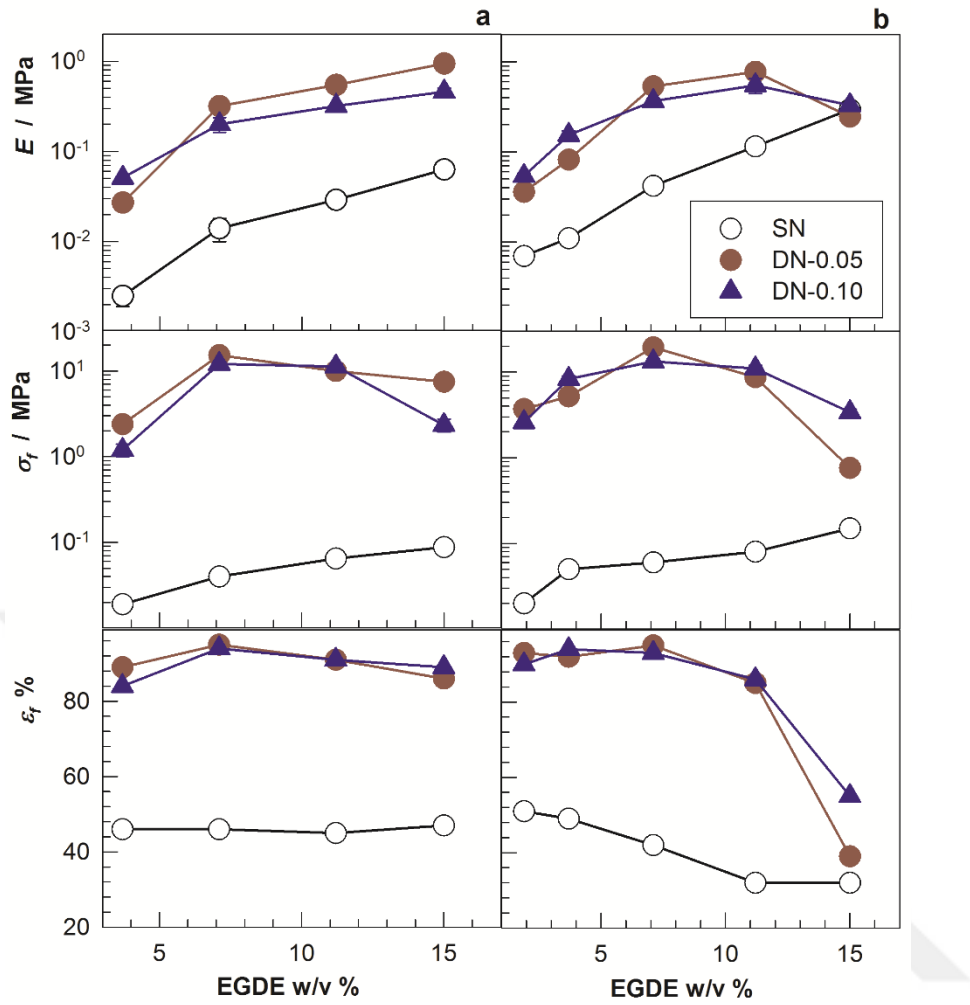

Figure 2.9 : Young's modulus E, the fracture stress σ_f and strain ε_f of SN (open symbols) and DN hydrogels (filled symbols) plotted against EGDE concentration. Preparation temperature of HA hydrogel = 50 ºC (a) and 25 ºC (b). Note that most of the error bars are smaller than the symbols.

To demonstrate the effect of the amount of the second PDMA ductile network on the mechanical performance of the hydrogels, we calculated the mass ratio w_{21} of PDMA to the HA first-network by:

$$w_{21} = \frac{(m_{rel} - 1) C_2}{C_1} \tag{2.3}$$

where m_{rel} is the swelling ratio of HA hydrogel in 30 w/v% DMA solution, C_1 and C_2 are the concentrations (in g.mL^{-1}) of HA and DMA in the preparation of the first- and double-network hydrogels, respectively. Note that eq (2.3) assumes that the densities of the hydrogels and DMA solution are equal to unity. Further, it neglects the exchange of water in the hydrogel with the external solution and thus, only consider monomer solution entering the gel phase during the swelling process to simulate real processes

[52,53]. Because both C_1 and C_2 are fixed by the experiments at 0.08 and 0.30 g.mL^{-1}, respectively, the ratio w_{21} only depends on the swelling capacity of HA hydrogels in the DMA solution.

In Fig. 2.10a-c, the filled symbols represent the fracture stress σ_f, Young's modulus E, and fracture strain ε_f of all DN hydrogels plotted against w_{21} ratio. For comparison, the data for SN hydrogels (w_{21} = 0) are also shown in the figures by the open symbols. The results demonstrate that the w_{21} ratio is an effective parameter determining the mechanical properties of the hydrogels. The fracture stress σ_f of SN hydrogels formed at two different temperatures (25 and 50 °C) and at various cross-linker contents (between 1.9 and 22.4 w/v% EGDE) is between 20-150 kPa (open symbols in Fig. 2.10a). After double networking, σ_f rapidly increases with increasing w_{21} and attains a maximum value of 19.4±0.9 MPa at w_{21} = 49. Further increase in w_{21} ratio again decreases the mechanical strength of the hydrogels up to 1.2±0.2 MPa at w_{21} = 126. Because a very high w_{21} ratio requires a high swelling capacity and thus, a loosely cross-linked HA first-network, crack propagation cannot be prevented during deformation leading to worsening the mechanical performance of DN hydrogels. A similar trend is also observable in the variations of Young's modulus E and fracture strain ε_f of the hydrogels as a function of w_{21} ratio. (Fig. 2.10b & c). We should note that, in classical DN hydrogels prepared from poly(2-acrylamido-2-methylpropanesulfonic acid) (PAMPS) first-network and polyacrylamide second-network, the maximum enhancement in the compressive stress at break occurs when the molar ratio of the second to the first-network is around 20 corresponding to the weight ratio w_{21} of 7 [33]. This means that for the present HA/PDMA double-network system, a much larger amount of the ductile component PDMA ($w_{21} \cong 50$) should be introduced in the first network to achieve the maximum enhancement in the mechanical properties. This feature could be related to the presence of a lesser number of linkages between the 1st and 2nd networks. Previous work shows that the formation of mechanically strong DN hydrogels requires strong chain entanglements or covalent links between the 1st and 2nd polymer networks [32,52,54]. In the case of SN hydrogels formed by vinyl–divinyl monomer copolymerization such as PAMPS hydrogels, the initiator molecules remaining in the first network as well as the pendant vinyl groups of divinyl monomer units are able to form potential cross-linking points between 1st and 2nd networks [54]. However, for the present DN system, HA chains are unable to

covalently link the first to the second network so that a larger amount of PDMA is required to create strong chain entanglements.

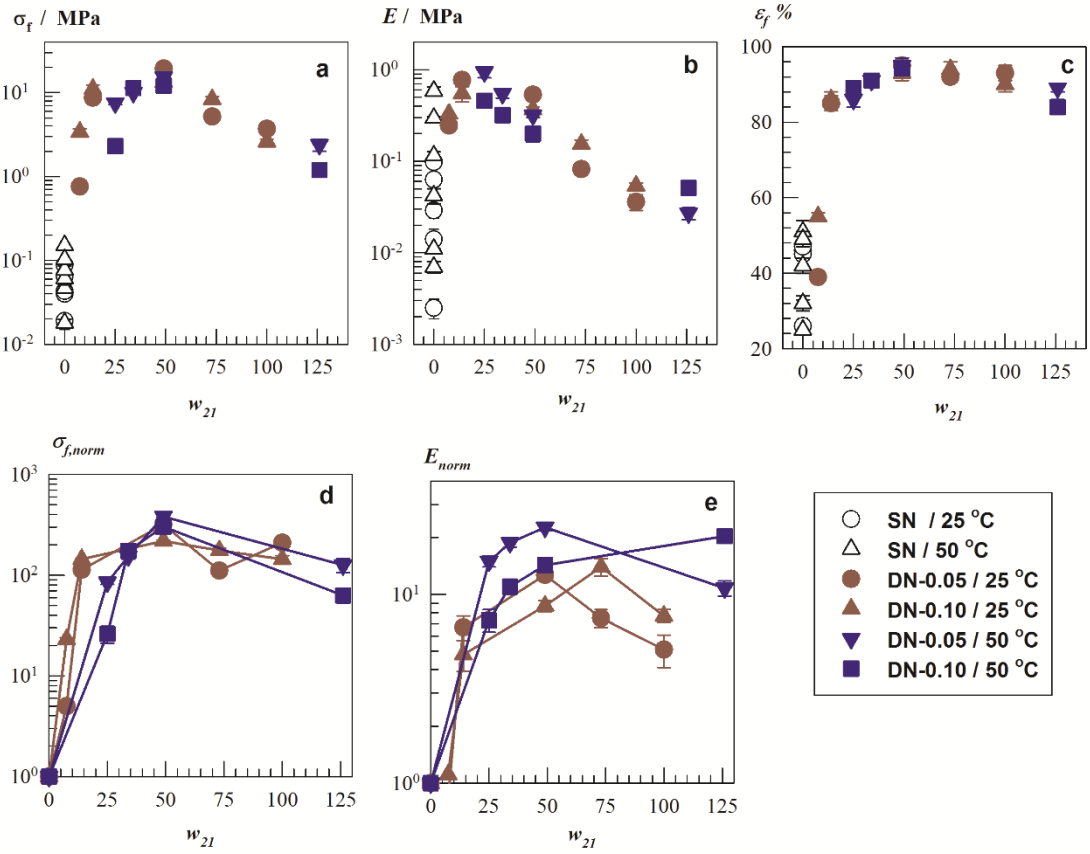

Figure 2.10 : Mechanical properties of DN hydrogels as a function of the w_{21} ratio. (a-c) The fracture stress σ_f (a), Young's modulus E (b), and strain at break ε_f (c) of SN (open symbols) and DN hydrogels (filled symbols) plotted against the w_{21} ratio. (d, e): Normalized fracture stress $\sigma_{f,norm}$ (d), and Young's modulus E_{norm} (e), of the hydrogels plotted against w_{21} ratio. Preparation temperature of HA hydrogel = 25 °C (dark red) and 50 °C (blue). Note that most of the error bars are smaller than the symbols.

We attribute the improvement in the mechanical properties of HA hydrogels after double networking to the higher cross-link density of the first HA network as compared to the second PDMA network. Because the short HA network chains attain a highly stretched conformation upon swelling in the second monomer solution, the resulting DN hydrogel consists of highly stretched HA and randomly coiled PDMA network chains. Thus, the first HA network internally fractures under low stresses by dissipating energy while the second PDMA network keeps the macroscopic gel sample together and prevents macro-crack formation. We have to mention that the mass ratio w_{21} of the second to the first-network achieved using HA hydrogels is much higher as compared to that obtained using GMHA hydrogels (w_{21} = 126 vs 29) [32]. This also

contributes to the mechanical strength of the present hydrogels. Thus, the internal fracture of HA network together with the high mass ratio of the second to the first-network components seem to be responsible for the extraordinary mechanical properties of the hydrogels. To demonstrate this internal fracture, a series of cyclic compression experiments were performed on DN hydrogels. Fig. 2.11a represents stress-strain curves of a DN hydrogel formed at w_{21} = 49 from a compression test composed of five successive cycles up to a maximum compression of 80% (λ_{max} = 0.20). The results are presented as the dependence of the true stress σ_{true} (= $\lambda\sigma_{nom}$) on the compression ratio λ (deformed length/initial length) The loading and unloading curves are indicated by up and down arrows, respectively. The loading path of the first compressive cycle conducted on a fresh hydrogel sample differs from the unloading path indicating damage in the sample and dissipation of energy. The hysteresis energy U_{hys} in this cycle, calculated from the area between the loading and unloading curves, is 220±20 kJ.m^{-3}. However, the following loading/unloading cycles are almost elastic with a small hysteresis area (U_{hys} = 18±1 kJ.m^{-3}), and they all closely follow the path of the first unloading. The results indicate the occurrence of an irrecoverable internal damage during the first compression of the gel sample.

The hysteresis energy U_{hys} can be interpreted as the energy released due to fracture of the first-network during deformation. This fracture can take place in EGDE cross-links as well as in the glycosidic linkages of HA chains. In both cases, breaking of C-O bonds results in a decrease in the effective cross-link density ν_e of the first-network. Thus, U_{hys} is equal to the product of C-O bond energy U_{xl} and the total number of effective cross-links broken down during the compression cycle [36,55], i.e.

$$U_{hys} = U_{xl}\left(\nu_e\ f_v\right) \tag{2.4}$$

where f_v is the fraction of effective cross-links broken during the mechanical cycles. Since C-O bond energy U_{xl} is 360 kJ.mol^{-1} and ν_e = 304±60 mol.m^{-3} (Fig. 2.6f), one may solve eq 2.4 for the fraction f_v of effective cross-links broken during the mechanical cycles in Fig. 2.11a. Calculations show that 25±4% of the cross-links are irreversible broken during the first loading while 2% additional bonds are broken in each of the following loadings.

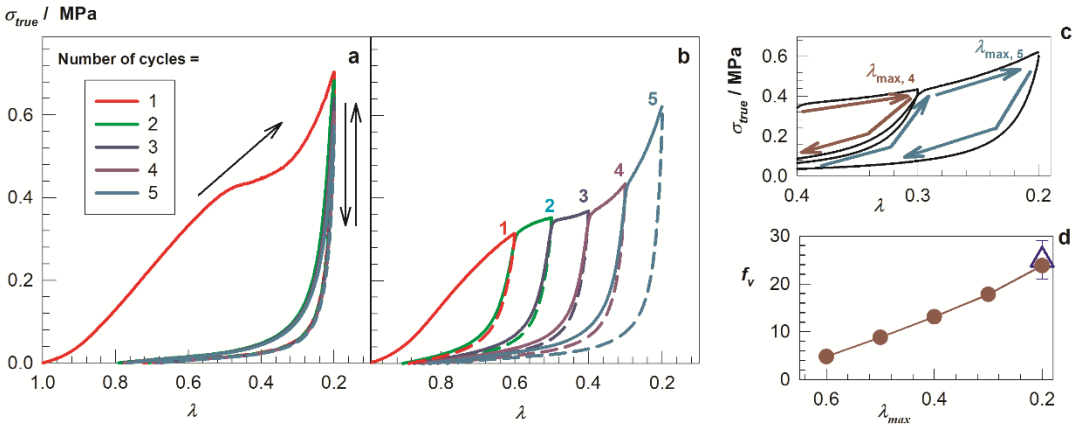

Figure 2.11 : Cyclic mechanical tests of DN hydrogels. (a, b) Typical stress-strain curves of a DN hydrogel from a compression test composed of five successive cycles. The true stress σ_{true} is plotted against the compression ratio λ (deformed length/initial length). The maximum compression was fixed at 80% (λ_{max} = 0.20) in (a) while in (b), it was stepwise increased from 40 to 80% in successive cycles (λ_{max} = 0.60 to 0.20). EGDE = 7.1 w/v%. BAAm = 0.05 w/v%. w_{21} = 49. The up and down arrows in (a) indicate loading and unloading curves, respectively. For clarity, loading and unloading curves are shown by the solid and dashed curves, respectively. (c) A zoom-in to Fig. 2.11b to highlight the damage and elastic regions of the 5th cycle. (d) The fraction f_v of EGDE cross-links broken during the mechanical cycles with increasing maximum compression from 40 to 80% (λ_{max} = 0.60 to 0.20). The open triangle represents the fraction f_v during a one-step mechanical cycle up to 80% compression.

The cyclic tests conducted up to a fixed maximum strain of 80% were repeated with a virgin gel sample with increasing maximum strain from 40 to 80 % in five successive cycles (λ_{max} = 0.6 to 0.2). The results are shown in Fig. 2.11b were the loading and unloading curves are presented by solid and dashed lines, respectively. After the first compressive cycle, each successive loading curve is composed of two regions, as also illustrated in Fig. 2.11c for the cycle 5 ($\lambda_{max,\,5}$ = 0.20). The first region is elastic and it follows the path of the unloading curve of the previous cycle while the second region creates an additional damage by continuing the loading curve of the previous cycle. The transition from the first (elastic) to the second (damage) region always occurred at the maximum strain of the previous cycle. Thus, due to the irreversible damage done during the previous cycle, additional damage only occurs at a higher maximum strain. In Fig. 2.11d, the fraction f_v of cross-links broken are plotted against the maximum strain λ_{max}. The open triangle in the figure represents the fraction f_v of broken cross-links during one-step cycle up to λ_{max} = 0.20 obtained from Fig. 2.11a. Increasing maximum strain also increases the number of broken bonds in the first network. Moreover, compression of the hydrogel sample with successive five-step cycles with

increasing maximum strain up to 80% results in the same number of broken bonds as in a one-step cycle with a maximum strain of 80%. This indicates that the extent of damage in the hydrogels is path-independent and it only depends on the maximum deformation ratio of the network chains.

2.3 Conclusions

We presented a two-step procedure for the preparation of high-strength HA hydrogels starting from native HA. In the first step, HA was cross-linked in aqueous solutions using EGDE cross-linker under various experimental conditions. It was found that EGDE-cross-linked HA hydrogels containing 97-99% water are fragile, and rupture when compressed to 25-51% strain under 0.02-0.15 MPa stresses. By applying the double-network approach in the second step, we were able to generate high strength HA/PDMA double-network hydrogels containing 84-94% water. Tuning the ratio of the network components could result in hydrogels exhibiting a compressive modulus of 0.9 MPa that sustain 19.4 MPa compressive stresses, which are much larger than those reported before for the hydrogels derived from the methacrylated HA macromers. Cyclic mechanical test results indicate that an irrecoverable internal damage occurs in DN hydrogels at compressions as low as 40% at which single-network HA hydrogels visibly rupture. The results indicate that the lightly cross-linked PDMA second-network holds the macroscopic gel sample together by hindering the micro-crack propagation to a macroscopic scale, while the gel sample internally fractures. This internal fracture of HA first-network together with the high mass ratio of the second to the first-network components are responsible for the extraordinary mechanical properties of the hydrogels. HA-based hydrogels presented here with good mechanical properties and high water contents are promising materials to make use the characteristics of HA in stress-bearing biomedical applications.

3. MECHANICALLY STRONG TRIPLE NETWORK HYDROGELS BASED ON HYALURONAN AND POLY(N,N-DIMETHYLACRYLAMIDE)[2]

Hyaluronan, or hyaluronic acid (HA), is a natural polyelectrolyte found in connectivity tissues and composed of repeating disaccharide units of β-1,4-D-glucuronic acid - β-1,3-N-acetyl-D-glucosamine (Figure 3.1) [1]. HA has distinctive biological functions, and therefore has been recognized as a potentially effective biomaterial for soft tissue regeneration [3–6,56]. Because HA is a non gelling macromolecule, it is either chemically modified or covalently cross-linked to generate a less degradable hydrogel for use in biomedical applications [8]. The functional groups in HA available for cross-linking are the hydroxyl and carboxyl groups. Hydroxyl groups may be cross-linked via an ether linkage and carboxyl groups via an ester linkage [9,10,12–15,18]. Methacrylation of HA with glycidyl methacrylate is another strategy for producing photocross-linkable macromers to form functional, cyto-compatible HA hydrogels (Figure 3.1) [21–23].

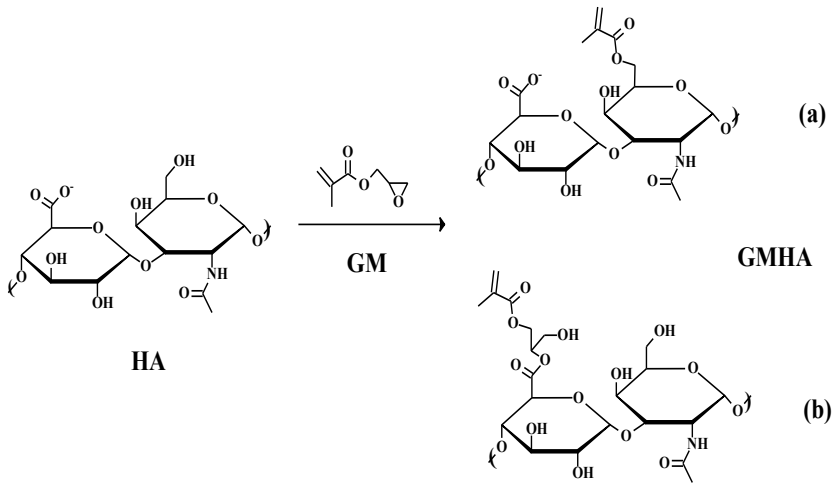

Figure 3.1 : Disaccharide repeat unit of HA and its methacrylation using glycidyl methacrylate (GM) through ring opening (a) and transesterification modes (b) to form methacrylated HA (GMHA).

[2] This chapter is based on the paper "Tavsanli, B. Can, V. Okay, O. (2015). Mechanically strong triple network hydrogels based on hyaluronan and poly(N,N-dimethylacrylamide). *Soft Matter*, 11, 8517-8524."

One limitation of HA hydrogels is that they are very brittle and/or easily dissolve in physiological environments which limit their use in load-bearing applications. This poor mechanical performance of covalently cross-linked HA hydrogels originates from their very low resistance to crack propagation due to the lack of an efficient energy dissipation mechanism in the gel network [16,57]. Weng and co-workers recently reported preparation of HA hydrogels containing 60-90% water and exhibiting a compressive modulus of 0.5 MPa and a fracture stress of 5.2 MPa [31]. The hydrogels were prepared by swelling a highly cross-linked methacrylated HA first network in N,N-dimethylacrylamide (DMA) monomer solution containing a small amount of a chemical cross-linker, and then polymerizing DMA to form a loosely cross-linked poly(N,N-dimethylacrylamide) (PDMA) second network. Thus, the hydrogels consist of interpenetrating brittle (HA) and ductile (PDMA) polymer network components [31]. One may expect that, under large strain, the highly cross-linked, brittle first network breaks up to form many cracks while the second ductile network keeps the gel sample together [58], which seems to be responsible for the improvement in the mechanical performance of brittle HA hydrogels.

The approach mentioned above is the double-network (DN) technique developed by Gong and co-workers in 2003 to prepare mechanically strong hydrogels [33–37,59,60]. DN hydrogels prepared from highly cross-linked poly(2-acrylamido-2-methylpropane sulfonic acid) polyelectrolyte network and linear or loosely cross-linked polyacrylamide exhibit exceptional compressive strengths of about 20 MPa and fracture energies in the hundreds of J m^{-2} [33]. Our preliminary experiments showed that the reduced mechanical performance of DN hydrogels based on HA and PDMA as compared to those reported by Gong *et al*. is due to the lesser degree of swelling of the first network hydrogels reducing the ratio of ductile-to-brittle components. For such cases, we recently developed the triple network (TN) approach to create mechanically strong hydrogels [52]. TN approach bases on the loss of the translational entropy of a second monomer upon its polymerization within the first network. The entropy of second monomer, if polymerized in a first network hydrogel, decreases so that additional solvent (3^{rd} monomer) enters into the gel phase to assume its new thermodynamic equilibrium. This means that DN will swell more than the first network so that triple networks could be prepared [52].

Our aim in the present study is to improve the mechanical performance of DN hydrogels based on HA and PDMA by applying the TN approach. As such biomaterials are non-cytotoxic and highly resistant to biodegradation [31], those with an excellent mechanical performance and a high degree of toughness will be a good candidate for load-bearing biomedical applications such as intervertebral disc prosthesis. As will be seen below, TN hydrogels containing 81-91% water sustain compressive stresses above 20 MPa and exhibit compressive moduli of 1 MPa.

TN hydrogels we described here consist of a highly cross-linked first HA network and loosely cross-linked PDMA as the second and third networks. This paper is organized as follows: Because the equilibrium degree of swelling and the elasticity of the first network significantly affect the mechanical strength of the resulting DN and TN hydrogels [33,52,58], we first describe properties of the first network (or, single network) hydrogels derived from methacrylated HA macromers of various methacrylation degrees. By tuning the methacrylation degree, we were able to generate DN hydrogels exhibiting a fracture stress of around 10 MPa, which is about twice that reported by Weng *et al* [31]. Swelling these double networks in DMA solutions following polymerization of DMA in the gel phase further increases the ratio of ductile-to-brittle components, and thus produces HA/PDMA/PDMA TN hydrogels capable of sustaining above 20 MPa of compressive stress.

3.1 Experimental Part

3.1.1 Materials

The sodium salt of hyaluronic acid (HA) from Streptococcus equi was purchased from Sigma-Aldrich. Glycidyl methacrylate (GM, Sigma Aldrich)), NaOH (Merck), N,N-dimethylacrylamide (DMA, Sigma-Aldrich), N.N′-methylene(bis)acrylamide (BAAm, Merck), triethylamine (TEA, Sigma-Aldrich), tetrabutylammonium bromide (TBAB, Sigma-Aldrich), 1-vinyl pyrrolidone (VP, Sigma-Aldrich) 2-oxoglutaric acid (Fluka), and Irgacure 2959 (Sigma-Aldrich) were used as received.

3.1.2 Methacrylation of HA

Methacrylated HA was prepared according to the following procedure [21–23]: HA (0.5 g) was first dissolved in 50 mL distilled water by gently stirring overnight. Then, *n* mL TEA, *n* mL GM, and *n* g TBAB were added separately in that order, and allowed

to fully mix for 1 h before the next addition. To vary the methacrylation degree of HA, the value *n* was taken as 1, 2, 4, and 8, corresponding to a molar ratio of GM to HA repeat units (n_{GM}/n_{HA}) of 6, 12, 24, and 49, respectively. Following complete dissolution, the reaction mixture was incubated at 55 °C for 1 h. After cooling, the solution was precipitated in acetone and the precipitate was dissolved in 30 mL water. After re-precipitation in acetone and re-dissolving in 10 mL water, it was lyophilized for 3 days to obtain methacrylated HA as a white product. Methacrylation degree of the samples was determined by nuclear magnetic resonance using a 500 MHz Agilent VNMRS spectrometer.

3.1.3 Hydrogel preparation

Single network hydrogels were prepared at 24 °C in aqueous solutions of the methacrylated hyaluronan (GMHA) of various methacrylation degrees using Irgacure 2959 as the initiator, and VP as a reactive comonomer and as a solvent for the initiator [21]. The initial concentration C_1 of GMHA was set to 0.01 and 0.02 g.mL^{-1}. Initiator concentration and the molar ratio of the initiator to VP were fixed at 2.2 wt.% (with respect to GMHA) and 0.012, respectively. Typically, GMHA (40 mg) was dissolved in 2 mL of distilled water overnight under continuous stirring. Then 34.2 μL of the initiator solution prepared by dissolving Irgacure 2959 (260 mg) in 10 mL of VP were added, and the reaction solution was transferred into plastic syringes to conduct the photopolymerization under UV light at 365 nm for 24h.

DN hydrogels were prepared by swelling the first network hydrogels in the 2nd DMA - BAAm solutions of concentration C_2 between 0.10 and 0.50 g.mL^{-1}, and photopolymerizing using 2-oxoglutaric acid initiator (0.1 mol% of DMA) at 24 °C. For this purpose, the first network hydrogel just after preparation (about 0.5 g) was immersed in 30 mL of 2nd monomer solution containing DMA, BAAm, and the initiator. After reaching the swelling equilibrium, which required about 4 days, the monomer + initiator solution containing the first network hydrogel was transferred into plastic syringes of 50 mL in volume and the photopolymerization was conducted under UV light at 365 nm for 24 h. We have to mention that due to the large volume of the 2nd DMA-BAAm solution as compared to the swollen SN hydrogel (30 mL vs 1-2 mL), the hydrogel is not in contact with the surface of the syringe and thus, the surface effects can be neglected. DN hydrogel was then separated by stripping off the external

loosely cross-linked 2nd PDMA hydrogel. TN hydrogels were prepared similar to DN hydrogels by swelling DN hydrogels in the 3rd DMA – BAAm solutions of concentration C_3 between 0.10 and 0.30 g.mL^{-1}, and photopolymerizing using 0.1 mol% 2-oxoglutaric acid initiator at 24 °C. Preparation conditions of SN, DN, and TN hydrogels are tabulated in Table 3.1 and 3.2.

3.1.4 Swelling and gel fraction measurements

Single network, DN, and TN hydrogel samples were immersed in a large excess of water or monomer solutions for at least 6 days by replacing solution every other day to extract any soluble species. The swelling equilibrium was tested by weighing the gel samples. All the synthesized gel samples in both as-prepared and equilibrium swollen states were transparent, indicating no macroscopic phase separation, and complete miscibility between the network components (Fig. 3.2A). The equilibrium relative weight swelling ratio $m_{rel,i}$, where the subindex i = 1, 2, and 3 stands for the first-, double-, and triple network hydrogels, respectively, was calculated as:

$$m_{rel,i} = m/m_o \tag{3.1}$$

where m is the mass of the equilibrium swollen gel sample, and m_o is its mass after preparation.

To determine the gel fraction, the equilibrium swollen gel samples were taken out of water and dried at 80 °C under vacuum to constant mass. The gel fraction W_g, that is, the conversion of monomers to the cross-linked polymer (mass of water-insoluble polymer / initial mass of the monomer in the 1st, 2nd, and 3rd monomer solutions) was calculated from the masses of dry polymer network and from the comonomer feed. W_g was found to be close unity for all first network, DN and TN hydrogels formed at various combinations.

3.1.5 Mechanical tests

Uniaxial compression measurements were performed on equilibrium swollen hydrogels at 24 °C on a Zwick Roell test machine using a 500 N load cell. Single network, DN, and TN hydrogels after equilibrium swelling in water were cut into cubic samples with the dimensions 3x3x3 mm. Before the test, an initial compressive contact to 0.01 N was applied to ensure a complete contact between the gel and the plates. Preliminary experiments showed that the use of Paraffin oil as lubricant to reduce

friction and adhesion between the plates and the gel surface is not necessary and the deviations of the data with and without use of Paraffin oil are within the limit of experimental error. The tests were conducted at a constant crosshead speed of 0.3 and 1 mm.min^{-1} below and above 15% compression, respectively. Load and displacement data were collected during the experiment. Compressive stress was presented by its nominal σ_{nom} and true values σ_{true} (= λ σ_{nom}), which are the forces per cross-sectional area of the undeformed and deformed gel specimen, respectively, and λ is the deformation ratio (deformed length/initial length). The compressive strain ε is defined as the change in the length relative to the initial length of the gel specimen, i.e., $\varepsilon = 1 - \lambda$. The strain is also given by the biaxial extension ratio λ_{biax} (=$\lambda^{-0.5}$) [36]. The Young's modulus E was calculated from the slope of stress-strain curves between 5 and 15% compressions. Cyclic compression tests were conducted at a constant crosshead speed of 1 mm.min^{-1} to a maximum strain ε_{max}, followed by retraction to zero force and a waiting time of 1 min, until the next cycle of compression. For reproducibility, at least five samples were measured for each gel and the results were averaged.

3.1.6 Calculations of the fracture stress and fracture strain

Since compression tests for soft materials are easier to perform and yield more consistent results than tensile tests, we conducted uniaxial compression measurements. We report here nominal stress values to make the results comparable to those of Weng *et al* [31]. Fig. 3.2B shows typical stress-strain curves of a DN hydrogel as the dependences of nominal σ_{nom} (dark red, solid curves) and true stresses σ_{true} (dark blue, dashed curves) on the compressive strain ε. Results of two samples from the same gel are shown in the figure. The inset is a zoom-in to the large strain region, i.e., between 85 and 99% compressions. The fracture stresses σ_f of the two samples obtained from σ_{nom} vs ε curves are 20 and 23 MPa at strains ε_f of 96.8 and 97.7%, respectively. Thus, the gel samples apparently sustain about 20 MPa stresses at 97% compression. However, when plotted the corresponding true stresses σ_{true} against ε (dashed curves), maxima in the stress-strain curves appear earlier, i.e., at much lower compressions (ε_f = 93.5 %). This indicates the onset of a microscopic failure in the samples which is not detectable in σ_{nom} vs ε plots. The arrows shown in the inset to Fig. 3.2B illustrate calculation of the real fracture stress from the maxima in σ_{true} vs ε curves. After such corrections conducted on 6 stress-strain curves, it was found that this DN hydrogel

sustains 12 ± 2 MPa stresses at 93.4 ± 0.9% compression. Noting that, without this correction, as repeatedly reported in the literature, the fracture stress of this hydrogel is around 20 MPa. In the following, we only report the corrected fracture stresses and strains of the hydrogels.

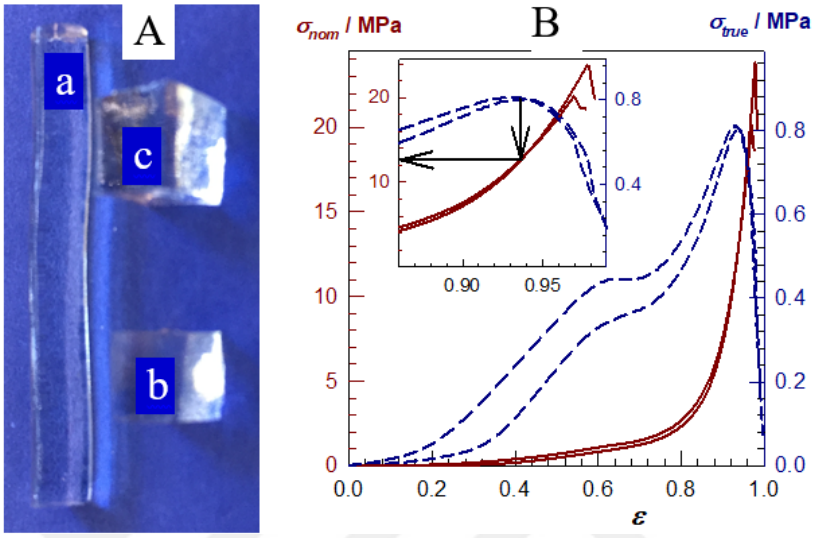

Figure 3.2 : Optical images of the first network (a), DN (b), and TN hydrogels (c) in equilibrium with water. The hydrogels were derived from 4% methacrylated HA. C_1 = 0.02 g.mL^{-1}. $C_2 = C_3$ = 0.30 g.mL^{-1}. BAAm = 0.05 mol%. **(B):** Typical stress-strain curves of a DN hydrogel under compression as the dependences of nominal σ_{nom} (dark red curves) and true stresses σ_{true} (dark blue curves) on the compressive strain ε. Results of two samples from the same gel are shown. The inset is a zoom-in to the large strain region. The arrows illustrate the calculation of real fracture stress from the maxima in σ_{true} vs ε curves. Gel synthesis conditions: DM = 4%. C_1 = 0.02 g.mL^{-1}. C_2 = 0.30 g.mL^{-1}. BAAm = 0.05 mol%. w_{21} = 29.

3.2 Results and Discussion

3.2.1 Single network hydrogels

Methacrylated hyaluronan (GMHA) of various degrees of methacrylation was used as a photocross-linkable macromer for the preparation of the single network hydrogels. The macromer GMHA was prepared by methacrylation of hyaluronan (HA) using glycidyl methacrylate (GM) in aqueous solutions. The reaction mechanism is quite complex and involves transesterification and ring opening modes to form GMHA (Fig. 3.1) [21–23]. GM attacks both the hydroxyl groups on the N-acetyl-D-glucosamine ring via opening of the epoxide group, and the carboxylate group on the glucoronic acid ring via transesterification. Methacrylate groups are thus incorporated pendant to HA molecules of molecular weight around 1.2x10^6 g.mol^{-1} [18]. Different degrees of

methacrylation were achieved by tuning the molar ratio (n_{GM}/n_{HA}) of glycidyl methacrylate to hyaluronan in the feed. Fig. 3.3 shows ^{1}H NMR spectrum of GMHA prepared at n_{GM}/n_{HA} = 49. The inset shows 5.1 – 5.6 ppm region of the spectra of GMHA samples prepared at various n_{GM}/n_{HA} ratios, and native HA (n_{GM}/n_{HA} = 0) as control. Compared to native HA, GMHA shows two new peaks at 5.2 and 5.5 ppm due to the methacrylate groups [22]. The degree of methacrylation (DM) was determined by integration the methyl peak of HA at 1.9 ppm and the methacrylate peaks. The results collected in the first two columns of Table 3.3 reveal that increasing n_{GM}/n_{HA} from 6 to 49 also increases the degree of methacrylation (DM) of GMHA from 4 to 25%.

Table 3.1 : Preparation conditions and mechanical data of SN and DN hydrogels. C_1 = 0.02 g.mL^{-1}. DN hydrogels were prepared without and with 0.05 mol % BAAm crosslinker in the 2nd monomer solution. Blue and red rows represent data for SN and DN hydrogels, respectively.

SN hydrogels	DN Hydrogels			Mechanical data	
DM [a]	C_2 [b]	BAAm % [c]	w_{21} [d]	σ_f [e] / MPa	ε_f [f] / %
4	0	0	0	0.024 (0.005)	43
4	0.10	0	13	0.03 (0.01)	38
4	0.10	0.05	13	11 (1)	94
4	0.30	0	29	0.07 (0.01)	36
4	0.30	0.05	29	12 (2)	93
14	0	0	0	0.050 (0.002)	45
14	0.10	0	6	0.16 (0.03)	40
14	0.10	0.05	6	6.2 (0.8)	92
14	0.30	0	15	0.4 (0.1)	34
14	0.30	0.05	15	6.7 (0.5)	88
25	0	0	0	0.026 (0.009)	34
25	0.10	0	8	0.1 (0.01)	52
25	0.10	0.05	8	3.1 (0.4)	77
25	0.30	0	15	0.3 (0.05)	53
25	0.30	0.05	15	9.4 (1)	90

[a] Methacrylation degree of GMHA (in %) formed at various n_{GM}/n_{HA} ratios, [b] DMA concentration in the 2nd monomer solution (in g.mL^{-1}), [c] BAAm concentration in the 2nd monomer solution (in mol %), [d] the mass ratio of the second to the first network units, [e] fracture stress, [f] strain at break. Standard deviations in parentheses.

Table 3.2 : Preparation conditions, mechanical data, and water contents of SN, DN, and TN hydrogels. $C_1 = 0.02$ g.mL^{-1}. DN hydrogels were prepared with 0.05 mol % BAAm crosslinker in the 2nd monomer solution. Blue, red, and white rows represent data for SN, DN, and TN hydrogels, respectively.

SN hydrogels	DN hydrogels		TN Hydrogels			Mechanical data		Water
DM [a]	C_2 [b]	w_{21} [c]	C_3 [d]	BAAm % [e]	$w_{32/1}$ [f]	σ_f [g] / MPa	ε_f [h] / %	content (%)
4	0	0	0	0	0	0.024 (0.005)	43	99.5
4	0.10	13	0	0	13	11 (1)	94	95
4	0.10	13	0.10	0.05	29	11.2 (0.7)	93	89
4	0.10	13	0.30	0.05	101	15 (3)	93	85
4	0.10	13	0.10	0	27	8.4 (0.8)	95	88
4	0.10	13	0.30	0	45	8.8 (0.7)	95	83
4	0.30	29	0	0	29	12 (2)	93	88
4	0.30	29	0.30	0.05	106	22 (5)	96	84
4	0.30	29	0.30	0	115	2 (0.4)	87	84
14	0	0	0	0	0	0.050 (0.002)	45	99.2
14	0.10	6	0	0	6	6.2 (0.8)	92	90
14	0.10	6	0.10	0.05	22	18 (2)	92	91
14	0.10	6	0.30	0.05	36	12 (2)	91	82
14	0.10	6	0.10	0	18	5.6 (0.5)	92	88
14	0.10	6	0.30	0	27	8.5(0.7)	95	84

Table 3.2 (continued) : Preparation conditions, mechanical data, and water contents of SN, DN, and TN hydrogels. C_1 = 0.02 g.mL^{-1}. DN hydrogels were prepared with 0.05 mol % BAAm crosslinker in the 2nd monomer solution. Blue, red, and white rows represent data for SN, DN, and TN hydrogels, respectively.

SN hydrogels	DN hydrogels		TN Hydrogels			Mechanical data		Water
DM [a]	C_2 [b]	w_{21} [c]	C_3 [d]	BAAm % [e]	$w_{32/1}$ [f]	σ_f [g] / MPa	ε_f [h] / %	content (%)
25	0	0	0	0	0	0.026 (0.009)	34	99.3
25	0.10	8	0	0	8	3.1 (0.4)	77	94
25	0.10	8	0.10	0.05	22	11.1 (1)	92	86
25	0.10	8	0.30	0.05	46	16.3 (2)	94	80
25	0.10	8	0.10	0	21	10.7 (1)	94	89
25	0.30	15	0.30	0	15	9.4 (0.8)	90	89
25	0.30	15	0	0,05	26	15.7 (2)	93	85
25	0.30	15	0.30	0.05	65	17.2 (1)	94	81
25	0.30	15	0.30	0	43	10.1 (1)	92	87
25	0.30	15	0	0	70	8.9 (0.8)	93	78

[a] Methacrylation degree of GMHA (in %) formed at various n_{GM}/n_{HA} ratios, [b] DMA concentration in the 2nd monomer solution (in g.mL^{-1}), [c] the mass ratio of the second to the first network units, [d] DMA concentration in the 3rd monomer solution (in g.mL^{-1}), [e] BAAm concentration in the 3rd monomer solution (in mol %), [f] the mass ratio of the second and third to the first network units, [g] fracture strain, [h] strain at break. Standard deviations in parentheses while for water contents; they are less than 5

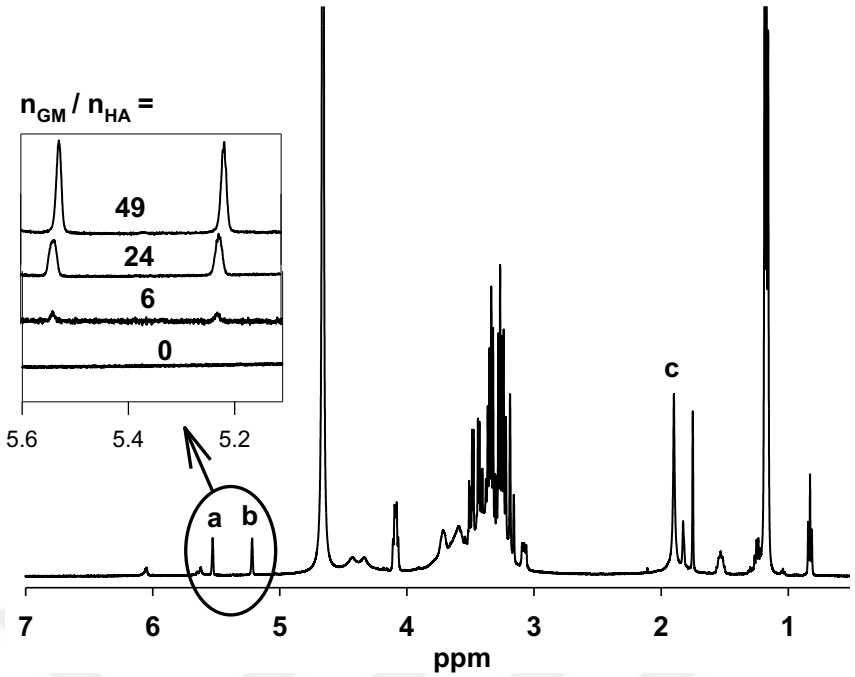

Figure 3.3 : ^{1}H NMR spectrum of GMHA prepared at n_{GM}/n_{HA} = 49. The inset shows 5.1 – 5.6 ppm region of the spectra of GMHA samples prepared at various n_{GM}/n_{HA} ratios together with native HA (n_{GM}/n_{HA} = 0) as control. Peaks at 5.5 and 5.2 denoted by *a* and *b* are indicative of methacrylate groups. HA methyl peak denoted by *c* is shown at 1.9 ppm.

GMHA macromers of various methacrylation degrees were photopolymerized at a concentration C_1 of 0.02 g.mL^{-1} using Irgacure 2959 as the initiator. All the single network hydrogels were insoluble in water with a gel fraction of unity. In Fig. 3.4A and B, the swelling degree m_{rel1} of the hydrogels and their Young's moduli E are plotted against the methacrylation degree (DM) of GMHA. Assuming a tetrafunctional phantom network, Young's modulus E is related to the effective cross-link density ν_e of the hydrogels by [49]:

$$E = 1.5\nu_e RT\left(\nu_2\right)^{1/3}\left(\nu_2^0\right)^{2/3} \tag{3.2}$$

where ν_2^0 and ν_2 are volume fractions of cross-linked GMHA at the gel preparation ($\cong$ 0.02), and in equilibrium with water ($\cong \nu_2^0/m_{rel1}$), respectively, R and T are in their usual meaning.

Table 3.3 : Characteristic data for SN and DN hydrogels

n_{GM} / n_{HA}	DM[a]	Water %[b]	E[c] / kPa		
			SN	DN[d]	DN[e]
6	4 (1)	99.5	17 (3)	211 (22)	370 (35)
12	8 (2)	99.5	48 (5)	305 (32)	549 (54)
24	14 (2)	99.2	52 (7)	611 (10)	409 (46)
49	25 (4)	99.3	28 (4)	224 (46)	442 (52)

[a] Methacrylation degree of GMHA (in %) formed at various n_{GM}/n_{HA} ratios, [b] water content of SN hydrogels, [c] Young's moduli of SN and DN hydrogels, [d] C_2 = 0.10 g.mL^{-1}, and [e] C_2 = 0.30 g.mL^{-1}. (Standard deviations in parentheses while for water contents; they are less than 5%.)

Open symbols in Fig. 3.4B show the cross-link density ve of the hydrogels plotted against DM. The lowest cross-link density ve and thus, the highest swelling ratio was obtained at 4% DM, i.e., at the lowest degree of methacrylation. v_e first increases with increasing DM but then decreases, which is attributed to the favourable intramolecular cross-linking reactions at high local concentration of methacrylate groups decreasing the number of effective cross-links [61]. Moreover, increasing monomer (DMA) concentration in the external solution decreases the swelling ratio of the hydrogels due to the osmotic pressure of DMA molecules in the external solution. Single network (SN) hydrogels were also subjected to uniaxial compression tests. Typical stress-strain curves of the hydrogels are shown in Fig. 3.5A where the nominal stress σnom is plotted against the compressive strain ε. In Fig. 3.5B, the fracture stress σ_f of the

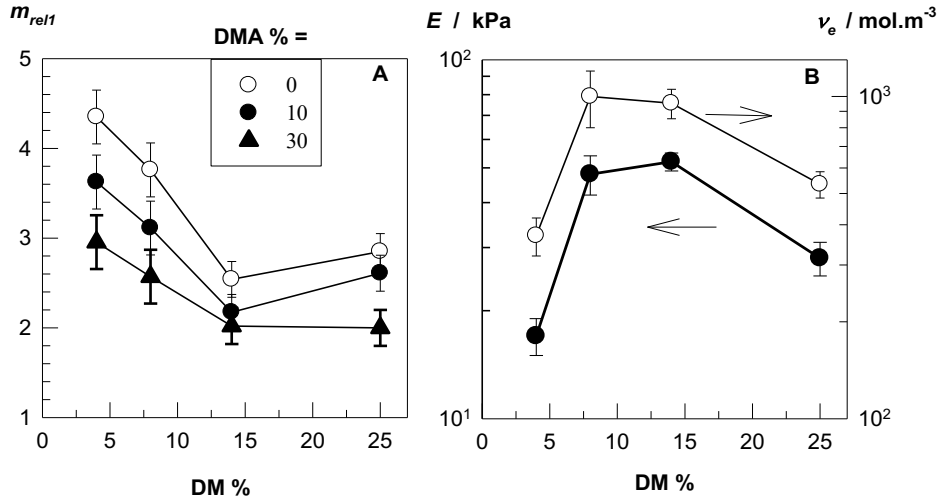

Figure 3.4 : The swelling degrees m_{rel1} of SN hydrogels in water and in DMA solutions (A), and their Young´s moduli E in equilibrium swollen state in water (filled symbols, B) both plotted against the methacrylation degree (DM) of GMHA. Open symbols in B show the cross-link density v_e of the hydrogels calculated using eqn (2) plotted against DM. C_1 = 0.02 g.mL^{-1}.

hydrogels is plotted against DM. The fracture stress σ_f of SN hydrogels is between 0.02 and 0.05 MPa while their fracture strains ε_f are around 0.4, i.e., the hydrogels rupture at around 40% compressions. This poor mechanical performance of SN hydrogels is typical for classical, chemically cross-linked hydrogels due to the lack of an efficient energy dissipation mechanism.

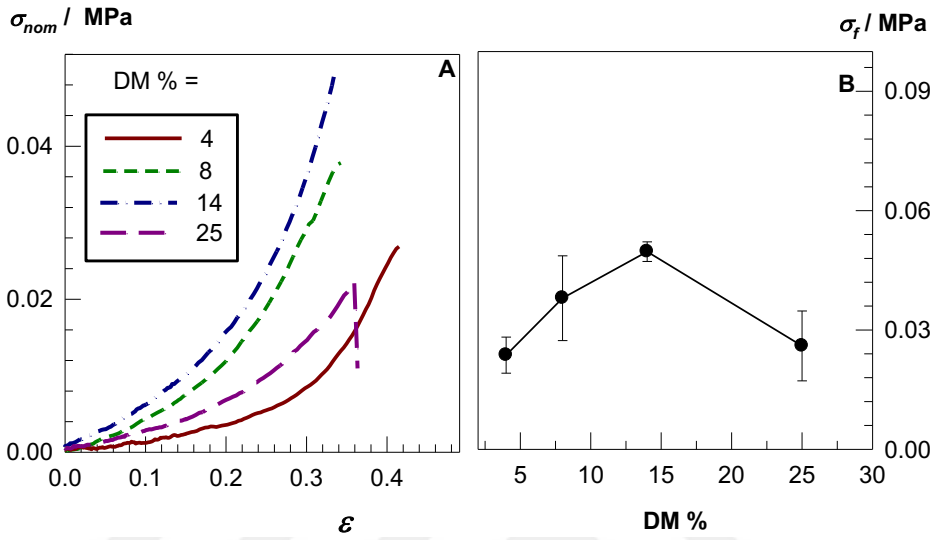

Figure 3.5 : (A): Typical stress-strain curves of SN hydrogels formed from GMHA macromers of various methacrylation degrees (DM) as indicated. C_1 = 0.02 g.mL^{-1}. (B): The fracture stress σ_f of SN hydrogels plotted against DM.

3.2.2 Double- and triple-network hydrogels

DN hydrogels were prepared by swelling SN hydrogels in DMA solutions containing the cross-linker BAAm and the initiator 2-oxoglutaric acid, following photopolymerization. DN hydrogels in equilibrium with water contained 87-95% water. We first fixed the methacrylation degree of GMHA at 4% while the cross-linker (BAAm) concentration in the second monomer solution was varied. Fig. 3.6A shows typical compressive stress-strain curves of SN (solid curves) and DN hydrogels (dashed curves) formed in DMA solutions at a concentration C_2 of 0.10 and 0.30 g.mL^{-1}, containing various amounts of BAAm. In Fig. 3.6B, the fracture stress σ_f and strain at break ε_f are plotted against BAAm concentration. In the absence of a cross-linker, the fracture stress of SN hydrogels slightly increases from 0.03 to 0.07 MPa after double networking (see the inset to Fig. 3.6A), while after addition 0.05 mol% BAAm cross-linker in the DMA solution, σ_f increases dramatically and becomes 12 ± 2 MPa at a DMA concentration C_2 of 0.30 g.mL^{-1}. The fracture strain also increases from 40 to 94% compression. Further increase of the cross-linker content again decreases σ_f of

DNs. This result highlights importance of the presence of a small amount of a chemical cross-linker in the second network solution. Previous work indeed shows that formation of mechanically strong DN hydrogels requires strong chain entanglements or covalent links between the 1st and 2nd polymer networks [31,33,58]. In case of SN hydrogels formed by vinyl-divinyl monomer copolymerization, no additional cross-linker was needed in the second network solution [52]. This is due to the initiator molecules remaining in the first network as well as the pendant vinyl groups of divinyl monomer units acting as potential cross-link points between 1st and 2nd networks [52]. For the present DN system, methacrylate groups of GMHA macromer seem to be sterically unable to effectively link the first to the second network in the absence of a chemical cross-linker. This could be related to the high molecular weight of HA (1.2 x10^6 g.mol^{-1}) [18] and thus, high viscosity of the gelation solutions.

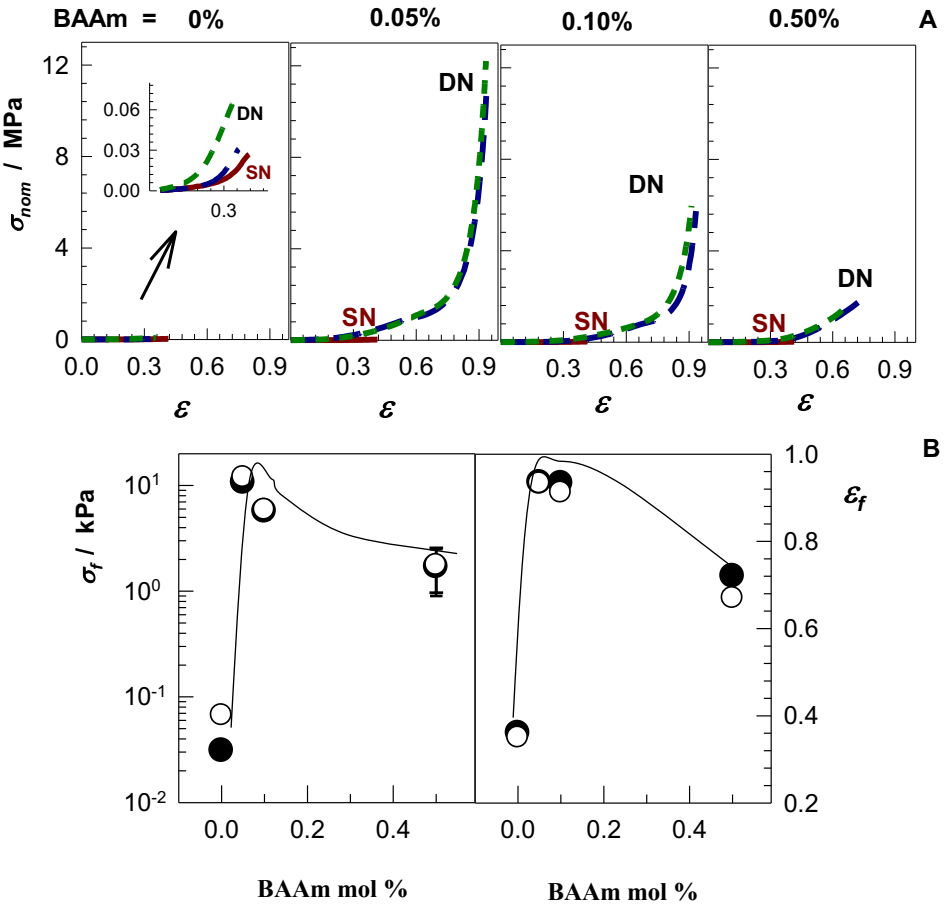

Figure 3.6 : (A): Compressive stress-strain curves of SN (solid curves) and DN hydrogels (dashed curves) formed from 4% methacrylated HA. C_1 = 0.02 g.mL^{-1}. C_2 = 0.10 (long dashed blue curves) and 0.30 g.mL^{-1} (short dashed green curves). (B): The fracture stress σ_f and strain ε_f of DN hydrogels plotted against BAAm concentration. C_1 = 0.02 g.mL^{-1}. C_2 = 0.10 (●) and 0.30 g.mL^{-1} (❍). Note that most of the error bars are smaller than the symbols.

As a next step, we fixed the cross-linker content at 0.05 mol% while the degree of methacrylation (DM) of GMHA was varied. Fig. 3.7 shows the stress – strain curves of SN (solid curves) and DN hydrogels formed at DM = 4, 14, and 25% (dashed curves). DN hydrogels were prepared by swelling SN hydrogels in DMA solutions of concentration C_2 = 0.10 and 0.30 g.mL^{-1} containing 0.05 mol% BAAm cross-linker. SN hydrogels formed from GMHA with the lowest methacrylation degree (4%) produces DNs with the highest fracture stresses, e.g., 11 ± 1 and 12 ± 2 MPa at C_2 = 0.10 and 0.30 g.mL^{-1}, respectively, while increasing methacrylation degree of GMHA deteriorates the mechanical performances of DN hydrogels. In the pioneering work by Weng and co-workers on hyaluronan based DNs [31], the maximum fracture stress achieved was 5.2 MPa which was obtained using methacrylated hyaluronan with DM of 10%. Thus, the results in Fig. 3.7 indicate that decreasing methacrylation degree down to 4% results in a 2.3-fold increase in the mechanical strength of DN hydrogels.

What is the reason for this improvement? Previous work shows that the molar or mass ratio of the second to the first network units is an important parameter determining the mechanical strength of DN hydrogels [33]. An extraordinary mechanical performance requires a high concentration of the second network as compared to the first one, i.e., a high ratio of these networks. For the present DN system, the mass ratio w_{21} of the second to the first network units can be estimated by [52]:

$$w_{21} = \frac{(m_{rel1} - 1) C_2}{C_1} \tag{3.3}$$

In Fig. 3.7, w_{21} ratios of DN hydrogels are indicated next to the curves within parenthesis. Because of the relatively high swelling ratio m_{rel1} of SN hydrogel formed using 4% methacrylated hyaluronan (Fig. 3.4A), it produces DN hydrogel with the highest w_{21} ratio so that the maximum improvement in the mechanical performance was achieved. Young's modulus E of the hydrogels also increased significantly after double-networking at C_2 = 0.10 and 0.30 g.mL^{-1} (Table 3.3). For instance, SN hydrogels formed using 4% methacrylated hyaluronan exhibit a Young's modulus of 17 kPa, while after double-networking at C_2 = 0.30 g.mL^{-1}, it increases to 370 kPa. The drastic increase of the modulus E upon formation of double network structures indicates a high degree of physical and chemical connectivity between the network components of DN hydrogels.

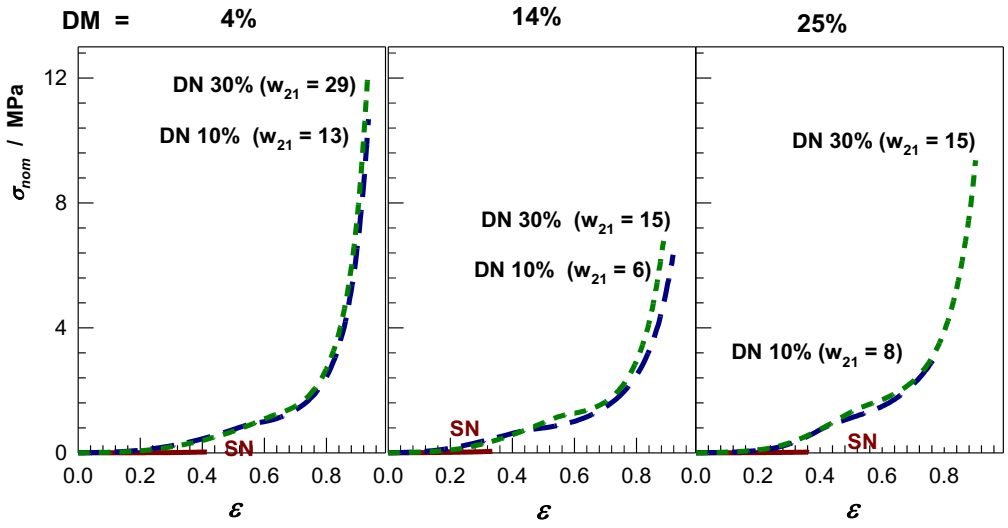

Figure 3.7 : Compressive stress-strain curves of SN (solid curves) and DN hydrogels (dashed curves) formed from HA with various degrees of methacrylation (DM), as indicated. C_1 = 0.02 g.mL^{-1}. C_2 = 0.10 (long dashed blue curves) and 0.30 g.mL^{-1} (short dashed green curves). BAAm = 0.05 mol%. w_{21} ratios calculated using eqn (3) are also indicated in the figures.

DN hydrogels were also prepared starting from SN hydrogels formed at a lower GMHA concentration (C_1 = 0.01 instead of 0.02 g.mL^{-1}). However, no further improvement in the mechanical properties was observed due to the limiting value of w_{21} ratio (Fig. 3.8 – 3.10). Because the key to obtain mechanically strong hydrogels is to increase the ratio of ductile-to-brittle network components, we used triple-network (TN) approach developed recently in our group [52]. Thus, DN hydrogels were first swollen in DMA solutions containing the cross-linker BAAm (0.05 mol%) and the initiator until equilibrium is reached, following photopolymerization to obtain TN hydrogels. The relative swelling ratios m_{rel2} of DN hydrogels in water and in DMA solutions were between 1.4 and 2.9. For a given methacrylation degree of GMHA, m_{rel2} increased with increasing w_{21} ratio of the DNs (Table 3.2). Increasing w_{21} ratio means that larger amount of the second monomer (DMA) is polymerized during the formation of DN hydrogels. Consequently, a larger decrease in the entropy occurs due to the monomer-to-polymer conversion within the gel phase so that more DMA solution can enter into the DN hydrogel leading to larger m_{rel2} values. The mass ratio $w_{32/1}$ of the second and third to the first network units was estimated as [52]:

$$w_{32/1} = \frac{m_{rel1}\left(m_{rel2}-1\right)C_3 + \left(m_{rel1}-1\right)C_2}{C_1} \qquad (3.4)$$

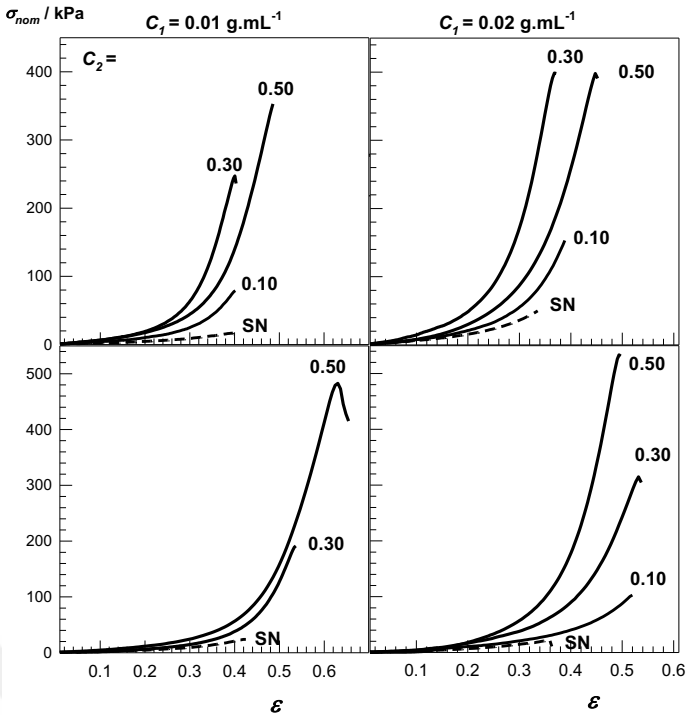

Figure 3.8 : Compressive stress-strain curves of SN and DN hydrogels formed from 14 (upper panel) and 25% methacrylated HA (bottom panel). C_1 = 0.01 (left) and 0.02 g.mL^{-1} (right). DN hydrogels were prepared without use of a chemical cross-linker in DMA solutions at a concentration (C_2) of 0.10, 0.30, and 0.50 g.mL^{-1}, as indicated.

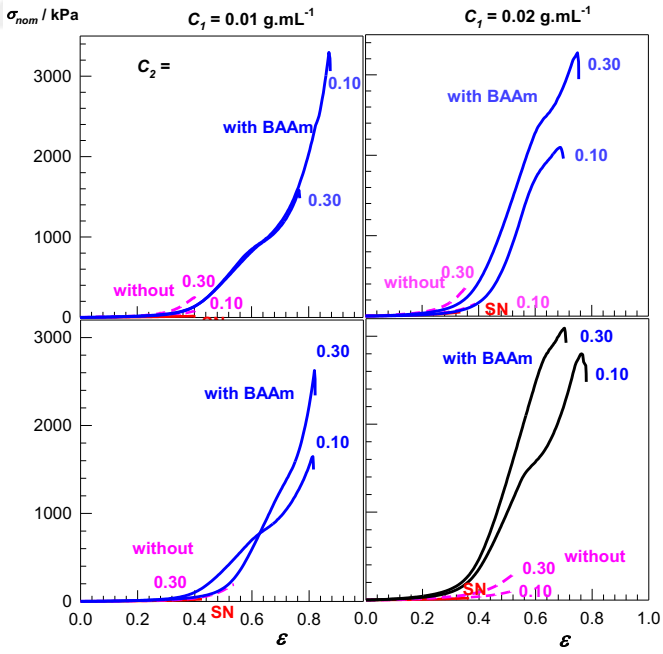

Figure 3.9 : Compressive stress-strain curves of SN and DN hydrogels formed from 14 (upper panel) and 25% methacrylated HA (bottom panel). C_1 = 0.01 (left) and 0.02 g.mL^{-1} (right). DN hydrogels were prepared without and with 0.1 mol% BAAm cross-linker in in DMA solutions at a concentration C_2 of 0.10 and 0.30 g.mL^{-1}, as indicated.

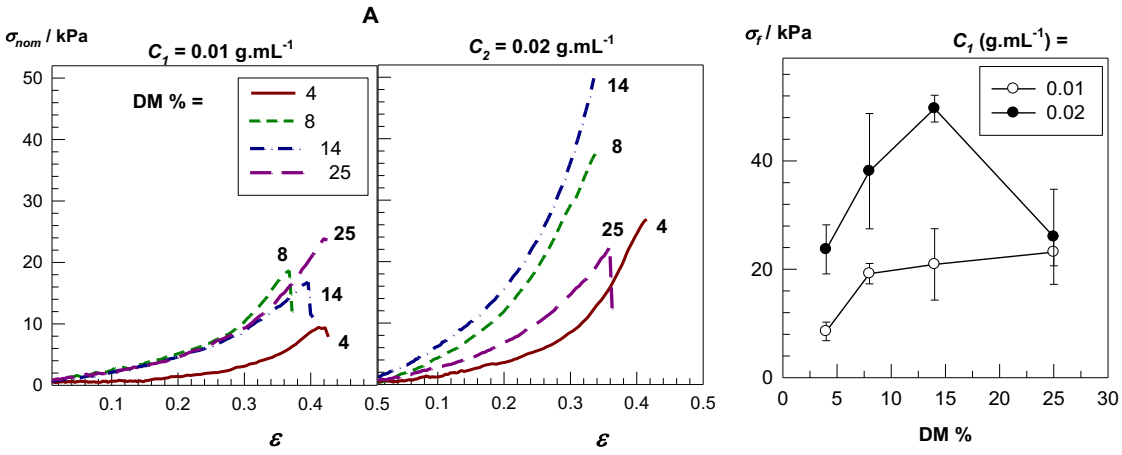

Figure 3.10 : (A): Compressive stress-strain curves of SN hydrogels formed GMHA macromer of various methacrylation degrees DM as indicated. C_1 = 0.01 (left) and 0.02 g.mL^{-1} (right). (B): Fracture stress of SN hydrogels plotted against the degree of methacrylation DM of the macromer.

The mass ratio $w_{32/1}$ of the second + third to the first polymer units was varied by changing DMA concentration C_3 in the 3rd monomer solution at a fixed w_{21} ratio of DN's. Similar to DN hydrogels, the gel fraction Wg was close to unity for all TN hydrogels formed at various $w_{32/1}$ ratios. In the swollen state, TN hydrogels contained 81 to 91% water; similar to the DN's, the swelling ratio m_{rel3} of TN hydrogels in water increased with increasing $w_{32/1}$ ratio (Table 3.5). This also means that quadruple-network hydrogels could also be prepared by swelling TNs in a 4th monomer solution.

Table 3.4 : Equilibrium swelling ratio m_{rel2} of DN hydrogels in water and DMA solutions. The hydrogels were prepared at various w_{21} ratios. SN hydrogels were prepared from GMHA of various methacrylation degrees (DM) indicated. Standard deviations for DM values are given in the parenthesis, while for the swelling ratios; they are less than 10 %.

DM %	w_{21}	m_{rel2}		
		water	10% DMA	30% DMA
4 (1)	13	1.4	2.0	1.6
	29	2.4	2.4	2.4
8 (2)	11	1.8	-	-
	24	2.4	-	-
14 (2)	6	1.4	1.8	1.5
	15	2.1	-	-
25 (4)	8	1.8	2.2	2.1
	15	2.7	2.9	2.6

Table 3.5 : Equilibrium swelling ratio m_{rel3} of TN hydrogels in water. The hydrogels were prepared at various w_{21} and $w_{32/1}$ ratios. SN hydrogels were prepared from GMHA of various methacrylation degrees (DM) indicated. Standard deviations for DM values are given in the parenthesis, while for the swelling ratios, they are less than 10 %.

DM %	w_{21}	$w_{32/1}$	m_{rel3}
4 (1)	13	29	1.8
		101	2.6
4 (1)	29	60	1.6
		106	3.1
14 (2)	6	22	1.9
		36	2.7
25 (4)	8	22	1.5
		46	2.5
25 (4)	15	26	1.4
		65	2.6

Fig. 3.11A and B show stress-strain curves of DN (solid curves) and TN hydrogels (dashed curves) formed from 4% methacrylated hyaluronan. Hydrogel samples are denoted in the figures as DN-x or TN-y, where x and y are w_{21} and $w_{32/1}$ ratios, respectively. The fracture stresses σ_f of DN hydrogels formed at w_{21} = 13 and 29 are 11 ± 1 and 12 ± 2 MPa, respectively. σ_f further increases to 15 ± 3 and 22 ± 5 MPa after triple-networking at $w_{32/1}$ ratios of 101 and 106, respectively. These values are the highest fracture stresses for such hydrogels reported so far in the literature. Thus, TN synthesis starting from the DN's leads to 4- to 8-fold increase in the mass ratio of ductile-to-brittle network components ($w_{32/1}$ / w_{21}), and produces hydrogels exhibiting very high fracture stresses. The results also show that the mechanical performance of DN hydrogels could be further strengthened by incorporation of additional ductile component (loosely cross-linked PDMA) via TN approach. Noting that, as in the case of DNs, no improvement in the mechanical performances of DN hydrogels was observed if the cross-linker BAAm is not included into the third monomer solution (Table 3.2, Fig. 3.12).

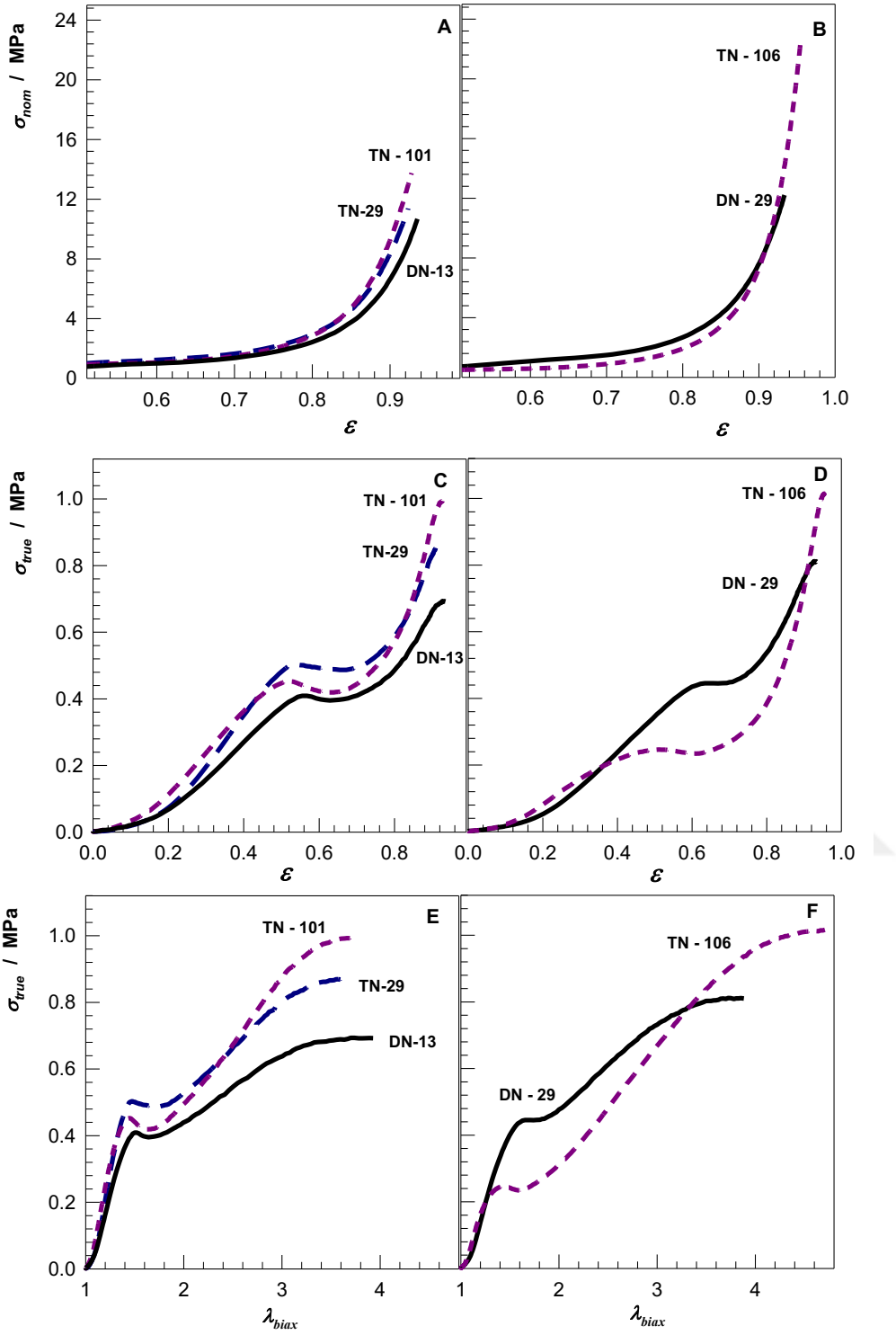

Figure 3.11 : (A, B): σ_{nom} vs. ε plots for DN (solid curves) and TN hydrogels (dashed curves) formed from 4% methacrylated HA. DNs were prepared in DMA solutions at a concentration C_2 = 0.10 (A) and 0.30 g.mL^{-1} (B) both containing 0.05 mol% BAAm. TNs were prepared in the presence of 0.05 mol% BAAm at C_3 = 0.10 and 0.30 g.mL^{-1}. C_1 = 0.02 g.mL^{-1}. Hydrogel samples are denoted in the figures as DN-x or TN-y, where x and y are w_{21} and $w_{32/1}$ ratios, respectively. **(C-F):** σ_{true} vs. ε (C,D) and σ_{true} vs. λ_{biax} plots derived from the curves given in A and B, respectively.

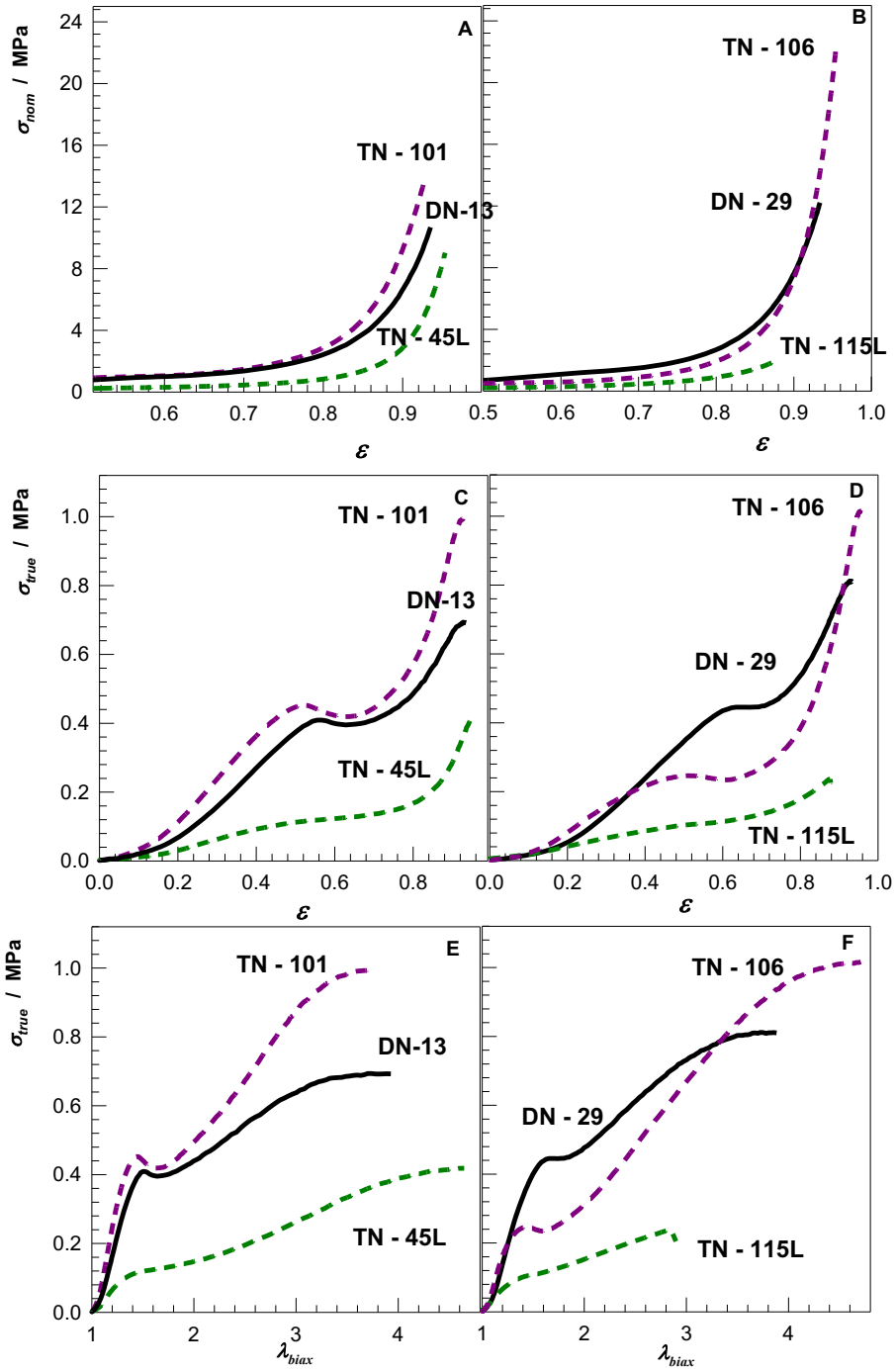

Figure 3.12 : (A, B): σ_{nom} vs. ε plots for DN (solid curves) and TN hydrogels (dashed curves) formed from 4% methacrylated HA. DNs were prepared in DMA solutions at C_2 = 0.10 (A) and 0.30 g.mL^{-1} (B), both containing 0.05 mol% BAAm. TNs were obtained in DMA solutions at C_3 = 0.30 g.mL^{-1} without and with 0.05 mol% BAAm. The letter L at the end of this abbreviation indicates that no cross-linker was used in TN preparation. C_1 = 0.02 g.mL^{-1}. Hydrogel samples are denoted in the figures as DN-x or TN-y, where x and y are w_{21} and $w_{32/1}$ ratios, respectively. (C-F): σ_{true} vs. ε (C,D) and σ_{true} vs. λ_{biax} plots derived from the curves given in A and B, respectively.

In Fig. 3.13, the filled circles show the fracture stress σ_f and fracture strain ε_f of all TN hydrogels formed using 0.05% BAAm cross-linker plotted against $w_{32/1}$ ratio. For comparison, σ_f of SN ($w_{32/1}$ = 0, open down-triangles) and DN hydrogels ($w_{32/1} = w_{21}$, gray up-triangles) are also shown in the figure. All TN hydrogels sustain 10 - 20 MPa compressive stresses at 95% compressions and exhibit a Young's modulus E up to 1 MPa (Fig. 3.14).

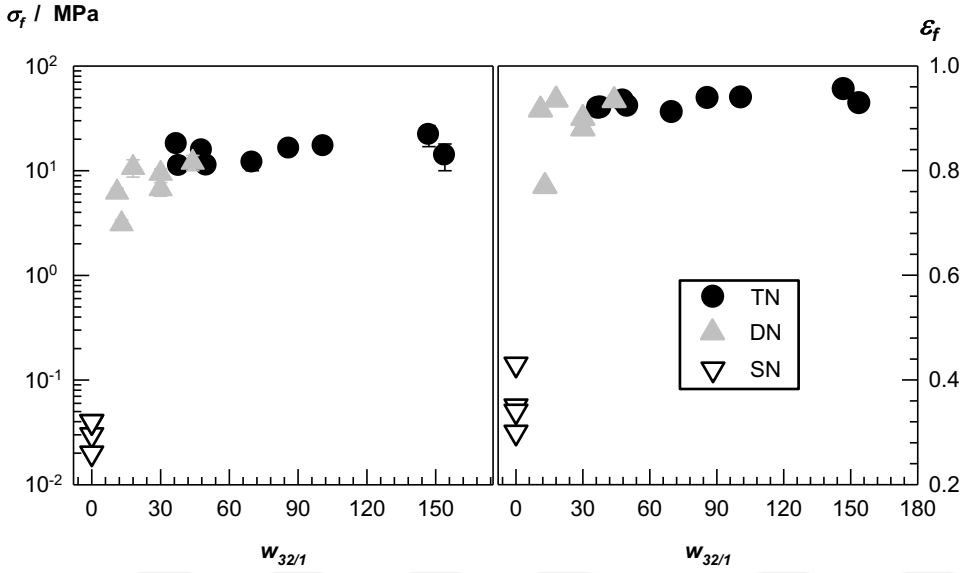

Figure 3.13 : Fracture stress σ_f (left) and fracture strain ε_f (right) of TN hydrogels formed using 0.05% BAAm plotted against $w_{32/1}$ ratio (filled circles). For comparison, fracture data obtained from SN ($w_{32/1}$ = 0, open down-triangles) and DN hydrogels ($w_{32/1} = w_{21}$, gray up-triangles) are also shown in the figure.

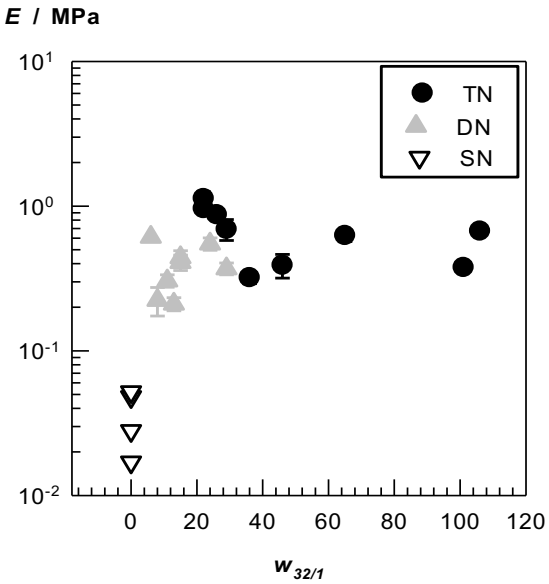

Figure 3.14 : Young's moduli E of SN, DN, and TN hydrogels plotted against $w_{32/1}$ ratio

Another characteristic of high strength DN and TN hydrogels is the appearance of a yielding region in stress-strain curves between 50 and 65% compression (Fig. 3.15). This feature becomes more apparent when the nominal stress σ_{nom} is converted to its true value σ_{true} and then plotted against ε or biaxial extension ratio λ_{biax}. This is illustrated in Fig. 3.11C – F derived from stress – strain curves in Fig. 3.11A and B. The yielding behavior of mechanically strong DN and TN hydrogels is attributed to a significant internal fracture under strain. To demonstrate this fracture, DN and TN hydrogels were subjected to cyclic compression tests by successive loading/unloading cycles up to a maximum strain ε_{max}.

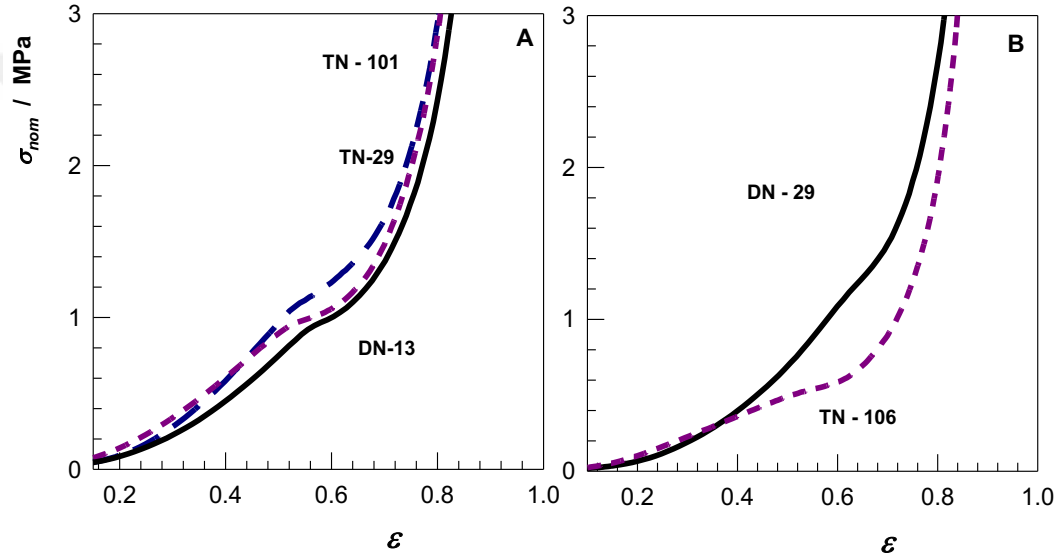

Figure 3.15 : σ_{nom} vs. ε plots for DN (solid curves) and TN hydrogels (dashed curves) formed from 4% methacrylated HA. DNs were prepared in DMA solutions at C_2 = 0.10 (A) and 0.30 g.mL^{-1} (B), both containing 0.05 mol% BAAm. TNs were obtained with 0.05 mol % BAAm. C_1 = 0.02 g.mL^{-1}

In Fig. 3.16A, five successive loading – unloading cycles of a TN hydrogel sample prepared at w_{21} = 29 and $w_{32/1}$ = 106 are shown up to a maximum strain of 80% (ε_{max} = 0.8). The loading curve of the first compressive cycle is different from the unloading curve indicating damage in the gel sample and dissipation of energy during the first cycle. The energy dissipated in this cycle, calculated from the area between the loading and unloading curves, is 160 kJ.m^{-3}. However, the following cycles are almost elastic with a small amount of hysteresis (22 – 24 kJ.m^{-3}), and they closely follow the path of the first unloading. The results show that an irreversible internal damage occurs in the gel sample. In Fig. 3.16B, the same but virgin hydrogel sample was subjected to five successive loading – unloading cycles with increasing maximum strain from 40 to

80%. After the first compressive cycle, each successive loading curve consists of elastic and damage regions due to the irreversible damage done during the previous cycle. Elastic region follows the path of the unloading curve of the previous cycle while the damage region continues the loading curve of the previous cycle (see the inset to Fig. 3.16B). The transition from elastic to damage region occurs at the maximum strain of the previous cycle. Thus, due to the irreversible damage done during the previous cycle, additional damage only occurs at a higher maximum strain. All these indicate the occurrence of a significant extent of internal fracture in the hydrogels even at 40% compressions where the single network hydrogels rupture (Fig. 3.5B). Thus, the ductile, loosely cross-linked PDMA second and third network components hinder macroscopic crack propagation by keeping the macroscopic gel sample together, while the sample internally fractures. This internal fracture is responsible for the extraordinary mechanical properties of the present DN and TN hydrogels based on HA and PDMA.

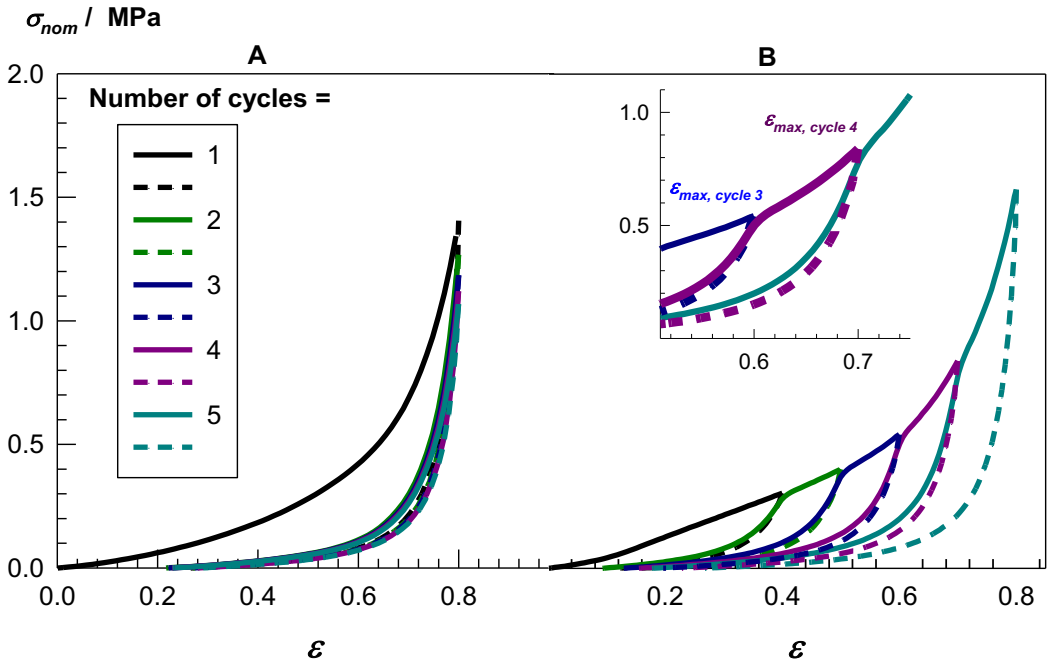

Figure 3.16 : Five successive loading / unloading cycles of a TN hydrogel up to a maximum compression of 80 % (A) and with increasing compression from 40 to 80% (B). The up and down arrows in A indicate loading and unloading curves, respectively. The inset to B is a zoom-in to highlight the damage and elastic regions of the 4th cycle. Synthesis parameters of TN hydrogels: w_{21} = 29, $w_{32/1}$ = 106. For clarity, loading and unloading curves are shown by the solid and dashed curves, respectively.

3.3 Conclusions

DN and TN hydrogels based on HA and PDMA with extraordinary mechanical properties were prepared by DN and TN approaches. The single network (SN) hydrogels were prepared by polymerization of HA of various degrees of methacrylation in aqueous solutions. SN hydrogels can sustain up to 40% compression and break at a stress of 0.02 – 0.05 MPa. By tuning the methacrylation degree of HA, DN hydrogels with a fracture stress above 10 MPa and a fracture strain of 96% were obtained. Triple-networking of DN hydrogels further increases the ratio of ductile/brittle components, and thus produces mechanically strong HA/PDMA/PDMA TN hydrogels. TN hydrogels contain 81-91% water and sustain compressive stresses above 20 MPa. Cyclic mechanical tests conducted on DN and TN hydrogels show a significant mechanical hysteresis and irreversible loading/unloading cycles, even under small strain conditions where the single network hydrogels rupture. The results indicate that the loosely cross-linked PDMA second and third network components hinder macroscopic crack propagation by keeping the macroscopic gel sample together while it internally fractures. This internal fracture is responsible for the extraordinary mechanical properties of the present DN and TN hydrogels based on HA and PDMA.

4. MECHANICALLY STRONG HYALURONIC ACID HYDROGELS WITH AN INTERPENETRATING NETWORK STRUCTURE[3]

Hyaluronan or hyaluronic acid (HA) is a natural glycosaminoglycan of high molecular weight composed of disaccharide repeat units of β-1,4-D-glucuronic acid and β-1,3-N-acetyl-D-glucosamine (Fig. 4.1) [1]. In physiological solutions, HA has a highly extended random coil conformation due to the hydrogen bonding between disaccharide units, and polyanionic properties [7,62]. HA is the major component of the extracellular matrix of vertebrate tissues with important biological and physicochemical functions. Due to the polyelectrolyte nature, HA can absorb large amounts of water and hence acts as lubricant in native extracellular matrix and controls the viscoelasticity of connective tissues [7].

Although HA is an attractive biomaterial for regeneration of soft tissues [2–6,56], it has limited application areas due to its rapid degradation and poor biomechanical properties. To overcome this drawback, HA has been physically or chemically cross-linked to form HA hydrogels [7,8,63,64]. The hydrogels based on HA are however generally brittle, or easily dissolve in aqueous solutions. For instance, HA hydrogels prepared by photopolymerization of methacrylated HA in aqueous solutions fracture at around 35% compressive strain under < 60 kPa stresses [32]. Cross-linking of native HA in aqueous solutions using cross-linkers such as divinyl sulfone, glutaraldehyde, and ethylene glycol diglycidyl ether (EGDE) also results in brittle materials [9–15,65]. For instance, EGDE-cross-linked HA hydrogels rupture when compressed to 25-51% strain under 20-150 kPa stresses [65]. To improve the mechanical performance of HA hydrogels, cryogelation technique has been employed which bases on conducting the gelation reactions below the freezing point of aqueous HA solutions [18,20,66]. Another strategy is the preparation double-network HA hydrogels consisting of brittle and ductile network components [31–33,65]. Double-network HA hydrogels were

[3] This chapter is based on the paper "Tavsanli, B. and Okay, O. (2017). Mechanically strong hyaluronic acid hydrogels with an interpenetrating network structure. *European Polymer Journal*, 90, 185-195."

prepared by swelling the brittle single-network HA hydrogel in a monomer solution and subsequent polymerization of the monomer to create an interconnected and interpenetrated network of HA and synthetic polymers [31]. Although double-network hydrogels based on HA exhibit improved mechanical strength as compared to the single-network ones [31,32,65], their synthetic procedure is lengthy and complicated. Thus, a simple one-pot synthesis of mechanically strong HA hydrogels would be attractive for many application areas.

Here, we describe preparation of mechanically strong single-network HA hydrogels via free-radical copolymerization of methacrylated HA and N,N-dimethylacrylamide (DMA) in aqueous solutions. The choice of the monomer DMA is due to the fact that poly(N,N-dimethylacrylamide) (PDMA) is a hydrophilic biocompatible polymer possessing strong associative properties and hydrogen-bonding interactions with HA [67–69]. The precursor of HA hydrogels, namely methacrylated HA (GMHA) at various levels of methacrylation between 4 and 25% was prepared by methacrylation of native HA using glycidyl methacrylate (Fig. 4.1) [21–23]. As will be seen below, GMHA acts as a multifunctional cross-linker during its copolymerization with DMA leading to the formation of interpenetrated and interconnected polymer network hydrogels. The effective functionality of GMHA increases with its degree of methacrylation as well as with the DMA concentration. The viscoelastic and mechanical properties of the hydrogels could be tuned by varying the degree of methacrylation of GMHA and DMA concentration. We also observed a significant improvement in the mechanical performance of the hydrogels when DMA is replaced with methacrylic acid (MAAc) monomer. By adjusting the synthesis parameters, hydrogels with a Young's modulus of around 200 kPa could be prepared that sustain up to 20 MPa stresses at 96% compression.

4.1 Experimental Part

4.1.1 Materials

Hyaluronic acid sodium salt (HA, Sigma-Aldrich, impurities: ≤1 protein) from Streptococcus equi has a viscosity averaged molecular weight of 1.2×10^6 g·mol^{-1} [18]. Glycidyl methacrylate (GM, Sigma Aldrich, 97%), N,N-dimethylacrylamide (DMA, Sigma-Aldrich, 99%), methacrylic acid (MAAc, Merck, 99%), triethylamine (TEA, Merck, 99%), tetrabutylammonium bromide (TBAB, Sigma-Aldrich, ≥99%), 1-vinyl

pyrrolidone (VP, Sigma-Aldrich), ammonium persulfate (APS, Sigma-Aldrich, ≥99%), N,N,N',N'-tetramethylethylenediamine (TEMED, Sigma-Aldrich, ≥99%), and acetone (Tekkim, 99.5%) were used as received. APS stock solution was prepared by dissolving 0.8 g of APS in 10 mL distilled water.

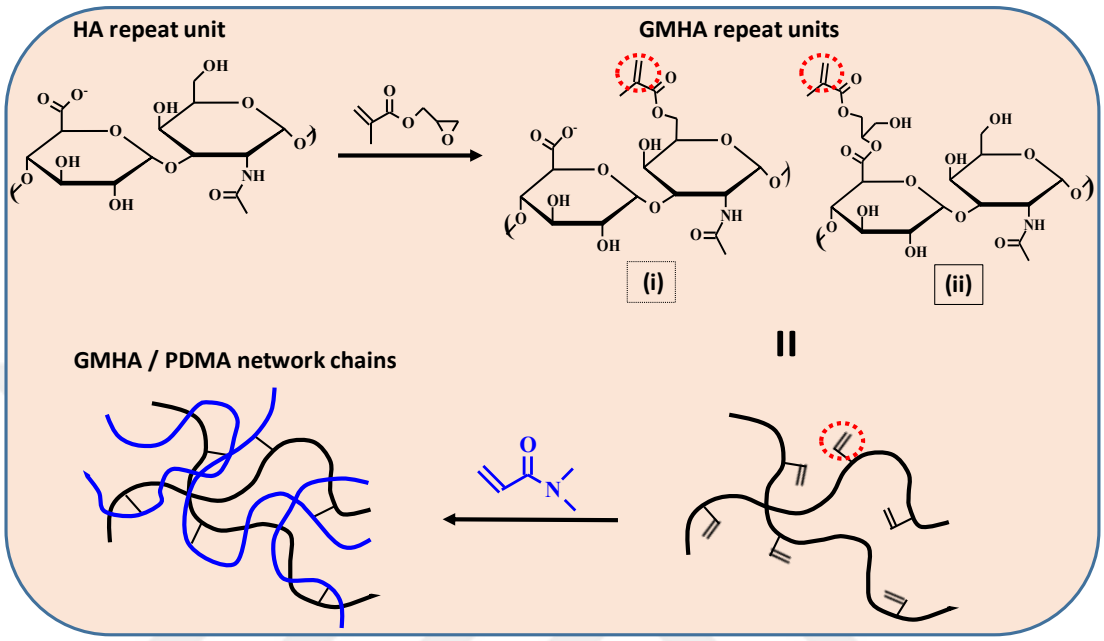

Figure 4.1 : Formation of methacrylated HA (GMHA) by methacrylation of native hyaluronic acid (HA) using glycidyl methacrylate via transesterification (i) and ring opening (ii), and its copolymerization with DMA to form interconnected and interpenetrated GMHA/PDMA network hydrogels. Red circles indicate the methacrylate groups incorporated as pendant into GMHA molecules acting as potential cross-link points during the copolymerization with DMA.

4.1.2 Methacrylation of HA

Methacrylated HA (GMHA) was synthesized by the reaction of HA with glycidyl methacrylate (GM), as described previously [21–23,32]. Typically, HA (0.5 g) was first dissolved under stirring overnight in 50 mL distilled water at room temperature. To prepare a reaction solution containing GM at a 6-fold molar excess to the disaccharide repeat unit of HA, TEA catalyst (1 mL), GM (1 mL), and TBAB (1 g) as phase transfer catalyst were mixed with the HA solution. The solution was then heated to 55 °C and stirred at this temperature for 1 h. After cooling to room temperature, the solution was precipitated twice in excess acetone and the precipitate was dissolved in water. The solution of GMHA in 10 mL water was then frozen at -25 °C for 1 day and freeze-dried using Christ Alpha 2e4 LD-plus freeze-dryer at -40 °C under 0.12 mbar vacuum for 1 day and at -60 °C under 0.011 mbar for an additional 1 day. ^{1}H NMR

spectroscopy (500 MHz Agilent VNMRS spectrometer) was used to determine the level of methacrylation of GMHA. Typical ^{1}H NMR spectrum of GMHA is shown in Fig. 4.2. The two peaks at 5.2 and 5.5 ppm are due to the methacrylate groups (a, b), while the methyl group of HA appears at 1.9 ppm (c) [22,32]. The methacrylation degree (DM) was calculated from the integration of the methyl peak of HA and the methacrylate peaks. In accord with previous work [32], the level of methacrylation was found to be 4, 8, 14, and 25% for the GM/HA molar ratios of 6, 12, 24, and 49, respectively.

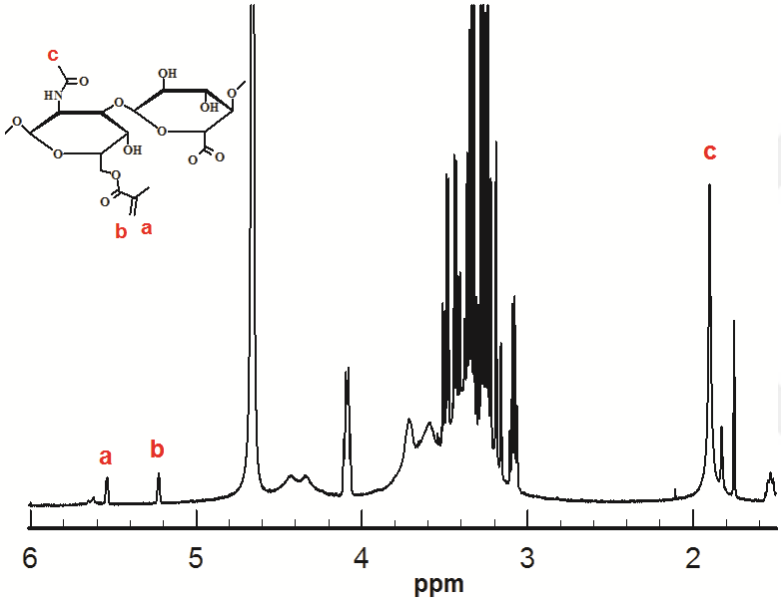

Figure 4.2 : Typical ^{1}H NMR spectrum of methacrylated hyaluronic acid. GM/HA molar ratio = 24.

4.1.3 Hydrogel preparation

The hydrogels were prepared at 4 °C in aqueous solutions of DMA and GMHA using a redox initiator system consisting of 3.5 mM APS and 0.25 v/v% TEMED. The initial concentration of GMHA was set to 1 w/v% while both DMA concentration and the methacrylation degree of GMHA were varied between 5 - 50 w/v% and 4-25%, respectively. To illustrate the synthetic procedure, we give details for the preparation of hydrogels at 30 w/v% DMA concentration: GMHA (100 mg) was dissolved in 6.8 mL of distilled water overnight under continuous stirring. DMA (3.1 mL) and TEMED (25 μL) were then added and the aqueous solution was stirred for 30 min under bubbling nitrogen. After addition of APS stock solution (0.1 mL), a portion of the reaction solution was transferred between the plates of the rheometer for the rheological measurements. For the swelling and mechanical measurements, the

remaining part of the solution was transferred into several plastic syringes of 4.6 mm internal diameter and the polymerization was conducted for 24 h at 4 °C.

4.1.4 Swelling and gel fraction measurements

After a reaction time of 24 h, hydrogel samples were immersed in a large excess of water at 25 °C for at least 4 days whereby the water was replaced every day to extract any soluble species. The swelling equilibrium was tested by weighing the gel specimens. The equilibrium swollen gel samples were taken out of water and dried at 80 °C under vacuum to constant mass. The equilibrium weight swelling ratios with respect to dry and as-prepared states, q_w and $q_{w,o}$, respectively, were calculated as:

$$q_w = m / m_{dry} \tag{4.1a}$$

$$q_{w,o} = m / m_o \tag{4.1b}$$

where m, m_o, and m_{dry} are the masses of the gel sample in equilibrium swollen, as-prepared and dry states, respectively. The gel fraction W_g was calculated from the masses of dry polymer network and from the comonomer feed.

4.1.5 Rheological experiments

The copolymerization reactions of GMHA and DMA were monitored at 4 °C within the rheometer (Gemini 150 Rheometer system, Bohlin Instruments) equipped with a cone-and-plate geometry (cone angle = 4°, diameter = 40 mm). The instrument was equipped with a Peltier device for temperature control. During the rheological measurements, a solvent trap was used and the outside of the upper plate was covered with a thin layer of low-viscosity silicone oil to prevent the evaporation of water. An angular frequency ω of 6.3 rad·s^{-1} and a deformation amplitude γ_o of 0.01 were selected to ensure that the oscillatory deformation is within the linear regime. After a reaction time of 17 h, the elastic moduli G' of the reaction solutions approached limiting values. Then, frequency-sweep tests were carried out at 25 °C. The viscosity measurements on aqueous DMA and MAAc solutions containing 1 w/v% native HA or GMHA were conducted at 25 °C between shear rates 10^{-2} and 10^{1} s^{-1}. We have to mention that because the rheological tests were conducted between the metal plates while swelling and mechanical tests were carried out on gel samples prepared in plastic syringes, gelation dynamics in both cases may differ due to different environments.

4.1.6 Mechanical tests

Uniaxial compression and elongation measurements were conducted at 25 ºC on a Zwick Roell Z0.5 TH test machine using a 500 N load cell. For the compression tests, the cylindrical gel samples in both as-prepared and swollen states were cut into cubic samples with dimensions 3x3x3 mm. Before the tests, an initial compressive contact of 0.01 N was applied to ensure a complete contact between the gel and the plates. The compression tests were performed at a constant cross-head speed of 0.3 and 1 mm·min^{-1} below and above 15% compression, respectively. The stress was presented by its nominal σ_{nom} and true values σ_{true} (= λ σ_{nom}), which are the forces per cross-sectional area of the undeformed and deformed gel specimen, respectively, and λ is the deformation ratio (deformed length/initial length). The compressive strain ε_c is defined as the change in the length relative to the initial length of the gel specimen, i.e., ε_c = 1-λ. The compressive strength and strain of the hydrogels were calculated from the maxima in σ_{true} *vs*. ε_c curves, as detailed before [52]. The uniaxial elongation tests were performed on cylindrical gel samples of 4.6 mm diameter in as-prepared state. The initial length of the gel samples between jaws and the cross-head speed were 10±2 mm and 5 mm·min^{-1}, respectively. The tensile strain ε is calculated as ε = λ -1. Young's modulus E of the hydrogels was calculated from the slope of stress-strain curves between 5 and 15% compression and elongation. For reproducibility, at least five samples were measured for each gel and the results were averaged.

4.2 Results and Discussion

4.2.1 Formation of HA hydrogels

The precursor of the present hydrogels, namely methacrylated hyaluronic acid (GMHA) was synthesized at various levels of methacrylation between 4 and 25% using glycidyl methacrylate by a competing reaction mechanism between transesterification and ring opening (Fig. 4.1) [21–23]. Because the average molecular weight of hyaluronic acid (HA) used in the hydrogel preparation is 1.2x10^6 g.mol^{-1} and the molecular weight of the disaccharide repeat unit is 416 g.mol^{-1}, 4 to 25% methacrylation indicate that 115 to 721 methacrylate groups were incorporated per molecule of GMHA as pendant vinyl groups. Thus, GMHA can be considered as a multifunctional macromolecular cross-linker able to form interpenetrated and

interconnected polymer networks when copolymerized with vinyl monomers such as N,N-dimethylacrylamide (DMA) (Fig 4.1).

Transparent hydrogels with tunable viscoelastic properties were prepared by copolymerization of GMHA and DMA in aqueous solutions using APS-TEMED redox initiator system. The amount of GMHA in the reaction solution was fixed at 1 w/v% while both the degree of methacrylation of GMHA and DMA concentration in the comonomer feed were varied. No gel formation could be detected by polymerization of GMHA alone, which we attribute to the low GMHA concentration making the intramolecular cross-linking reactions favorable. Because GMHA was insoluble in aqueous solutions containing more than 50 w/v% DMA, we conducted the copolymerization reactions below 50 w/v% DMA. We have to mention that the polymerization of aqueous 5-50% DMA solutions in the absence of GMHA resulted in semi-dilute PDMA solutions revealing that the self-cross-linking efficiency of DMA is insufficient for the onset of gelation [70]. The gelation reactions were initially carried out at both 4 and 25 °C. Typical gelation profiles of the reaction solutions obtained by rheometry using oscillatory deformation tests are shown in Fig. 4.3 where the storage modulus *G'* and loss factor *tan* δ (= *G''*/*G'*, where *G''* is the loss modulus) are plotted against the polymerization time. The initial reaction solutions contain 30 w/v% DMA and 1 w/v% GMHA with methacrylation degrees of 4 and 14%. It is seen that, although increasing the polymerization temperature from 4 to 25 °C significantly reduces the induction period of the reaction, the limiting values of both *G'* and *tan* δ are close together after 10 h. However, to eliminate the possibility of degradation of GMHA during gelation [41], all the hydrogels reported below were prepared at 4 °C.

Frequency-sweep results of the hydrogels after a reaction time of 17 h are shown in Fig. 4.3 where the storage *G'* and loss moduli *G''* are plotted against the angular frequency ω. In Fig. 4.3a, the hydrogels were prepared at 5 w/v% DMA and at two different degrees of methacrylation (DM) while in Fig. 4.3b, DM was fixed at 14% while DMA concentration was varied between 5 and 30 w/v%. The general trend is that, at DMA contents below 20 w/v%, the hydrogels exhibit predominantly elastic or viscous nature depending on the frequency, i.e., on the time scale of the rheological tests. At low frequencies, *G''* attains very low values (~10^1 Pa) and the loss factor *tan* δ approaches to 0.01 corresponding elastic, solid-like behavior. At high frequencies, *G''* approaches to *G'* and the gels exhibit a viscous character. This feature is opposite

to what is observed in semi-dilute polymer solutions, but similar to hydrogel systems with strong hydrogen bonding interactions [46–48,65]. Thus, the intermolecular hydrogen bonds between GMHA and GMHA-PDMA molecules seem to act as physical cross-links at low frequencies and thus contribute to the gel elasticity. Because these bonds are broken at high frequencies, increasing amount of energy is dissipated with increasing frequency so that *G''* increases leading to the appearance of a strong-to-weak gel transition. Moreover, as indicated by the arrows in Fig. 4.4, *G'* increases with the methacrylation degree, or with the monomer concentration DMA%, while the loss modulus *G''* is only affected by DMA%.

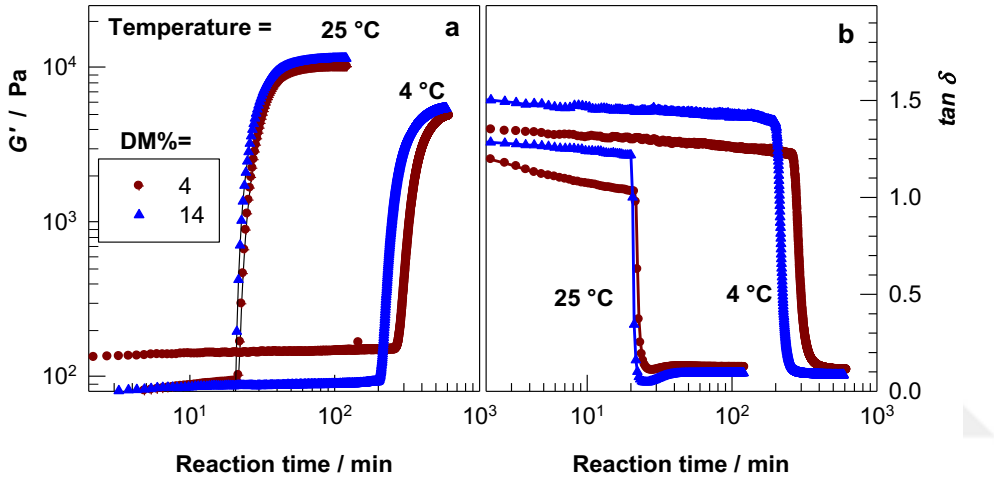

Figure 4.3 : Storage modulus *G'* (a) and the loss factor *tan δ* (b) during the copolymerization of GMHA and DMA shown as a function of the reaction time. The degree of methacrylation DM is 4 (circles) and 14% (triangles). DMA = 30 w/v%. GMHA = 1 w/v%. The reaction temperatures are shown in the Figure.

To highlight the effect of the synthesis parameters on the viscoelastic properties of the hydrogels, *G'* and *tan δ* of all hydrogels measured at 6.3 rad·s^{-1} are shown in Fig. 4.5a as a function of the DMA concentration. The arrows indicate direction of increasing methacrylation degree (DM) of GMHA. Increasing DMA% also increases the storage modulus *G'* while the loss factor remains almost unchanged revealing that the viscoelastic nature of the hydrogels is not much affected with increasing polymer concentration. However, when the methacrylation degree is increased at a fixed DMA%, *G'* increases while *tan δ* decreases indicating increasing elastic character of the hydrogels.

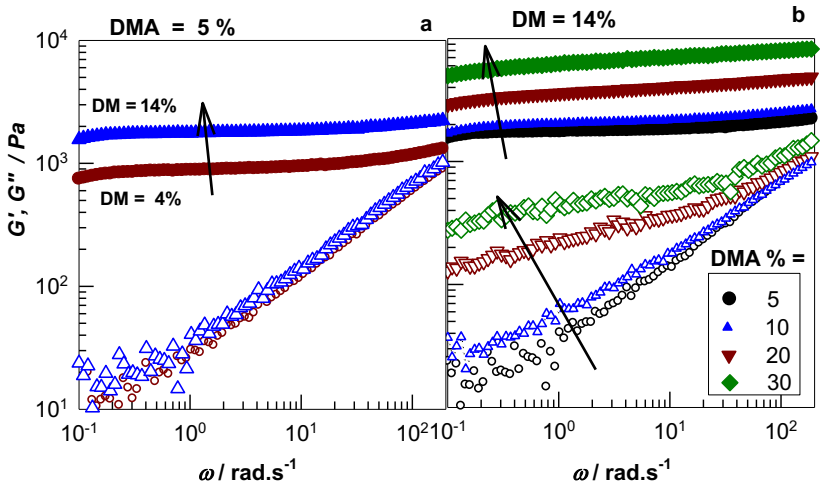

Figure 4.4 : Storage moduli *G'* (filled symbols) and loss moduli *G''* (open symbols) shown as a function of the angular frequency ω measured after 17 h of reaction time. (a): DMA = 5 w/v%. DM = 4 (circles) and 14% (triangles). (b): DM = 14%. DMA concentrations are indicated. The arrows show the direction of increasing DM (a) and DMA % (b).

Assuming that *G'* measured at 6.3 rad·s^{-1} corresponds to the equilibrium shear modulus *G*, one may calculate the effective cross-link density v_e of the hydrogels. According to the phantom network model, *G* at the state of gel preparation is related to v_e by [49,50]:

$$G = \left(1 - 2/f_e\right) v_e \, RT \, v_2^0 \tag{4.2}$$

where f_e is the average effective functionality of GMHA macromer, that is the number of elastically effective PDMA network chains per GMHA cross-link, v_2^0 is the volume fraction of cross-linked polymer in the gel, *R* and *T* are in their usual meanings. At the highest degree of methacrylation of 25% corresponding to the existence of 720 pendant methacrylate groups per GMHA molecule, the functionality f_e is expected to be much larger than unity so that the first term at the right hand side of Eq. 4.2a reduces to unity (affine limit), i.e.,

$$G = v_e \, RT \, v_2^0 \tag{4.2b}$$

Thus, using the modulus data of the hydrogels formed using GMHA with DM = 25% (Fig. 4.5a), the cross-link density v_e of the hydrogels can be calculated using Eq. 4.2b. Substituting these v_e values for each DMA concentration into Eq. 4.2a allows estimation of the average functionality f_e as a function of the methacrylation degree. In Fig. 4.5b & c, the effective cross-link density v_e and the average functionality f_e are

plotted against DMA% and DM%, respectively. For calculations, the volume fraction v_2^0 of polymer in the as-prepared hydrogels was estimated using the equation $v_2^0 = 10^{-2}$ (DMA%)/d_2, where d_2 is the density of PDMA (1.21 g·mL^{-1} [71]). Except the initial drop in v_e between 5 and 10% DMA, v_e continuously increases with increasing DMA% indicating formation of larger number of effective cross-links per dry polymer volume. Moreover, the effective functionality f_e of GMHA varies between 4 and 13, and increases both with the methacrylation degree of GMHA and DMA concentration. Thus, although GMHA macromonomer acts as a multifunctional cross-linker, its effective functionality is much smaller than the number of methacrylate groups incorporated as pendant into HA molecules. This is attributed to the cyclization reactions as well as reduced reactivity of pendant methacrylate groups that are generally observed in free-radical cross-linking copolymerization [72].

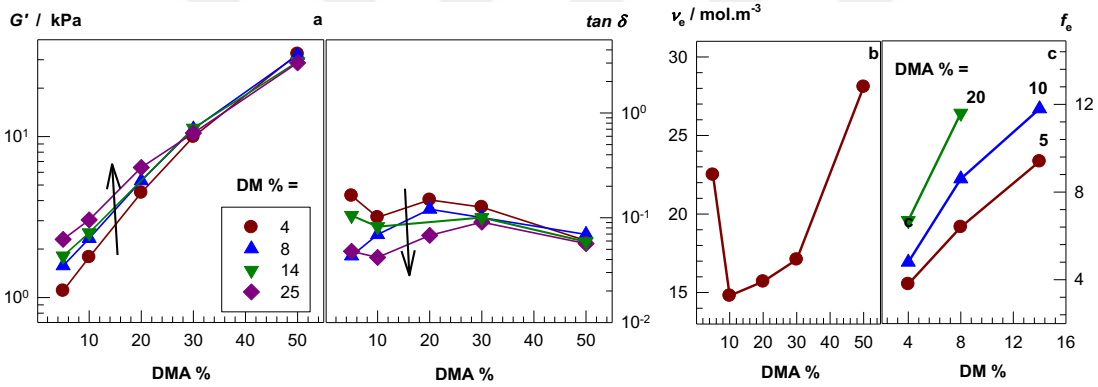

Figure 4.5 : (a): The storage modulus *G'* and loss factor *tan δ* measured at 6.3 rad·s^{-1} shown as a function of the monomer (DMA) concentration. The arrows indicate direction of increasing methacrylation degree (DM) of GMHA. Methacrylation degrees DM of GMHA are indicated. (b): Cross-link density v_e of the hydrogels calculated using eq 4.2b plotted against DMA concentration. (c) Variation of the effective functionality f_e of GMHA with the level of methacrylation DM. The solid curves are guide to the eye.

4.2.2 Mechanical properties of as-prepared HA hydrogels

HA hydrogels after a reaction time of 24 h were subjected to uniaxial compression and elongation tests. Fig 4.6a & b show typical tensile stress-strain curves of the hydrogels formed at 10 and 30 w/v% DMA, respectively, where the nominal stress σ_{nom} is plotted against the tensile strain ε. The methacrylation degree (DM) of GMHA used in the hydrogel preparation is indicated in the figures. The hydrogels formed at 10 w/v% DMA and at DM > 8% were brittle in tension and they already broke at the start of the mechanical tests. The maximum tensile strength σ_f observed at the lowest

methacrylation degree of 4% was 5±1 kPa. Stronger hydrogels could be obtained at 30 w/v% DMA concentration (Fig. 4.6b); they all sustain above 600% elongation ratios and their tensile strength σ_f increases from 55±3 to 111±13 kPa with increasing DM from 4 to 14% while further increase in DM decreases σ_f of the hydrogels. Fig. 4.6c shows compressive stress σ_{nom} – strain ε_c curves of the hydrogels formed at 10 and 30 w/v% DMA with varying DM of GMHA. The hydrogels formed at 10 and 30 w/v% DMA sustain 7±1 and 11±1 MPa compressive stresses, respectively, at 96±1% compressions.

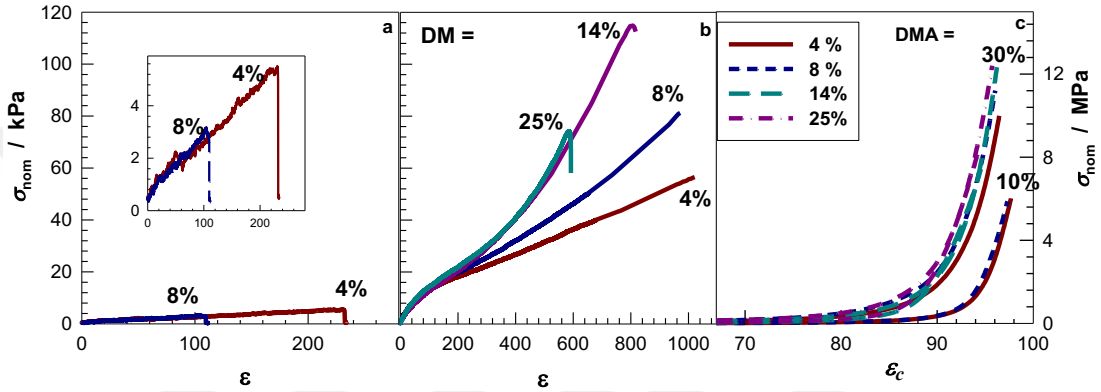

Figure 4.6 : (a, b): Tensile stress-strain curves of HA hydrogels formed at 10 (a) and 30 w/v% DMA (b) as the dependence of nominal stress σ_{nom} on the strain ε. Methacrylation degree DM of GMHA is indicated (c)**:** Compressive stress – strain curves of HA hydrogels as the dependence of σ_{nom} on the compressive strain ε_c. DMA concentration and DM% are indicated.

The results thus reveal that the simple one-pot free-radical copolymerization of GMHA and DMA provides formation of mechanically strong HA hydrogels by adjusting the degree of methacrylation of GMHA as well as the DMA concentration at gelation. Because of the existence of extensive hydrogen bonding interactions in HA solutions [62], and PDMA is a polymer with associative properties [67–69], the good mechanical performance of the hydrogels can be attributed to the existence of both hydrophobic and hydrogen bonding interactions acting as physical cross-links. These cross-links are reversibly broken under load and thus, resisting the crack propagation by dissipating energy and contributing to the mechanical properties [16,57]. Recently, Hu et al. demonstrated formation of tough physical hydrogels consisting of copolymer chains composed of DMA and methacrylic acid (MAAc) units [73]. We conducted gelation reactions by replacing half of the DMA with MAAc monomer but observed any further improvement in the mechanical properties of the final hydrogels. However, total replacement of DMA with MAAc resulted in stronger

hydrogels. Tensile and compressive stress-strain curves of HA hydrogels formed using 30 w/v% MAAc and GMHA with methacrylation degrees of 4 and 8% are shown in Fig. 4.7a & b, respectively. For comparison, the data obtained using 30 w/v% DMA are also shown in the figures by the gray curves. The inset in Fig. 4.7b shows the portion of the curves below 30% compression. It is seen that the initial slope of the stress-strain curves corresponding to the Young's modulus significantly increases when DMA is replaced with MAAc monomer.

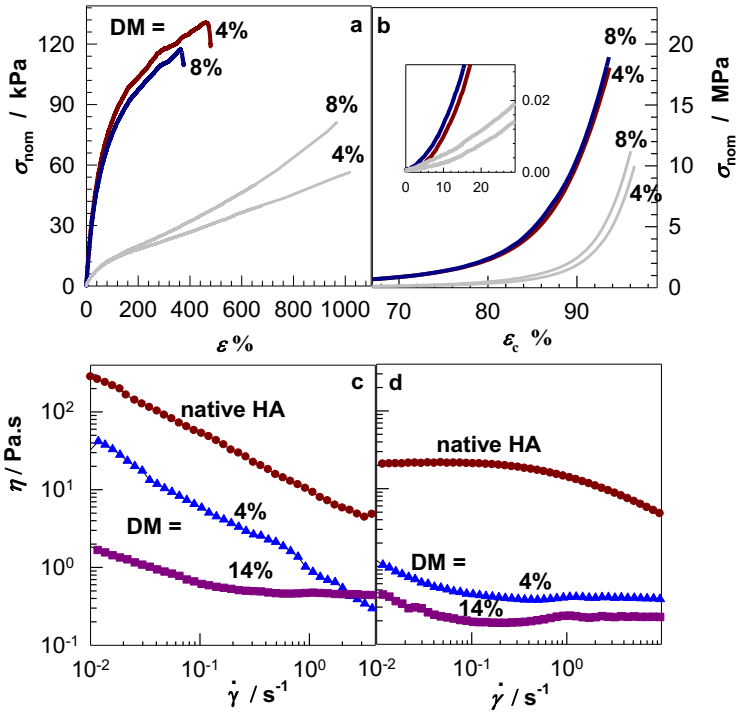

Figure 4.7 : (a, b): Tensile (a) and compressive stress-strain curves (b) of HA hydrogels formed using MAAc at a concentration of 30 w/v%. For comparison the data of the hydrogels formed using 30 w/v% DMA are also shown by gray curves. (c, d) Viscosities η of 1 w/v% native HA and GMHA at 2 different methacrylation degrees in aqueous solutions of 30 w/v% MAAc (c) and DMA (d) plotted against the shear rate $\dot{\gamma}$.

In Fig. 4.8a-d, Young's modulus E, elongation at break ε_f, compressive and tensile strengths σ_f of HA hydrogels are shown as a function of methacrylation degree DM of GMHA. The hydrogels formed using MAAc monomer exhibit a modulus E between 175 and 218 kPa that increases with increasing degree of methacrylation, as compared to 33-36 kPa obtained using DMA monomer at the same concentration. Thus, GMHA/poly(methacrylic acid) (PMAAc) hydrogels exhibit about 5-fold larger modulus as compared to GMHA/PDMA ones indicating the contribution of non-covalent cross-links to the effective cross-link density. Moreover, tensile strength

increases from 62±7 to 117±4 kPa while compressive strength increases from 10 to 20 MPa when MAAc is used in the gel preparation instead of DMA.

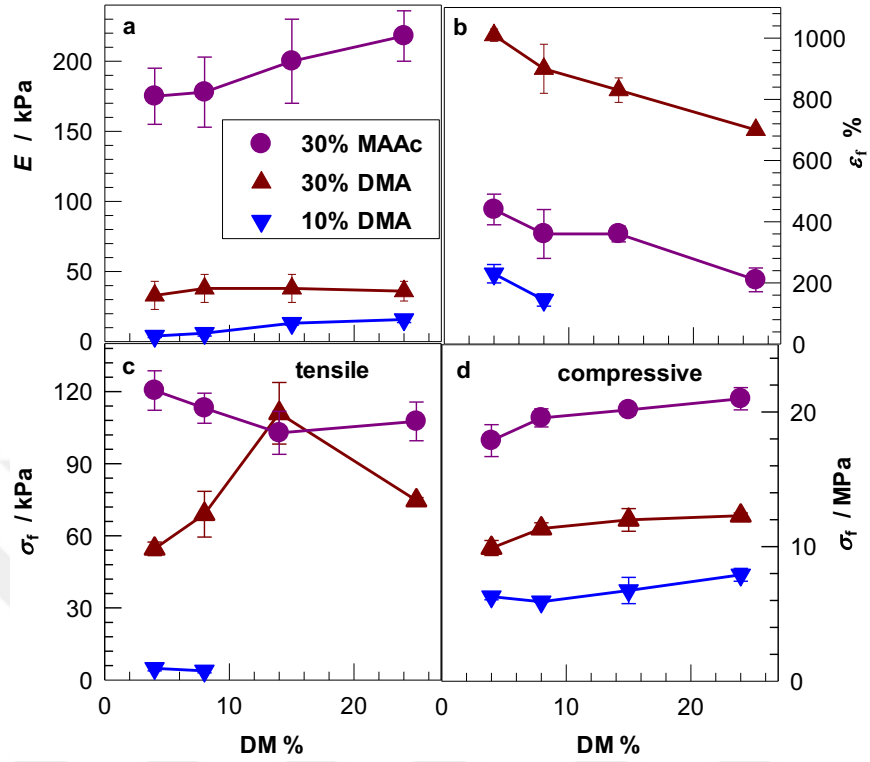

Figure 4.8 : Young's modulus E (a), elongation at break ε_f (b), tensile and compressive strengths σ_f (c and d, respectively) of the hydrogels shown as a function of methacrylation degree DM of GMHA. The type and concentration of the monomer are indicated.

Stronger extent of non-covalent interactions in hydrogels based on GMHA/PMAAc as compared to those based on GMHA/PDMA seems to be responsible for the improved mechanical properties of the resulting hydrogels. To compare the extent of non-covalent interactions, viscosity measurements at 25 °C were conducted on aqueous solutions of DMA and MAAc at a concentration of 30 w/v% containing 1 w/v% HA or GMHA. Fig. 4.7c & d present the viscosity versus shear rate curves for native HA and GMHA in MAAc (c) and DMA solutions (d). Note that pH's of the solutions are 2.6±0.1 and 5.7±0.1 for MAAc and DMA, respectively. The viscosity decreases with increasing methacrylation degree of GMHA due to the increasing hydrophobicity of HA upon incorporation of methacrylate groups [32]. Moreover, both native HA and GMHA exhibit higher viscosities at low shear rates and marked shear-thinning in the presence of MAAc as compared to DMA. This indicates increasing associativity of GMHA chains in MAAc environment and thus support the experimental findings.

4.2.3 Swelling behavior and mechanical properties of HA hydrogels in equilibrium swollen state

Gel fraction W_g of the hydrogels formed using DMA monomer was above 0.95 after a reaction time of 24 h and they contained 94-99% water in their equilibrium swollen states in water. Hydrogels formed using MAAc exhibited very large swelling ratios due to the osmotic pressure of counterions of carboxylate groups. They also became too weak to perform any meaningful gel fraction, swelling and mechanical tests. In Fig. 4.9a, the equilibrium weight swelling ratios of GMHA/PDMA hydrogels with respect to their dry (q_w) and as-prepared states ($q_{w,o}$) are plotted as a function of the methacrylation degree DM of GMHA. As expected, q_w decreases with increasing methacrylation degree as well as with increasing DMA concentration due to the simultaneous increase of the cross-link density ν_e and cross-link functionality f_e (Fig. 4.5). However, when considering the swelling ratios with respect to the preparation state of the hydrogels, the higher DMA concentration, the higher is the degree of swelling $q_{w,o}$. This is due to the fact that the translational entropy of DMA monomer upon its polymerization decreases so that more water enters into the as-prepared hydrogel with increasing DMA% to assume its new thermodynamic equilibrium [52].

Fig. 4.9b & c show compressive stress-strain curves of swollen HA hydrogels formed at 10 and 30 w/v% DMA, respectively. In accord with the mechanical behavior of as-prepared hydrogels, those formed at 30 w/v% DMA exhibit better mechanical properties as compared to 10 w/v% DMA hydrogels. In Fig. 4.10, Young's modulus E, compressive strength σ_f, and strain at break ε_f of swollen HA hydrogels formed at 10 and 30 w/v% DMA are shown as a function of methacrylation degree DM of GMHA. For comparison, the data obtained from as-prepared hydrogels are also shown by gray symbols. It is seen that the ultimate properties of the hydrogels, e.g., the fracture stress and fracture strain decrease after swelling of HA hydrogels. However, the modulus E does not change much and remains at around 10-30 kPa although swelling results in a 7- to 9-fold dilution of the hydrogels (Fig. 4.8a). This suggests increasing effective cross-link density of the hydrogels upon their swelling which is attributed to increasing extent of hydrogen bonding and hydrophobic interactions between GMHA and PDMA chains acting as additional cross-links [67–69].

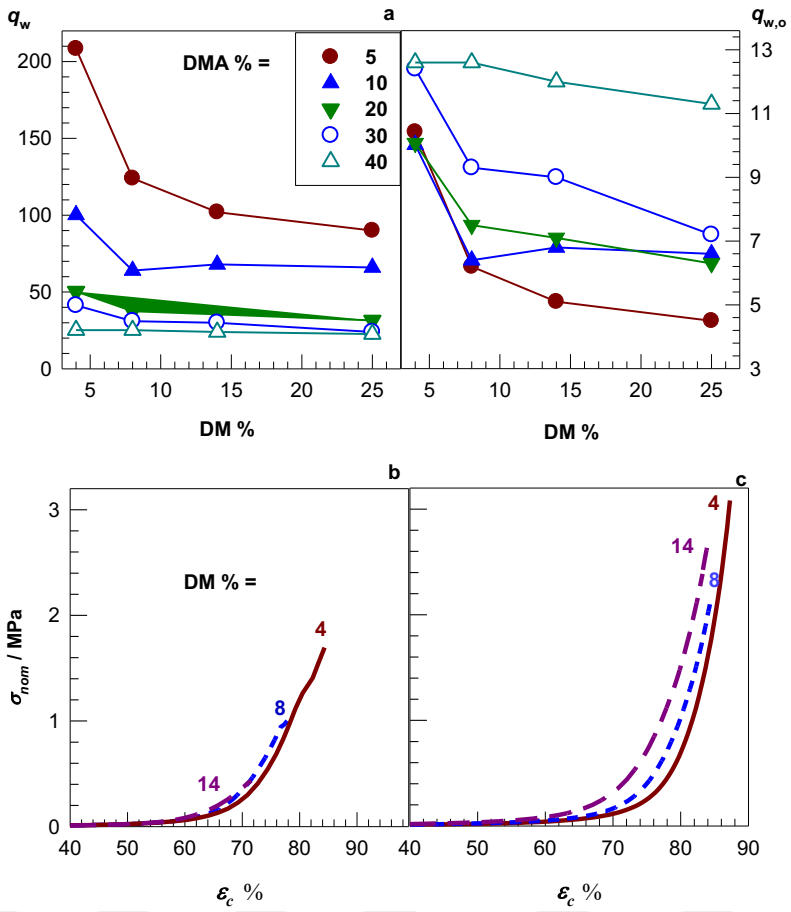

Figure 4.9 : (a): Equilibrium weight swelling ratios of HA hydrogels with respect to their dry q_w and as-prepared states $q_{w,o}$ shown as a function of the methacrylation degree of GMHA. DMA concentrations are indicated. (b, c): Compressive stress-strain curves of swollen HA hydrogels formed at 10 (b) and 30 w/v% DMA (b). Methacrylation degree of GMHA is indicated.

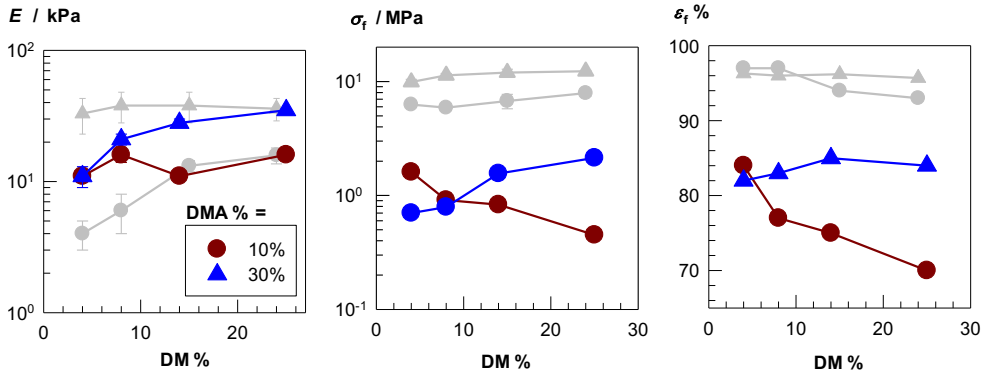

Figure 4.10 : Young's modulus E, compressive strength σ_f, and strain at break ε_f of swollen HA hydrogels formed at 10 (circles) and 30 w/v% DMA (triangles) shown as a function of methacrylation degree DM of GMHA. Gray symbols represent data of the hydrogels in their preparation states.

4.3 Conclusions

We presented a simple one-pot procedure for the preparation of mechanically strong HA hydrogels with tunable viscoelastic and mechanical properties. The precursor of the hydrogels, namely methacrylated hyaluronic acid (GMHA) was synthesized by methacrylation of native HA using glycidyl methacrylate at various levels of methacrylation between 4 and 25%, corresponding to 115 to 721 pendant methacrylate groups per GMHA molecule. The hydrogels were prepared via free-radical copolymerization of GMHA and N,N-dimethylacrylamide (DMA) in aqueous solutions. It was found that GMHA acts as a multifunctional cross-linker during its copolymerization with DMA leading to the formation of interpenetrated and interconnected polymer networks. The average functionality of GMHA for intermolecular cross-linking reactions increases with its methacrylation degree as well as with the DMA concentration. Both the methacrylation degree of GMHA and DMA concentration strongly affect the properties of HA hydrogels both in their as-prepared and equilibrium swollen states. We also observed a significant improvement in the mechanical performance of the hydrogels when DMA is replaced with methacrylic acid monomer. By adjusting the synthesis parameters, hydrogels with a Young's modulus of around 200 kPa could be prepared that sustain up to 20 MPa stresses at 96% compression.

5. MECHANICALLY ROBUST AND STRETCHABLE SILK/HYALURONIC ACID HYDROGELS[4]

Hydrogels derived from natural polymers such as silk or hyaluronic acid have been used in a wide range of biological and biomedical applications because of their advantages including good biocompatibility and controlled degradability [3,74–78] Silk consists mainly of two components, namely fibroin and sericin proteins which are produced in the glands of domesticated silkworm *Bombyx mori* [79,80]. Silk fibroin (SF) has a microstructure similar to multiblock copolymers composed of hydrophobic and hydrophilic blocks inside, together with hydrophilic terminal blocks [81,82]. The less ordered hydrophilic blocks of SF provide water solubility, elasticity and toughness whereas large hydrophobic blocks form intermolecular associations leading to a conformational transition from random-coil or helix to β-sheet structure. The β-sheets in silk fibroin acting as physical cross-links by connecting the fibroin molecules into a 3D network are responsible for the high strength of fibroin hydrogels.

Hyaluronic acid (HA) is a naturally occurring polyanion composed of disaccharide repeating units of β-1,4-D-glucuronic acid - β-1,3-N-acetyl-D-glucosamine [1]. HA has unique lubricating properties and biological functions and hence, plays important roles in cell differentiation, cell motility, and wound-healing processes [2,83]. Although HA is an important biomaterial for soft tissue regeneration, poor biomechanical performance and rapid degradation of HA limit its applications [84,85]. To produce slowly degradable HA, it was physically or chemically cross-linked or, alternatively, methacrylate groups are incorporated into HA to generate HA macromers, which are then polymerized to form hydrogels [21,22,32].

Our aim in this study was to combine the material and biological properties of SF and HA in a single composite hydrogel that would expand the range of properties and hence applications available to SF and HA individually. The ionic nature of the HA

[4] This chapter is based on the paper "Tavsanli, B. and Okay, O. (2019). Mechanically robust and stretchable silk/hyaluronic acid hydrogels. *Carbohydrate Polymers*, 208, 413-420."

component in such composites will provide enhanced water retention and structural support, whereas relative slow degradation and mechanical strength of SF component will contribute to the mechanical integrity and control of water interactions of HA. SF/HA scaffolds, hydrogels, patches, and films have been prepared in the past years using several techniques including unltrasonication [86,87], cross-linking using enzymes [88], or chemical cross-linking agents such as genipin and carbodimides [89–92]. The resulting composites exhibit, however, poor mechanical properties and have no stretchability limiting their applications. More recently, Zhou et al. prepared SF/HA films without a cross-linker or any post treatment capable of sustaining up to around 140% stretches [93]. It was shown that the presence of HA enhances β-sheet formation in SF, which well correlates with improved mechanical properties of SF/HA films or hydrogels [94].

We describe here a novel strategy for the preparation of mechanically robust SF/HA hydrogels exhibiting a high stretchability up to around 400%. Instead of HA, methacrylated HA (GMHA) prepared by the reaction of HA with glycidyl methacrylate was used in the gel preparation (Fig. 5.1). Previous work shows that the hydrogels derived from GMHA show good biocompatibility and reduced degradation rate as compared to the native HA [21,23,31]. GMHA of various methacrylation degrees between 4 and 25% and SF isolated from *Bombyx mori* cocoons are the starting materials of the present composite hydrogels (Fig. 5.1). Due to the presence of pendant vinyl groups on GMHA molecules, they act both as a macromer and multifunctional chemical cross-linker during the radical polymerization in aqueous solutions [95]. By conducting polymerization of GMHA in the presence of SF at an elevated temperature, we intend to induce β-sheet domains between SF molecules and hence, to produce additional cross-links of physical nature (Fig. 5.1). Preliminary experiments, however, showed no gel formation in aqueous solutions of GMHA and SF, likely because of the steric effect of SF hindering the cross-linking reactions between GMHA. Therefore, N, N-dimetylacrylamide (DMA) monomer was also included into the reaction system as a spacer to connect GMHA's through their pendant vinyl groups. The in situ formed poly(DMA) (PDMA) is known to exhibit both associative and enhanced proton acceptor properties, which would contribute to the cooperativity of the non-covalent bonds in the composite hydrogels [67,69]. As will be seen below, the presence of SF significantly enhances the mechanical strength and toughness of GMHA hydrogels by

creating an energy dissipation mechanism under load. Further, a wide range of tunable mechanical and swelling properties could be achieved by varying the methacrylation degree of GMHA. Because the hydrogel components GMHA, SF, and PDMA exhibit good biocompatibility, the composite hydrogels presented here are a good candidate as biomaterials in biological and biomedical applications.

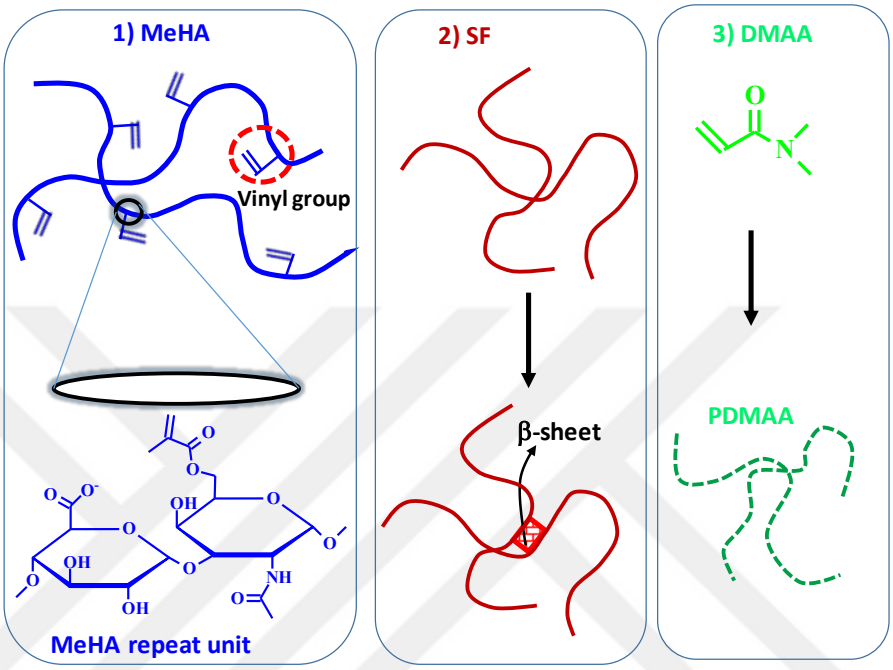

Figure 5.1 : Components of composite hydrogels. 1) methacrylated hyaluronic acid (GMHA), 2) silk fibroin (SF), and 3) in-situ formed PDMA.

5.1 Experimental Part

5.1.1 Materials

Hyaluronic acid sodium salt (HA, Sigma-Aldrich) from Streptococcus equi having a viscosity average molar mass of 1.2×10^6 g mol^{-1} was used as received [18]. Silk fibroin (SF) protein was separated from *Bombyx mori* cocoons (Koza Birlik, Bursa, Turkey), as reported earlier [96]. Briefly, the cocoons were placed in boiling aqueous 0.02 M Na_2CO_3 solution for 1 h for the removal of sericin protein. After thorough rinsing, the remaining fibroin was dissolved in 9.3 M LiBr aqueous solution at 60 °C and then the solution was dialyzed in a dialysis tube (10000 MWCO, Snake Skin, Pierce) against deionized water for 3 days. This procedure yielded an aqueous 5 wt. % SF solution. N,N-dimethylacrylamide (DMA, Sigma-Aldrich, 99%), glycidyl methacrylate (GM, Sigma Aldrich, 97%), tetrabutylammonium bromide (TBAB, Sigma-Aldrich, ≥99%), triethylamine (TEA, Merck, 99%), ammonium persulfate

(APS, Sigma-Aldrich, ≥99%), N,N,N',N'-tetramethylethylenediamine (TEMED, Sigma-Aldrich, ≥99%), LiBr (Merck), and Na_2CO_3 (Merck) were used as received.

5.1.2 Methacrylation of HA

HA was methacrylated according to a procedure described previously [21]. Briefly, 0.5 g of HA was dissolved in 50 mL distilled water and stirred overnight at 23±2 °C. To prepare a solution containing 6-fold molar excess of GM with respect to the disaccharide repeat unit of HA, 1 mL of GM, 1 mL of TEA and 1 g of TBAB were added to the HA solution. After heating the solution to 55 °C and stirring for 1 h, it was cooled to 23±2 °C and precipitated twice in a large excess of acetone. After dissolving the precipitate in water, the solution of methacrylated HA (GMHA) was freeze-dried (Christ Alpha 2e4 LD-plus) for 2 days. The degree of methacrylation (DM) of GMHA was determined by nuclear magnetic resonance using a 500 MHz Agilent VNMR spectrometer, as detailed before [32].

5.1.3 Preparation of composite hydrogels

The initial concentrations of DMA, and SF were fixed at 5, and 2.5 w/v %, respectively, while GMHA was used at 1 and 2 w/v % concentrations at methacrylation degrees (DM) of 4, 14, and 25%. Typically, GMHA (0.100 or 0.200 g) was first dissolved overnight in 4.38 mL of water under gently stirring. After addition of DMA monomer (0.500 g) and stirring for 30 min, 5 mL of a 5 w/v % SF solution were dropwise, slowly added to this solution with a rate of 1 mL min^{-1} to prevent aggregations during fast mixing of the solutions [86]. After bubbling nitrogen for 10 min and cooling to 4 °C, TEMED (25 μL) and 0.1 mL of APS stock solution (0.08 g mL^{-1}) were added. The solution was then transferred into 1-mL plastic syringes and the reactions were conducted at 50 ºC for 2 days. For 1 and 2 w/v % GMHA in the synthesis feed, the total solid contents of the hydrogels after preparation (C_o) were 8.9 and 10.0 w/v %, whereas GMHA:SF weight ratios were 1:2.5 and 1:1.25, respectively.

5.1.4 Rheological measurements

A Gemini 150 rheometer system (Bohlin Instruments) in the cone-and-plate mode (cone angle = 4°, diameter = 40 mm) equipped with a Peltier device for temperature control was used to measure the storage G' and loss moduli G'' as functions of the reaction time and angular frequency ω. To prevent evaporation of water, a solvent trap

was used during the rheological measurements. The strain amplitude γ_o in the measurements was fixed at 1% which was within the linear viscoelastic range of the hydrogels.

5.1.5 Swelling tests

The gel specimens were placed in an excess of water at 23±2 °C for 4-7 days, replacing the water every other day. After reaching swelling equilibrium, the relative weight swelling ratio m_{rel} of the hydrogels was calculated as $m_{rel} = m/m_o$, where m and m_o are the masses of the gel specimen in equilibrium swollen and as-prepared states, respectively. To determine the dry mass of the specimens, they were placed in acetone for 1 day which is a poor solvent for the polymers. After drying at 80 °C under vacuum to constant mass m_{dry}, the gel fraction Wg, that is, the fraction of the total mass of GMHA, SF, and DMA incorporated into the 3D polymer network was calculated as $W_g = m_{dry}/ (m_o C_o)$.

5.1.6 XRD, DSC, and ATR-FTIR measurements

X-ray diffraction (XRD) patterns of freeze-dried samples were recorded in reflection mode on a PANalytical X-Pert PRO X-ray generator using Ni-filtered Cu Kα (λ = 0.15418 nm) irradiation (45 kV, 40 mA) in the range of 2θ = 5−40°. Differential scanning calorimetry (DSC) measurements were carried out on a Perkin Elmer Diamond DSC under nitrogen atmosphere. The freeze-dried polymer specimens sealed in aluminum pans were scanned between 30 and 300 °C with heating and cooling rates of 10 °C·min^{-1}. Fourier transform infrared (FTIR) spectra of the polymers were recorded on a Nicolet Nexus 6700 spectrophotometer using a single-bounce diamond attenuated total reflectance (ATR) accessory equipped with a liquid nitrogen cooled mercury – cadmium − telluride (MCT) detector. 64 interferograms at 4 cm^{-1} resolution were co-added to generate each spectrum.

5.1.7 Mechanical tests

Uniaxial compression and tensile tests were carried out at 23±2 °C with a Zwick Roell test machine, model Z0.5 TH, using a 500 N load cell. For the compression tests, cubic gel specimens with dimensions 3x3x3 mm were prepared by cutting as-prepared and swollen hydrogels. To ensure a complete contact between the specimen and the plates, an initial compressive force of 0.01 N was applied before the test. The tests were

conducted at a strain rate of 0.3 and 1 mm·min^{-1} below and above 15% compression, respectively. Nominal σ_{nom} and true σ_{true} stresses ($\sigma_{true} = \lambda\ \sigma_{nom}$) were used in the calculations, which are the forces acting per unit area of the undeformed and deformed gel specimens, respectively, and λ is the deformation ratio. The strain is given by fractional deformation ε which is equal to $1 - \lambda$ or $\lambda - 1$, for compression and elongation, respectively. Compressive fracture stress σ_f was calculated from the maxima of σ_{true} vs ε curves, as detailed previously [52]. Young's modulus E was calculated from the slope of the stress-strain curves between 5 and 15% deformations. Cyclic compression tests were carried out by compressing the gel specimens at a strain rate of 1 mm·min^{-1} up to a predetermined maximum strain, and then unloading with the same strain rate to zero strain. These loading and unloading steps were repeated with a wait time of 1 min between the cycles. Uniaxial tensile tests were conducted using cylindrical gel specimens of 4.6 mm in diameter and 10±2 mm in length at a strain rate of 5 mm·min^{-1}.

5.2 Results and Discussion

Methacrylated hyaluronic acid (GMHA), silk fibroin (SF), and N, N'-dimethyl acrylamide (DMA) are the starting materials of the present biocompatible, biodegradable composite hydrogels (Fig. 5.1). The methacrylation degree of GMHA was determined as 4, 14, and 25% for the molar ratios of glycidyl methacrylate to disaccharide repeat units of 6, 24, and 49, respectively. The initial concentrations of DMA, and SF were fixed at 5.0, and 2.5 w/v %, respectively, while GMHA was used at 1 and 2 w/v % concentrations with methacrylation degrees (DM) of 4, 14, and 25%. To highlight the effect of SF, all gelation reactions were also conducted in the absence of SF. In the following paragraphs, we first discuss gelation mechanism of the reaction system and then describe the viscoelastic, swelling, and mechanical properties of the hydrogels by highlighting significant effects of SF and methacrylation degree of HA on the hydrogel properties.

5.2.1 Gelation

We monitored hydrogel formation by rheometry using oscillatory deformation tests at an angular frequency ω of 6.3 rad s^{-1} and strain amplitude γ_o of 1%. Blue symbols in Figures 5.2a, b show the storage modulus G' and the loss factor $tan\ \delta$ (= G''/G' where

G'' is the loss modulus) of the reaction solutions, respectively, plotted against the reaction time. GMHA macromers with three different degrees of methacrylation (DM) were used in the gel preparation, as indicated in the figure. During the initial period of the reaction, *G'* rapidly increases to around 1 kPa and *tan δ* decreases to around 0.1 followed by a plateau regime where *G'* and *tan δ* remain almost unchanged. However, at longer times, *G'* starts to increase again and approaches to a second plateau at 10^2 kPa. We have to note that, to prevent evaporation of water, the reactions between the plates of the rheometer could be monitored up to 5 h (Figure 5.2a). Therefore, the limiting moduli G'_∞ of the hydrogels was estimated by fitting the data of the second reaction period to the modified Hill equation [42,43,65]:

$$G'(t) = G'_\infty \frac{t^n}{t^n + \theta^n} \tag{5.1}$$

where θ and n are constants. The solid red curves in Figure 1a are the best fits of eq 5.1 to the experimental data yielding G'_∞ as 65, 78, and 20 kPa at 4, 14, and 25% DM, respectively (Figure 5.2c).

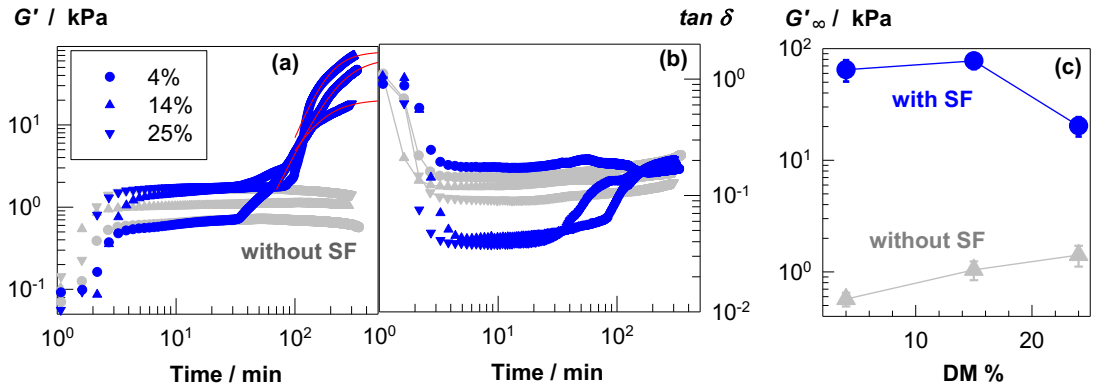

Figure 5.2 : (a, b): Storage modulus *G'* (a) and the loss factor *tan δ* (b) of the reaction solutions plotted against the reaction time. ω = 6.3 rad s^{-1}. γ_o = 0.01. Temperature = 50 °C. GMHA = 1 w/v%. Methacrylation degrees (DM) of GMHA are indicated. Gray symbols represent the data obtained in the absence of silk fibroin. **(c)**: Limiting modulus (G'_∞) of the hydrogels with and without SF plotted against DM.

To explain this unusual two-step gelation profile of the reaction system, we repeated the measurements on the same reaction solutions but without including silk fibroin (SF). The results are also shown in Figures 5.3a, 3b by gray triangles. It is seen that, in the absence of SF, the first reaction period closely matches to that with SF whereas the second period disappears from the gelation profile, suggesting that the second rise

in *G'* is due to the presence of SF in the reaction system. The final modulus of the hydrogels without SF shown in Figure 5.2c by the gray symbols is more than one-order of magnitude smaller than that with SF. The results indicate that the cross-linking copolymerization of GMHA and DMA during the first reaction period dominates the viscoelastic properties of the reaction system and produces hydrogels with a modulus of around 1 kPa, whereas at longer times fibroin gelation dominates their viscoelasticity by further increasing the modulus to 20-78 kPa.

Previous work shows that gelation of aqueous SF solutions occurs due to the conformational transition in SF from random-coil or helix to β-sheet structures leading to the formation of SF hydrogels in which intermolecular β-sheets act as physical cross-links [97,98]. Because the rate of fibroin gelation is slow as compared to many proteins gels, one may expect that β-sheet structures start to form in the present reaction system during the second period of the reaction accompanied with a significant increase in the modulus *G'*. FTIR technique is a mean to detect conformational transitions in silk fibroin and to estimate the β-sheet contents. Amide I region of the FTIR spectrum of SF is characterized by a broad peak at around 1640 cm^{-1} due to the presence of primarily random-coil and α-helix conformations while appearance of a main peak at 1620 cm^{-1} indicates β-sheet conformation (Figure 5.3) [40,99]. However, PDMA component of the hydrogel also exhibited a peak at 1610 cm^{-1} due to C=O stretching and hence, this technique could not be used to estimate the content of the β-sheets in the hydrogels (Figure 5.3).

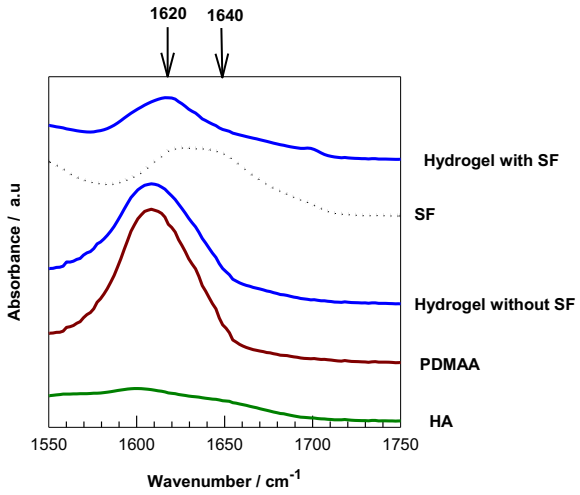

Figure 5.3 : Amide-I region of FTIR spectra of freeze-dried SF solution (dotted curve), HA, PDMA, and hydrogels with and without SF.

Therefore, the structure of SF in the hydrogels was assessed by XRD measurements. Figure 5.4a shows typical X-ray profiles of freeze-dried hydrogels with and without SF together with SF alone. SF exhibits a broad peak from 15 to 28° indicating an amorphous structure (dotted curve) [96]. To induce β-sheet domains in SF, an aqueous solution of 2.5 w/v% SF was heated at 50 °C for 2h. The blue curve in Figure 5.4b represents XRD pattern of this SF solution after freeze-drying. It exhibits diffraction peaks at 2θ values of 11°, 20.5°, and a shoulder at 24° corresponding to crystalline spacings of 0.80, 0.43, and 0.37 nm, which are typical for Silk II structure [96,100]. Thus, as expected, a conformation transition from random-coil and helix to the β-sheet structure occurs after heating SF solution to 50°C. Figure 5.4a also shows that freeze dried hydrogels exhibit the same peaks while no distinct peaks appear in the XRD pattern of SF-free hydrogel. Thus, XRD results confirm the formation of β-sheet structure during the gelation reactions leading to a significant increase in the modulus of the hydrogels.

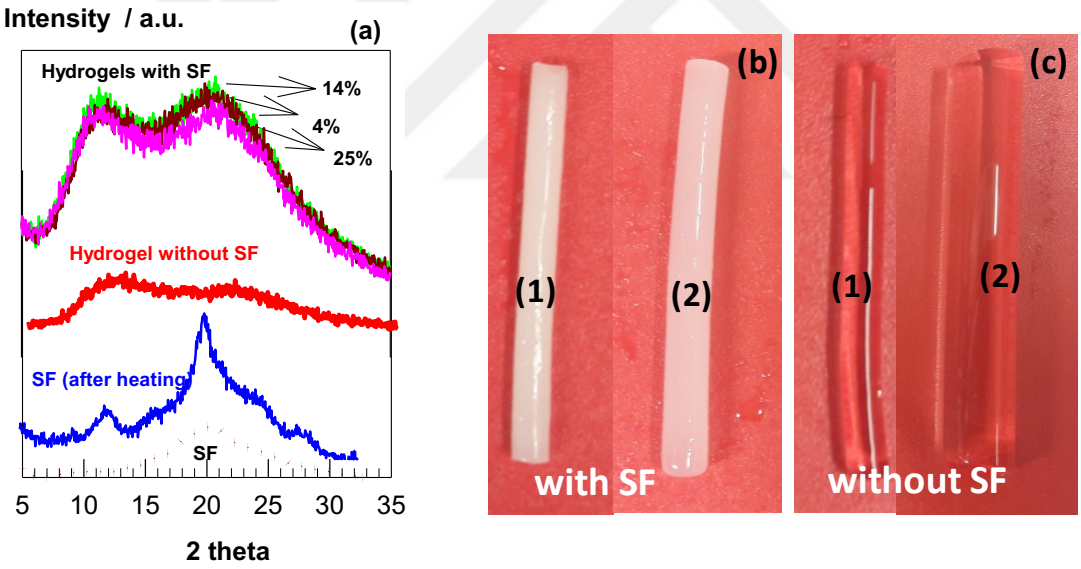

Figure 5.4 : (a): X-ray diffraction of freeze-dried 2.5 w/v % SF solutions before (dotted curve) and after heating to 50 °C (blue curve), and composite hydrogels with and without SF. Methacrylation degree DM of GMHA is indicated. (b, c): Photographs of the hydrogels with (b) and without SF in as-prepared (1) and swollen states in water (2).

Formation of nano-sized crystalline domains in the hydrogels was also reflected from their visual appearances. Figures 5.4b, c show images of the hydrogels prepared with and without silk fibroin, respectively, in as-prepared (1) and equilibrium swollen states in water (2). As compared to the transparent SF-free hydrogels, those containing SF are opaque and exhibit a lesser degree of swelling reflecting the effect of β-sheets as

additional cross-links. DSC measurements conducted on freeze-dried hydrogels showed a broad endothermic peak at around 100 °C due to the loss of moisture remaining after freeze-drying (Figure 5.5). However, the characteristic peaks of the gel components SF, GMHA, and PDMA did not appear in the DSC scans of the hydrogels, and they all start to degrade at around 300 °C (Figure 5.5).

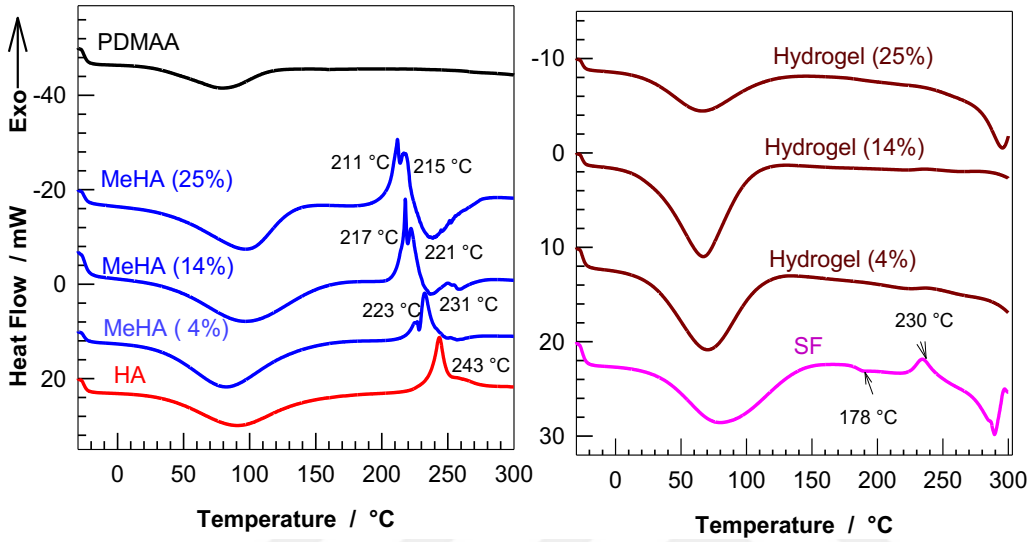

Figure 5.5 : DSC scans of freeze-dried gel components and composite hydrogels. The numbers in parentheses are the methacrylation degrees of GMHA.

The following scenario may explain the two-step gelation mechanism of the present system (Fig. 5.6). After addition of APS/TEMED redox initiator system into the reaction solution containing GMHA, DMA and SF, primary radicals attack to DMA monomer to produce growing PDMA chains interconnected by GMHA cross-links (Fig. 5.6a-c). These reactions result in GMHA-cross-linked hydrogels with a storage modulus of around 1 kPa (Fig. 5.6c). Because of the slow rate of fibroin gelation, conformational transition in fibroin starts at longer reaction times leading to a second rise in the storage modulus due to the increasing number of β-sheets acting as additional cross-links (Fig. 5.6d).

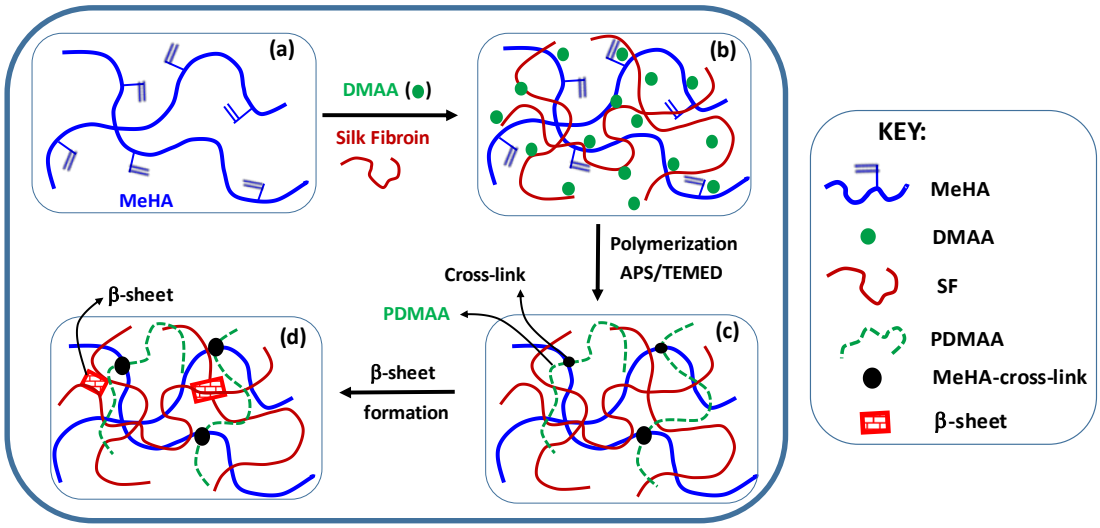

Figure 5.6 : Cartoon showing formation of silk-hyaluronic acid hydrogels using DMA monomer acting as a spacer.

5.2.2 Hydrogel properties

Composite hydrogels after a reaction time of 5 h were subjected to frequency-sweep tests at 25 °C and at a strain amplitude γ_o of 1%. Figure 5.7 shows the storage *G'* (filled symbols) and loss moduli *G''* (open symbols) of the hydrogels prepared with and without SF plotted against the angular frequency ω. The methacrylation degree of GMHA is 4 (a), 14 (b), and 25% (c). The hydrogels prepared without SF exhibit typical behavior of HA hydrogels [65], i.e., at low ω, G'' attains low values and $tan\ \delta$ approaches to 0.01 (not shown in the figures), corresponding elastic, solid-like behavior. At high ω, G'' approaches to G' and the gels exhibit a viscous character. After incorporation of fibroin into the hydrogel network, both moduli become slightly frequency dependent and no crossover of *G'* and *G''* occurs. Further, *G'* modulus becomes one-order of magnitude higher than that of SF-free gels highlighting significant effect of fibroin on the hydrogel properties. The results also show that *G'* first increases with increasing DM from 4 to 14% but then decreases with a further increase in DM to 25%. The decrease of the modulus at 25% DM is also observable in the gelation profiles (Figure 5.2) which is attributed to the steric effect of chemical GMHA-cross-links hindering formation of β-sheet domains.

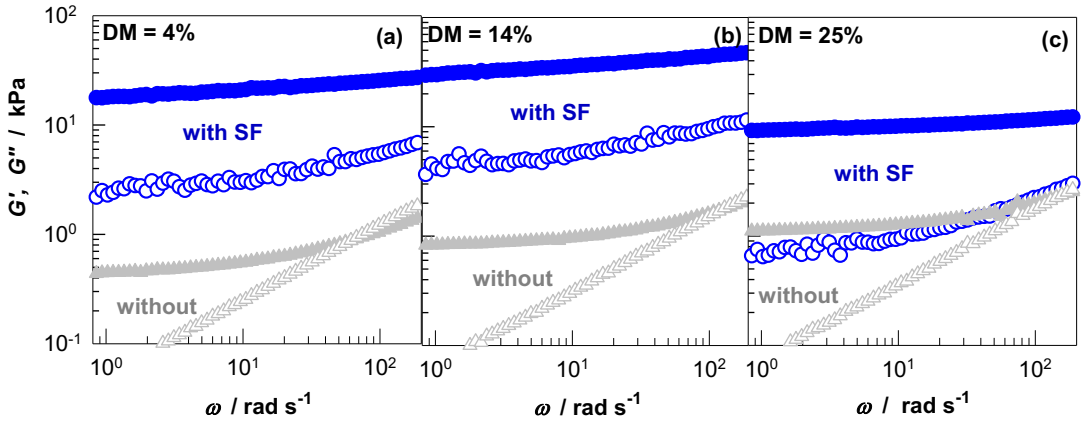

Figure 5.7 : *G'* (filled symbols), and *G''* (open symbols) of the hydrogels with (blue circles) and without SF (gray triangles). γ_o = 0.01. GMHA = 1 w/v%. DM = 4 (a), 14 (b), and 25% (c). Temperature = 25 °C.

After a reaction time of 2 days, hydrogels were subjected to the solubility and swelling tests in water. All hydrogels with or without SF were insoluble in water with a gel fraction between 0.85 and 0.98 indicating that GMHA, SF, and PDMA components are incorporated into the 3D network (Table 5.1). Figure 5.8a shows the degree of swelling (m_{rel}) of the hydrogels plotted against the methacrylation degree (DM) of GMHA. As expected from the storage moduli of the hydrogels (Figure 5.2c), those with SF swell much less than without SF because of the presence of β-sheet cross-links. Further, the higher the DM, the lower is the degree of swelling of the hydrogels with or without SF, reflecting the effect of the functionality of GMHA cross-linker on the gel cross-link density. Mechanical properties of the hydrogels were determined by uniaxial compression and tensile tests. Figures 5.9a, b show compressive stress-strain curves of the hydrogels prepared using GMHA with different degrees of methacrylation DM in their as-prepared (a) and swollen states (b). The gray curves are the data obtained from hydrogels prepared without SF addition. A significant increase in both stiffness and fracture stress is observable upon incorporation of SF in the gel network. For instance, at DM = 4%, both Young's modulus *E* and fracture stress σ_f of as-prepared gels increase from 5 to 54±5 kPa and from 0.6 to 4.9 MPa, respectively, after incorporation of SF in the gel network (Figure 5.10). Simultaneously, the toughness W calculated from the area under the stress-strain curves up to the fracture point increases from 19±2 to 320±6 kJ m^{-3} after SF addition (Table 5.3).

Table 5.1 : Compositions, swelling and compressive mechanical properties of the hydrogels. Standard deviations are shown in the parentheses. They are less than 5% for m_{rel} and W_g values. Note that for each hydrogel, at least five swelling and mechanical measurements from different specimens were averaged. (see Table 5.2 for the tensile mechanical properties)

DM %	GMHA w/v%	SF w/v%	m_{rel}	H_2O %	W_g	σ_f / MPa	E / kPa	ε_f %	σ_f / kPa	E / kPa	ε_f %
						As-prepared state			After equilibrium swelling		
4	1	2.5	2.8	98	0.92	4.9	54 (5)	94	448 (98)	14 (1)	78
14	1	2.5	2.2	98	0.95	3.4	82 (5)	91	323 (49)	41 (9)	70
25	1	2.5	1.9	99	0.96	2.5	99 (11)	86.6	288 (21)	48 (3)	70
4	2	2.5	4.7	97	0.87	3	30 (3)	85	224 (40)	42 (5)	63
14	2	2.5	3.1	97	0.89	1.1	52 (4)	77	207 (39)	59 (5)	59
25	2	2.5	2.2	98	0.85	0.9	81 (11)	70	118 (19)	99 (8)	48
4	1	0	17.2	98	0.96	0.6	5	88	85 (7)	4	72
14	1	0	9.3	96	0.97	0.4	8	84	51 (5)	5	62
25	1	0	5.3	98	0.97	0.4	13 (2)	79	26 (6)	11 (2)	53
4	2	0	13.6	99	0.96	1.2	11(1)	88	31 (3)	6	62
14	2	0	7.1	97	0.97	0.6	17 (3)	82	79 (3)	13 (1)	59
25	2	0	4.5	98	0.98	0.4	22 (3.3)	74	57 (4)	18 (1)	54

Table 5.2 : Tensile mechanical properties of the hydrogels. Standard deviations are shown in the parentheses.

DM %	GMHA w/v%	SF w/v%	σ_f / kPa	ε_f %	W / $kJ\ m^{-3}$
4	1	2.5	65 (5)	4.4 (0.5)	170 (40)
14	1	2.5	57 (2)	2.9 (0.3)	83 (16)
25	1	2.5	52 (2)	2.1 (0.1)	38 (8)
4	1	0	3 (0.5)	5.4 (0.5)	9 (2)
14	1	0	4 (0.6)	3.9 (0.1)	8 (0.8)
25	1	0	6 (0.7)	3.2 (0.3)	8 (2)

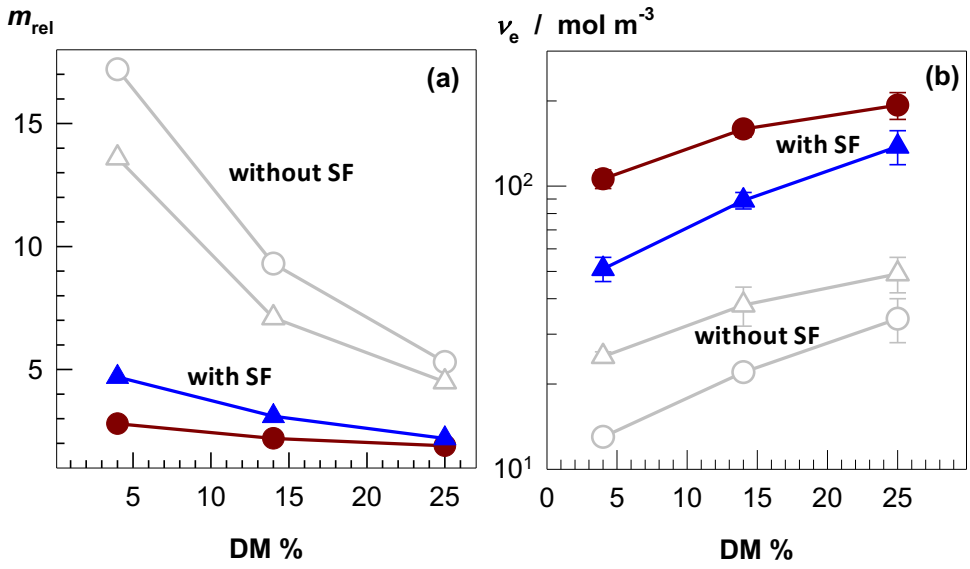

Figure 5.8 : Swelling ratio m_{rel} (a) and effective cross-link density ν_e of composite hydrogels plotted against the methacrylation degree (DM) of GMHA. Gray symbols represent data of the hydrogels without SF. GMHA = 1 (●, ○), and 2 w/v % (▲, △).

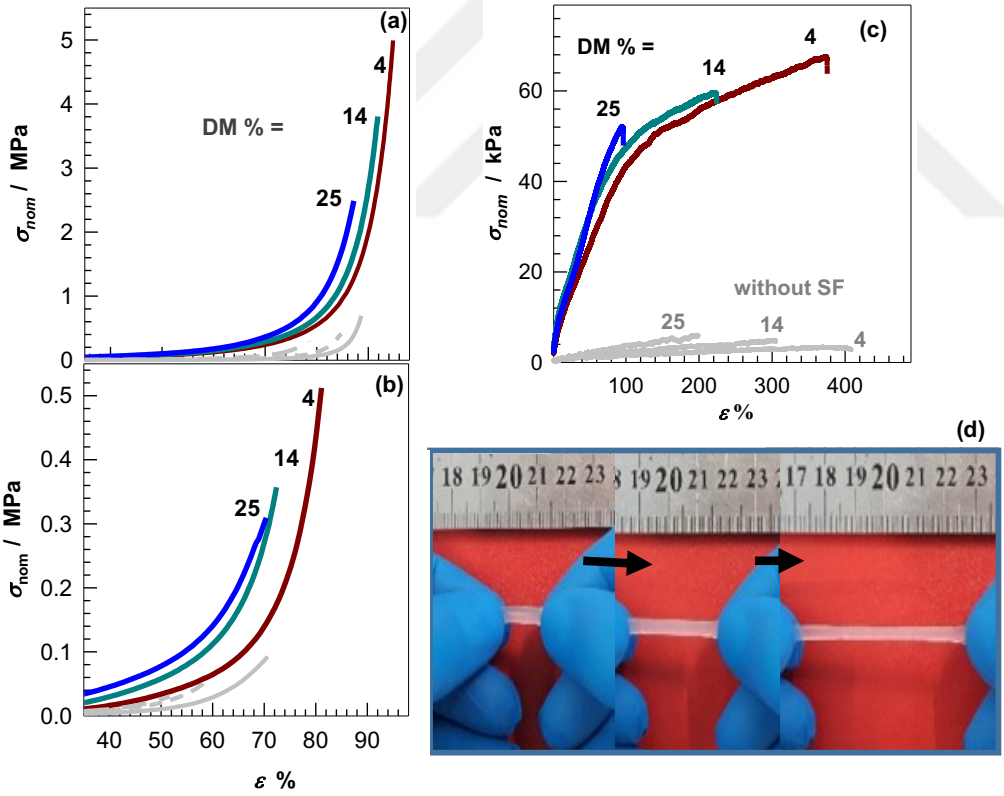

Figure 5.9 : (a, b): Compressive stress-strain curves of the hydrogels in as-prepared (a) and water-swollen states (b). GMHA = 1 w/v %. The data of SF-free hydrogels are shown by the gray solid, short-dash, and long-dash curves corresponding to DM = 4, 14, and 25%, respectively. (c): Tensile stress-strain curves of the hydrogels in as-prepared state. GMHA = 1 w/v %. (d): Photograph of a hydrogel sample with DM = 4% during stretching by hand to around 300% stretch ratio.

Table 5.3 : Toughness (*W*) of the hydrogels. Standard deviations are shown in the parentheses.

DM %	GMHA w/v%	SF w/v%	W / kJ m^{-3}	
			As-prepared state	After equilibrium swelling in water
4	1	2.5	320 (6)	42 (2)
14	1	2.5	250 (30)	37 (1)
25	1	2.5	200 (30)	40 (3)
4	2	2.5	166 (17)	26 (6)
14	2	2.5	97 (20)	25 (4)
25	2	2.5	76 (10)	15 (1)
4	1	0	19 (2)	6
14	1	0	17 (2)	4
25	1	0	20 (4)	3 (1)
4	2	0	43 (4)	3
14	2	0	32 (5)	7
25	2	0	24 (1)	6

Moreover, increasing the methacrylation degree DM also increases the modulus E of the hydrogels whereas the fracture stress σ_f and strain ε_f decrease (Figure 5.10). A similar effect was observed upon increasing GMHA content of the hydrogels (Figure 5.11). Because increasing DM or GMHA concentration also increases the number of pendant vinyl groups in the reaction system, the chemical cross-link density and hence the modulus increases but the toughness decreases due to the stress localization in chemically cross-linked networks under stress [101]. An opposite effect appears upon incorporation of SF indicating that fibroin molecules interconnected by the β-sheet domains reduces stress localization and creates energy dissipation mechanism in the gel network. The results also show that swelling of the hydrogels decreases their mechanical properties due to the dilution of the network chains. However, they still exhibit a high modulus (up to 99±8 kPa) in equilibrium with water (Figure 5.10). Uniaxial tensile tests could only be conducted on as-prepared hydrogels because they were too slippery after equilibrium swelling in water. Tensile stress-strain curves shown in Figure 5.9c reveal that highly stretchable hydrogels were obtained at the lowest methacrylation degree DM of 4%. They sustain up to 350±50% stretch ratio under a stress of 70±10 kPa (Figure 5.10f). Because silk fibroin hydrogels are usually brittle in tension, presence of GMHA seems to contribute to the stretchability of the

composite hydrogels. Comparing tensile behavior of the hydrogels with and without SF reveals that stretch at break slightly reduces while tensile strength more than one order of magnitude increases after inclusion of SF in the gel network.

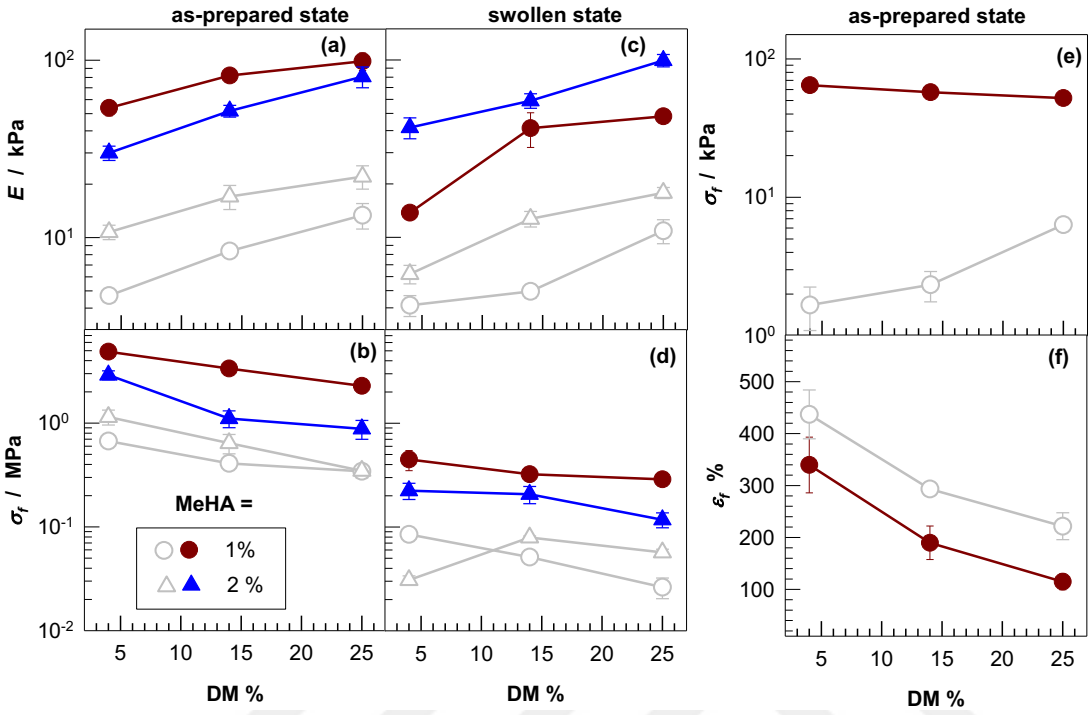

Figure 5.10 : (a-d): Young's modulus E and compressive strength σ_f of the hydrogels in as-prepared (left panel) and water-swollen states (right panel) plotted against the methacrylation degree (DM) of GMHA. Gray symbols represent the data of the hydrogels without SF. (e, f): Tensile strength σ_f and strain ε_f of the hydrogels with (filled symbols) and without SF (open symbols). GMHA = 1 w/v%.

From the swelling ratios m_{rel} of the hydrogels in water together with their Young's moduli E, we estimated their effective cross-link densities ν_e using the theory of elasticity [49,50]:

$$E = 3\nu_e RT\left(m_{rel}\right)^{2/3} \tag{5.2}$$

where R is the gas constant and T is the absolute temperature. Eq (5.2) assumes affine deformation of the polymer chains in the hydrogels under strain, and equality of the mass and volume swelling ratios. Figure 5.8b shows the cross-link density ν_e of the hydrogels with (filled symbols) and without SF (open symbols) plotted against DM. Incorporation of SF into the gel network enhances its cross-link density, and the enhancement effect becomes stronger with increasing degree of methacrylation of GMHA. For instance, assuming additivity of the cross-links due to the GMHA cross-links and β-sheets, the contribution of β-sheets to the cross-link density increases from

~30 to 60-70% with increasing DM from 4 to 25%. Thus, composite hydrogels exhibit a hybrid cross-linked structure composed of chemical and physical cross-links.

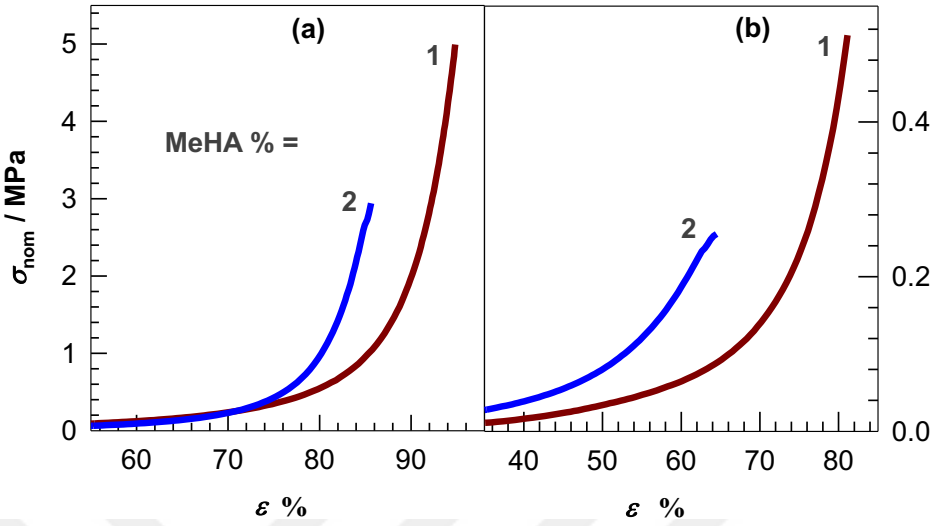

Figure 5.11 : Compressive stress-strain curves of the hydrogels with 1 and 2 w/v % GMHA in as-prepared (a) and water-swollen states (b). DM = 4%. SF = 2.5 w/v %.

For a deeper understanding of the nature of intermolecular bonds and the enhanced mechanical properties due to SF incorporation into the composite hydrogels, successive cyclic compression tests were conducted on the hydrogels prepared at DM = 4%. The tests consist of a loading step up to a maximum strain ε_{max} followed by the unloading step to zero strain. For an ideal elastic material, stress-strain curve of the unloading should follow that of the loading because there is no dissipation of the mechanical energy given to the material. Existence of energy dissipation under strain is reflected by the deviation between the paths of loading and unloading steps. Figure 5.12a shows five successive compressive cycles up to ε_{max} = 80% while Figure 5.12b shows the same cycles but with successively increasing ε_{max} from 40 to 80% in five steps. The wait time between each cycle for the relaxation of the gel specimens was fixed at 1 min. For a fixed ε_{max} of 80%, the first unloading strongly deviates from the loading indicating a significant energy dissipation due to the damage in the sample, i.e., due to the breaking of intermolecular bonds. However, the extent of this deviation decreases in the following cycles revealing that most of the bonds are broken during the first loading step.

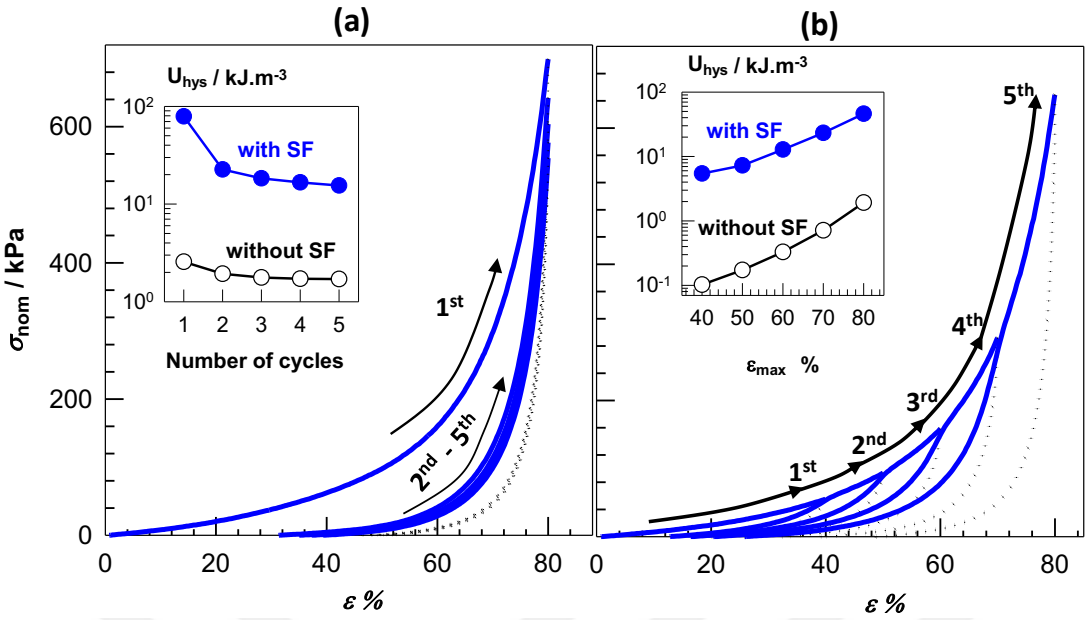

Figure 5.12 : Five successive compressive cyclic tests conducted up to a constant ε_{max} of 80% (a) and with successively increasing ε_{max} from 40 to 80% in five steps (b). Loading curves are indicated by the arrows. DM = 4%. GMHA = 1 w/v %. The insets show U_{hys} plotted against the number of cycles (a) and ε_{max} (b).

The filled and open symbols in the insets to the figures represent the hysteresis energies U_{hys} of the hydrogels with and without SF, respectively, calculated from the area between loading and unloading curves. Note that the hysteresis energy U_{hys} is directly related to the total number of bonds broken during compression up to ε_{max} [101,102]. As compared to the SF-free hydrogel, a significant hysteresis appears in composite hydrogel revealing damage of a larger number of β-sheet cross-links of the SF component (Figure 5.12a). The inset to Figure 5.12b show that the dissipated energy U_{hys} also increases with increasing maximum strain ε_{max}, and the extent of U_{hys} increase is much larger in the composite hydrogels as compared to the SF-free ones. We attribute the enhancement in the mechanical properties of the hydrogels upon incorporation of SF to the energy dissipation of SF network under strain. For instance, the toughest hydrogel reported so far in the literature are double-network (DN) hydrogels composed of a brittle first network and ductile second network [33]. The first network in DN's breaks into smaller clusters under strain by dissipating energy whereas the second network keeps the macroscopic gel sample together, leading to extraordinary mechanical properties. For the present composite hydrogels, β-sheet domains of the brittle SF network break under strain by dissipating energy leading to improved mechanical properties as compared to the individual SF or HA hydrogels.

5.3 Conclusions

We presented a novel strategy for the preparation of mechanically robust and stretchable hydrogels composed of HA and SF components. Composite hydrogels were synthesized from methacrylated HA (GMHA), SF, and DMA in aqueous solutions in the presence of APS/TEMED redox initiator system. It was found that in-situ produced PDMA chains are interconnected by GMHA cross-links whereas SF undergoes a conformation transition from random coil to β-sheet structures. A significant enhancement in the mechanical strength of the hydrogels was observed upon incorporation of SF due to its β-sheet domains acting as additional physical cross-links. Cyclic mechanical tests reveal that the damage in SF network under strain leads to a significant energy dissipation, which is responsible for the improved mechanical properties of SF/HA hydrogels. A wide range of tunable mechanical and swelling properties could be achieved by varying the methacrylation degree of GMHA. Because GMHA, SF, and PDMA exhibit good biocompatibility, the composite hydrogels presented here are a good candidate as biomaterials in biological and biomedical applications. Moreover, because HA and SF components were combined in a single hydrogel material, present results would expand the range of properties and applications available to HA and SF individually.

6. MACROPOROUS METHACRYLATED HYALURONIC ACID CRYOGELS OF HIGH MECHANICAL STRENGTH AND FLOW-DEPENDENT VISCOELASTICITY[5]

Hyaluronic acid (HA), a significant component of the extracellular matrix, is a high-molecular weight natural polysaccharide with a large water holding capacity due to its polyelectrolyte nature [1]. Although HA attracts significant interest over many years in soft tissue regeneration due to its excellent lubricating, self-healing, and biological functions [2,83], easy degradability and weak mechanical behavior of HA limit its application areas [84,85]. To overcome these limitations, hydrogels based on native or chemically modified HA have been reported [21,22,32,85]. Several cross-linkers including ethylene glycol diglycidyl ether (EGDE), glutaraldehyde, and divinyl sulfone have been used in the preparation of HA hydrogels [9–15]. Alternatively, HA was first modified to incorporate methacrylate groups to enable cross-linking, and then polymerized to form HA hydrogels [21–23]. It was shown that the hydrogels based on both native and methacrylated HA exhibit a good biocompatibility as well as a slow rate of degradation as compared to the native uncross-linked HA [31]. However, these hydrogels are generally brittle in nature because of the lack of an effective energy dissipation in the covalently cross-linked HA network [16,57].

Recently, we have shown that an improvement in the mechanical properties of HA hydrogels could be achieved when silk fibroin is incorporated into the HA network that forms β-sheet crystallites acting as physical cross-links [103]. Another strategy is double- or triple-networking of HA hydrogels with ductile network components based on poly(N,N-dimethylacrylamide) (PDMA) [31,32], a non-cytotoxic polymer for various applications interfacing with biological systems such as in medicine [104–108]. Although a mechanical property improvement in the resulting double- or triple-

[5] This chapter is based on the paper "Tavsanli, B. and Okay, O. (2020). Macroporous methacrylated hyaluronic acid cryogels of high mechanical strength and flow-dependent viscoelasticity. *Carbohydrate Polymers*, 229, 115458."

network HA hydrogels could be achieved, this multi-step synthetic procedure is lengthy and complicated.

Cryogelation is a simple and versatile technique for the fabrication of macroporous hydrogels, also called cryogels [20,66,109]. It is also more environmentally friendly as compared to alternative techniques because water is generally used as the solvent, and there is no need to use organic solvents as porogens. The principle of this technique is to carry out the cross-linking reactions of linear polymers in aqueous solutions below their freezing points. As water freezes, polymer chains rejected from the ice and concentrated in the unfrozen regions result in the formation of a highly concentrated solution phase, called cryoconcentration. Thus, cryogelation system at thermal equilibrium with the surrounding is composed of a concentrated polymer-cross-linker solution together with the ice template distributed along the system [20]. Cryogelation leads to the formation of cross-linked polymers even at very low polymer concentrations due to the fact that the effect of the cryoconcentration commonly dominates over the reduction in the cross-linking rates at low temperatures. After cryogelation and melting of ice temple, a 3D polymer network containing macropores is obtained.

Physically cross-linked HA cryogels exhibiting a storage modulus of around 100 Pa were prepared via freeze-thaw induced gelation at a low pH [110]. HA cryogels sustaining up to around 30 kPa compressive stresses have also been prepared in an aqueous NaOH solution (pH > 10) of HA at -18 °C using EGDE as a chemical cross-linker [18]. However, the selection of a NaOH solution as the solvent to conduct the cross-linking reactions is not appropriate as it promotes the degradation of HA [19,65]. It seems challenging to produce macroporous HA hydrogels and scaffolds with appropriate mechanical properties to closely mimic mechanical properties of the extracellular matrix, structural stability, and an effective mechanism of energy dissipation under strain.

We present here a new cryogelation approach for the fabrication of macroporous HA cryogels with a wide variety of properties, flow-dependent viscoelasticity (poroelasticity), complete squeezability, and a high mechanical strength. HA cryogels were synthesized from methacrylated HA of varying methacrylation degree in aqueous solutions at -18 °C by free-radical mechanism using a redox initiator system. Our preliminary experiments showed that methacrylated HA alone could not form water-

insoluble cryogels likely due to the steric effect of HA molecules. However, incorporation of a small amount of a vinyl monomer such as N, N-dimethylacrylamide (DMA) in the feed resulted in a complete gelation at -18 °C. This reveals spacer effect of PDMA chains interconnecting HA units, as illustrated in Fig. 6.1. As will be seen below, HA cryogels in swollen state sustain up to 2.6 ± 0.2 MPa compressive stress, which is around 2 orders of magnitude higher than those obtained by EGDE cross-linker [18]. HA cryogels confined between parallel plates also exhibit reversible strain-dependent apparent gel-to-sol transition behavior due to the flowing-out and flowing-in water through the pores, similar to water squeezing out of a sponge. This flow-dependent viscoelasticity of HA cryogels, known as poroelasticity [111–113], is similar to that observed with articular cartilage [114], a low-friction and load bearing soft tissue, providing the joint with vital biomechanical functions, such as wear resistance, load bearing, and shock absorption for around a century. Under compression, the liquid within the cartilage flows out of the tissue through the pores, as observed in HA cryogels, which produces high frictional resistance and hence frictional energy dissipation responsible for the viscoelastic behavior of articular cartilage [114]. Gel-to-sol transition behavior of HA cryogels presented here is also of great interest in biomaterial and biomedical applications as it protects HA network from damage under large strain conditions and hence acts as a self-defense mechanism.

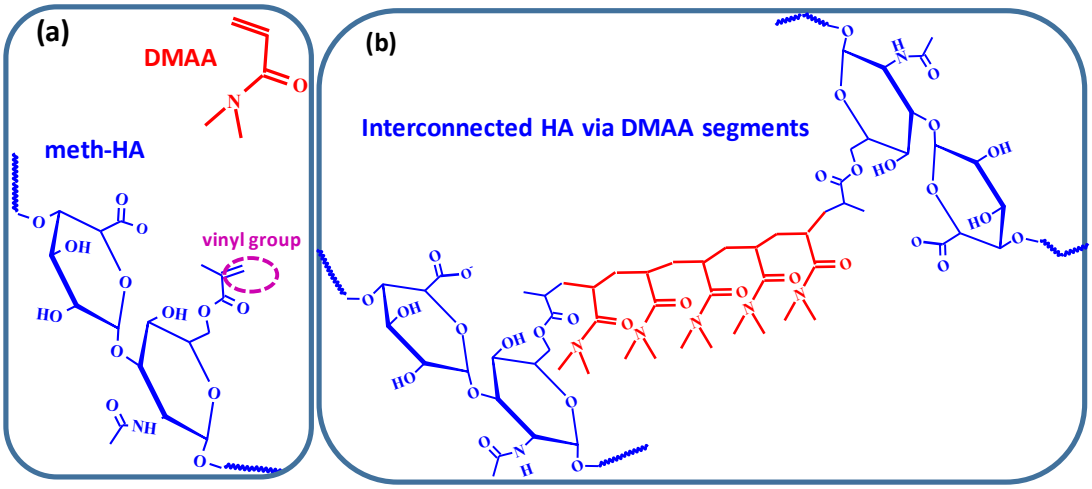

Figure 6.1 : DMA and repeat unit of methacrylated HA (GMHA, blue) before (a) and after interconnecting with DMA segments (red). Note that the reaction between glycidyl methacrylate and HA to form GMHA proceeds via transesterification and ring opening routes [21,32]. For the sake of clarity, the chemical structure of GMHA formed by the former route is shown in (a).

6.1 Experimental Part

6.1.1 Materials

The sodium salt of hyaluronic acid from Streptococcus equi (HA) with a viscosity average molecular weight of ~1.2×10^6 g·mol^{-1} [18], glycidyl methacrylate (GM), N,N-dimethylacrylamide (DMA), tetrabutylammonium bromide (TBAB), ammonium persulfate (APS), N,N,N',N'-tetramethylethylenediamine (TEMED), all from Sigma-Aldrich, triethylamine (TEA, Merck), and acetone (Tekkim, Turkey), were used as received. A stock solution of APS was prepared by pipetting 10 mL distilled water onto 0.8 g APS and dissolving at 23 ±2 °C. HA was methacrylated following a protocol by Leach et al. [21]. In short, 0.5 g of HA was added into 50 mL distilled water and stirred overnight for complete dissolution. GM (1 mL), TEA (1 mL), and TBAB (1 g) were then dissolved in this HA solution to obtain a GM / disaccharide repeat unit molar ratio of 6. After the reaction at 55 °C, the solution was precipitated in an excess of acetone and dissolved in distilled water twice. The solution of methacrylated HA (GMHA) was then freeze-dried for 2 days. Fourier transform infrared (FTIR) spectroscopy was used to demonstrate the incorporation of methacrylate groups onto the HA backbone (Figure 6.2). The methacrylation degree of GMHA was determined from nuclear magnetic resonance (NMR) spectra recorded on a 500 MHz Agilent VNMR spectrometer, as reported before [21,32] (Figure 6.3).

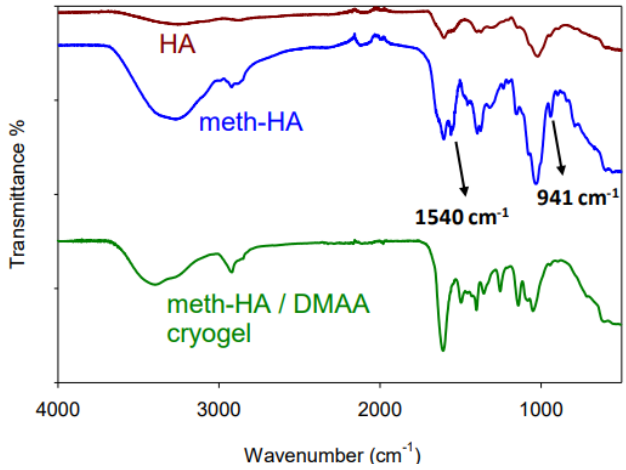

Figure 6.2 : FTIR-ATR spectra of native HA, GMHA, and freeze-dried HA cryogel. GMHA was prepared at a GM/HA molar ratio of 6. DMA content of the cryogel = 0.5 wt %. The spectra were recorded on a Nicolet Nexus 6700 spectrophotometer using a single-bounce diamond ATR accessory equipped with a liquid nitrogen cooled mercury–cadmium–telluride (MCT) detector. 64 interferograms at 4 cm^{-1} resolution were co-added to generate each spectrum.

The appearance of the peaks at 941 and 1540 cm^{-1} in the spectrum of GMHA indicates the presence of the methacrylate carbon-to-carbon double bonds that disappear after cryogelation indicating incorporation of GMHA into the cryogel network.

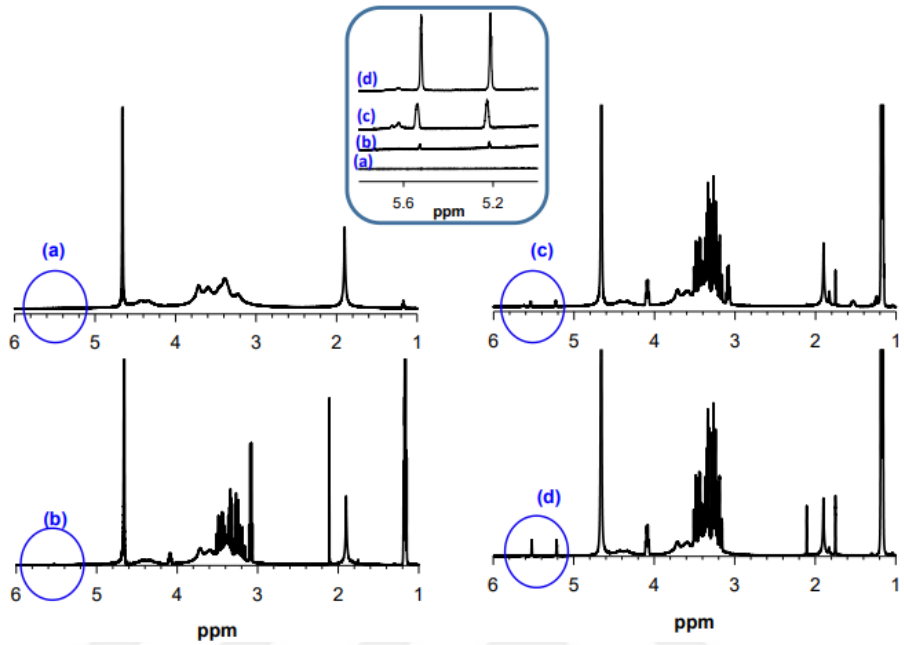

Figure 6.3 : ^{1}H NMR spectra of native HA (a) and GMHA prepared at GM/HA molar ratios of 6 (b), 24 (c), and 49 (d). The region between 5 and 6 ppm is highlighted in circles. The inset is a zoom-in of the 5.0–5.8 ppm region of the spectra. The peaks at 5.5 and 5.2 ppm are indicative of methacrylate groups. The degree of methacrylation was determined by integration of the methyl peak of HA at 1.9 ppm and the methacrylate peaks. The methacrylation degrees are 4, 14, and 25% for b, c, and d, respectively.

6.1.2 Preparation of cryogels

Methacrylated HA (GMHA) with methacrylation degrees of 4, 14, and 25% was used in the synthesis of the cryogels. In our experiments, the concentration of GMHA was set to 1 wt % whereas DMA concentration was varied between 0.5 and 5 wt %. Typically, to prepare cryogels at 1 wt % DMA, GMHA (0.100 g) was added into 9.8 mL distilled water and gently stirred overnight for complete dissolution. DMA (0.100 g) was then dissolved in this solution under stirring for 30 min. After cooling the solution to 4 °C under bubbling nitrogen to prevent gelation before freezing at -18 °C, TEMED (25 µL) and APS stock solution (0.1 ml) were added. The solution was then poured into 1-mL plastic syringes and cylindrical glass vials of 4.6 and 40 mm in internal diameters, respectively, that were immersed in a deep freezer at -18 ºC and the cryogelation reactions were conducted for 5 days.

6.1.3 Quantifying the amount of unfrozen water during cryogelation

Differential scanning calorimetry (DSC) was used to estimate the unfrozen water content and the true monomer concentration during cryogelation. Reaction solutions with 1 wt % GMHA and various amounts of DMA were first prepared without addition of the initiator system to avoid gelation. GMHA/DMA solutions were then poured into plastic syringes that were placed in a deep freezer at -18 °C for 24 h. Frozen specimens weighing approximately 20 mg were placed into the DSC pans of Perkin- Elmer Diamond DSC instrument which were then sealed and weighed. Each pan was cooled in the DSC to -18 °C, held at this temperature for 2 h, and then heated to 30 °C at a rate of 1 °C min^{-1}. The mass fraction f_{unf} of water remaining unfrozen in GMHA/DMA solution at -18 °C was calculated as:

$$f_{unf} = 1 - \frac{\Delta H}{\Delta H_m} \tag{6.1}$$

where ΔH and ΔH_m are the melting enthalpies of frozen water in the specimen in kJ mol^{-1}, and of ice (6.01 kJ mol^{-1}), respectively.

6.1.4 Characterization of HA cryogels

The measurements of the swelling degrees and gel fractions were performed by immersing the cryogel specimens of about 1 cm in length in an excess of water at 23 ± 2 °C for 1 week to remove soluble species, followed by freeze-drying (Christ Alpha 2e4 LD-plus) for 2 days. The gel fraction W_g, that is the mass of water-insoluble HA-DMA network obtained from one gram of GMHA and DMA was calculated as:

$$W_g = \frac{m_{dry}}{m_o C_o} \tag{6.2}$$

where m_{dry} and m_0 represent the masses of the specimens in freeze-dried state and just after preparation, respectively, C_o is the concentration of GMHA and DMA in the initial reaction solution. The equilibrium swelling ratios of HA cryogels in water by weight q_w and volume q_v were calculated as:

$$q_w = \frac{m_s}{m_{dry}} \tag{6.3}$$

$$q_v = \left(\frac{D_s}{D_{dry}} \right)^3 \tag{6.4}$$

where m_{dry} and D_{dry} are the mass and the diameter of freeze-dried samples, respectively, and m_s and D_s are the same quantities for samples in their equilibrium swollen states in water.

Rheological measurements were carried out on a Gemini 150 rheometer system (Bohlin Instruments) equipped with 40 mm parallel plates, a solvent trap filled with water to avoid water evaporation, and a Peltier device for temperature control. The gap distance was set to 800-1200 μm depending on the sample thickness. The measurements were conducted on the cryogels prepared in cylindrical glass vials of 40 mm in internal diameter that were cut into 1.0 ± 0.2 mm slices with a razor blade. The angular frequency ω dependences of the storage G' and loss moduli G'' of the cryogels were determined at a fixed strain γ_o of 1% which was within the linear viscoelastic range of HA cryogels.

The porous structure HA scaffolds was investigated using scanning electron microscopy (SEM) measurements conducted on a Tescan GAIA 3 Field Emission SEM. The measurements were performed on freeze-dried gel specimens after sputter-coating with gold-palladium on a Leica ACE 600 instrument. The average diameter D of the pores was calculated using ImageJ image processing software (NIH) with data from 50 pores of at least 10 SEM images of different magnification. The porous morphology of freeze-dried HA scaffolds was also studied using micro-computed tomography (μ-CT) scanning conducted on a μ-CT Skyscan 1272 instrument (Skyscan, Bruker, Belgium), as detailed before [115]. The following parameters were used: Voltage = 55 kV, current = 60 μA, pixel resolution = 8 μm, integration time = 70 ms.

Mechanical compression tests were conducted at 23 ± 2 °C on a Zwick Roell instrument using 500 N load cell. An initial compressive force of 0.01 N was applied before the tests to ensure a complete contact between the specimen and the plates. Cubic gel specimens with dimensions 3x3x3 mm were used for the measurements. The tests were carried out at 0.3 and 1 mm·min^{-1} strain rates below and above 15% compression, respectively. The nominal stress σ_{nom} which is the force per cross-sectional area of undeformed specimen and the fractional deformation ε were recorded.

Young's modulus E was calculated from the 5-15% strain region in the stress–strain curves. The compressive strength and compression at break were estimated from the maxima of true stress–strain curves [52] (for details, see the section 6.1.5 and Figure 6.4).

The swelling ratios, gel fractions, and mechanical data reported here are averages of experiments performed at least in duplicate. They all are collected in Table 6.1 and expressed as means ± SD.

6.1.5 Determination of compressive fracture stress of the cryogels

The compressive fracture stress values of the cryogels were calculated from the maxima of true stress–strain curves, where the true stress σ_{true} is the force per cross-sectional area of the deformed gel specimen and, assuming isotropic deformation during compression, it is related to the nominal stress σ_{nom} by $\sigma_{\text{true}} = \lambda\, \sigma_{\text{nom}}$, where λ is the deformation ratio, i.e., $\lambda = 1 - \varepsilon$. For instance, Figures 6.4a, 6.4b show stress-strain curves of two cryogel samples as the dependences of the nominal σ_{nom} (solid black curves) and true stresses σ_{true} (dashed blue curves) on the strain ε. Although the nominal stress σ_{nom} continuously increases with increasing strain up to around complete compression, the corresponding $\sigma_{true} - \varepsilon$ plots pass through maxima at 96-99% compressions. This behavior is a result of the gel samples with microscopic cracks still supporting the stress and nonisotropic deformation of gel samples under large strain. Therefore, the fracture nominal stress σf and strain ε_f at failure were calculated from the maxima in $\sigma_{true} - \varepsilon$ plots, as indicated by the red arrows in the figures. The corrected $\sigma_{nom} - \varepsilon$ plots are shown in the figures by thick black curves. Thus, for the samples in Figures 6.4a and 6.4b, the fracture stresses σf are 3.6 and 2.5 MPa, respectively.

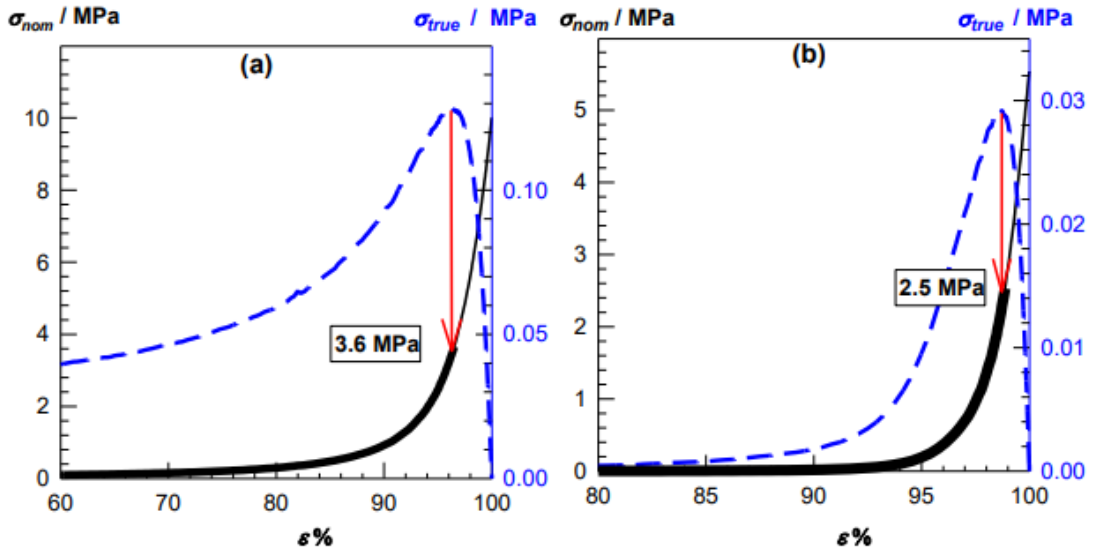

Figure 6.4 : Typical stress-strain curves of cryogels under compression as the dependences of nominal σ_{nom} (solid black curves) and true stresses σ_{true} (dashed blue curves) on the strain ε. The thick black curves are corrected $\sigma_{nom} - \varepsilon$ plots. (a): Freeze-dried HA cryogel formed at 4% Meth and 5 wt %. DMA. (b): Swollen HA cryogel formed at 4% Meth and 0.5 wt % DMA.

6.2 Results and Discussion

Hyaluronic acid (HA) cryogels were fabricated from methacrylated HA (GMHA) in aqueous solutions at -18 °C using APS-TEMED redox initiator system. GMHA with 3 different methacrylation degrees, namely 4, 14, and 25 % was used at a fixed concentration of 1 wt %. Because HA and its disaccharide repeating units have molecular weights of 1.2×10^6 and 416.2 g mol^{-1}, respectively, increasing the degree of methacrylation from 4 to 25% also increases the average number of pendant vinyl groups per HA chain from 115 to 720 and hence, increases its cross-linking functionality. Preliminary experiments conducted at various subzero temperatures and initiator concentrations showed no gel formation when GMHA was used alone in the cryogelation, which we attribute to the steric hindrance of HA molecules restricting the cross-linking reactions. However, incorporation of a small amount of a spacer such as N, N-dimethylacrylamide (DMA) into the monomer feed resulted in complete gelation. It is likely that GMHA acts as a multifunctional macro-cross-linker during the free- radical polymerization of DMA (Fig. 6.1). We selected DMA for the present research because poly(DMA) (PDMA) is a biocompatible polymer with several attractive properties [31,67,102,104–108]. Moreover, previous work shows that the redox-initiated polymerization of DMA without a chemical cross-linker in a moderately frozen aqueous medium leads to the formation of water-insoluble cryogels

[116]. Although the cross-link density of the resulting cryogels is low, the self-cross-linking ability of DMA may further contribute to the elasticity of the present HA cryogels. To highlight the effect of DMA on the cryogel properties, its concentration in the reaction solution was varied from 0.5 up to 5 wt %, above which no gel could be obtained.

6.2.1 Swelling behavior, squeezability, and flow-dependent viscoelasticity

After the cryogelation reactions, the reaction components GMHA and DMA were completely incorporated into the cryogel network, as evidenced by the gel fraction tests (Table 6.1). Figure 6.5a shows the equilibrium weight q_w (filled symbols) and volume swelling ratios q_v (open symbols) of HA cryogels with various DMA contents in water as a function of the methacrylation degree (Meth) of HA. HA cryogels have a large degree of swelling by weight q_w varying between 22 and 140, that decreases with increasing DMA content or Meth of HA. In contrast, the swelling ratio by volume q_v is 20- to 100- times smaller than q_w and almost independent of DMA content and methacrylation degree of HA (Table 6.1, Figure 6.6). For instance, Figure 6.5b shows images of a cryogel specimen formed at 5 wt % DMA and 25% Meth after preparation (image 1), after freeze-drying (image 2), and after swelling equilibrium in water colored with a dye (image 3). Although the volume change of the cryogel is negligible after swelling (q_v = 1.06±0.02), its mass 22-fold increases after swelling suggesting filling of the micro-voids in the cryogel with water without changing its volume. This is an indirect indication of the existence of a 3D open pore structure in HA cryogels, as will be detailed in the next section.

Another feature of water-swollen HA cryogels is that they can almost completely and reversibly be squeezed under force without any damage. This behavior is illustrated in Figure 6.5c showing the images of a swollen cryogel specimen in water colored with crystal violet. Compressing the specimen under load up to 90% strain squeezes out water from the cryogel network (down arrows in the images), whereas upon unloading, water released from the network is sucked back immediately and hence, the specimen autonomously recovers its original shape (up arrows). These cycles composed of squeezing followed by autonomic reswelling steps could be repeated 20 times without a change in the weight swelling ratio q_w of the cryogels and it remained at 22 ± 2. In

contrast to HA cryogels, the corresponding HA hydrogels prepared at 23 ± 2 °C were not squeezable and they all fractured at around 60% compression (Figure 6.7).

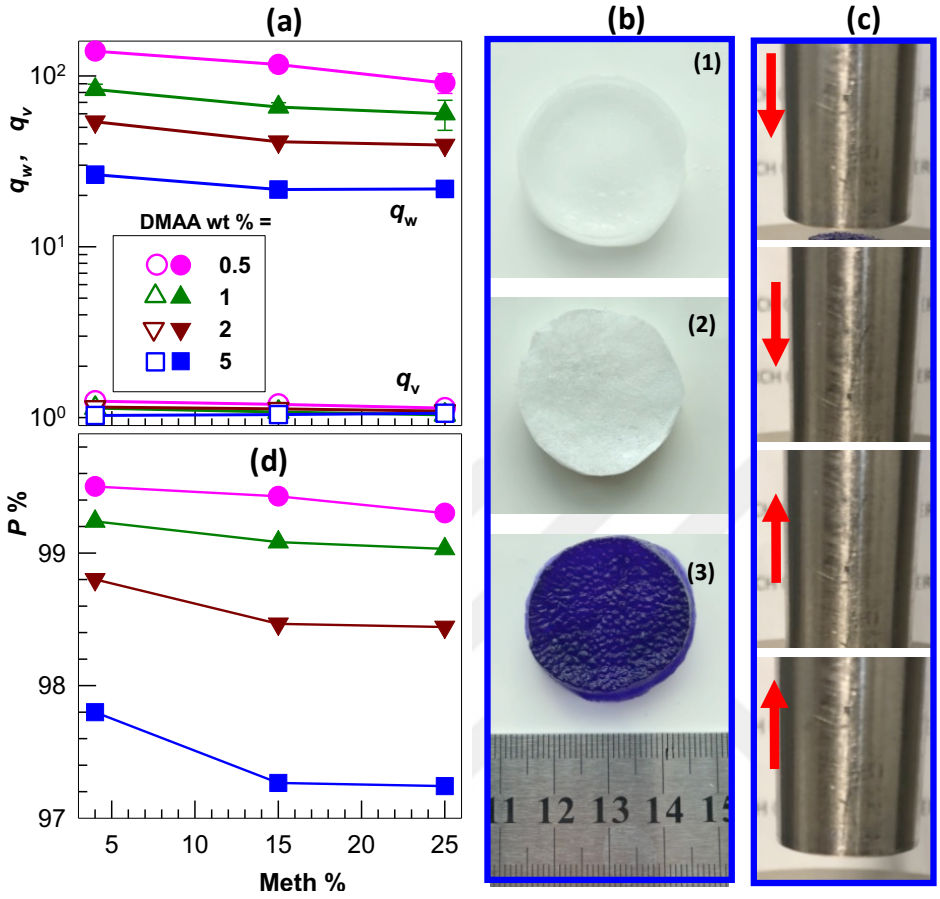

Figure 6.5 : (a): Equilibrium weight q_w (filled symbols) and volume swelling ratios q_v (open symbols) of HA cryogels in water shown as a function of the methacrylation degree (Meth) of HA. DMA contents are indicated. Most of the error bars showing standard deviations of experiments performed at least duplicate are smaller than the size of the symbols. (b): Cryogel images after preparation (1), after freeze-drying (2), and after swelling equilibrium in water that was colored before with crystal violet. DMA = 5 wt %. Meth = 25%. (c): Cryogel images under loading up to 90% strain and then unloading, indicated by down and up arrows, respectively. DMA = 5 wt %. Meth = 25%. (d): Porosity P of the cryogels plotted against Meth %. Symbol explanations are displayed in Figure 6.5a.

To measure the fatigue resistance properties of the cryogels, they were subjected to cyclic compression tests at a constant strain rate of 1 mm·min^{-1}. The samples were first compressed up to a maximum strain of 90% and then unloaded to zero strain. This loading-unloading cycle was repeated 20 times with a waiting time of 1 min between the cycles. It was found that each loading or unloading curve follows the previous one indicating that the cycles are reversible and the cryogels are self- recoverable (Figure S5). Indeed, the area between the loading and unloading curves, i.e., the hysteresis

energy U_{hys} is almost independent on the number of cycles and equals to 2.1±0.3 kJ·m^{-3} (Figure 6.8). Because U_{hys} is the dissipated energy during the cyclic loading [117], this indicates recovery of the virgin microstructure of the cryogels during the wait time between the cycles. Thus, self- recoverability of the cryogels reveals a high fatigue resistance against successive loadings.

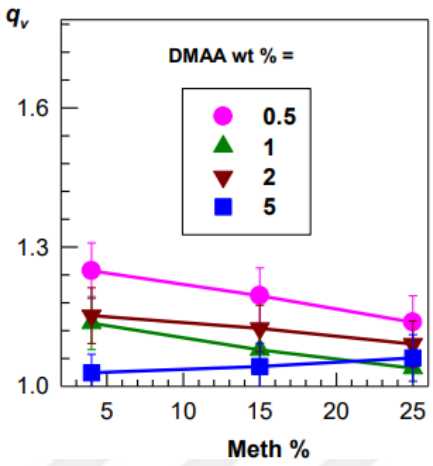

Figure 6.6 : Equilibrium volume swelling ratio qv of HA cryogels in water shown as a function of Meth of HA. DMA contents are indicated.

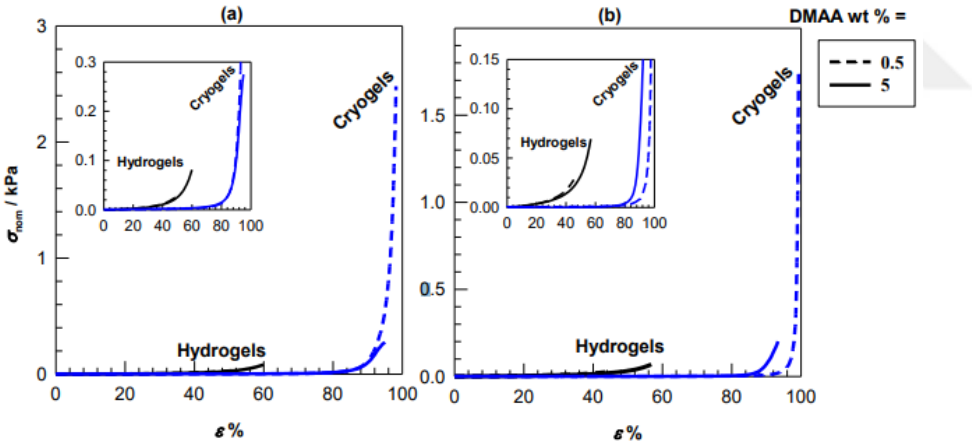

Figure 6.7 : Stress-strain curves of swollen HA cryogels (blue curves) and the corresponding hydrogels prepared at 23±2 °C (black curves). The insets are zoom-in of low strain region. Meth of HA = 14 (a) and 25% (b). DMA wt % indicated.

Squeezability of HA cryogels as demonstrated in Figure 6.5c reveals reversible flow-out and flow-in of water through the pores under high and low strain, respectively. Thus, if the strain is applied to a cryogel specimen confined between the parallel plates of a rheometer, one may expect that the flow-out water will surround the specimen providing its liquid-like response to the stress whereas upon reducing the applied strain, flow-in water will recover its gel-like response [118]. In order to verify this for HA cryogels, cyclic strain-sweep tests were carried out between 1 and 1000% strains

(γ_o) at a fixed frequency ω of 6.3 rad s^{-1}. Figure 6.9 shows γ_o-dependent variations of the storage modulus *G'* (filled symbols), loss modulus *G''* (open symbols), and the loss factor *tan* δ (= *G''/G'*, lines) of a cryogel specimen formed at 5 wt % DMA and 25% Meth. Results of up and down strain sweep tests are shown by circles and triangles, respectively. It is seen that *G''* starts to dominate over *G'*, i.e., an apparent gel-to-sol transition takes place at ~20% strain above which the cryogel behaves as a low density liquid. The cryogel regain its initial viscoelastic properties after reducing the strain back to 1%, revealing the reversibility of the solid to liquid-like transition (Figure 6.9). Similar results were also observed for all cryogels formed at various DMA contents and Meth %. This behavior thus verifies the effect of flowing-out and flowing-in water on the viscoelastic response of the cryogels. It is worth to mention that this gel-to-sol transition is only an apparent transition because the gel network remains intact under strain while the rheometer measures the response of the flowing-out water surrounding the gel. The observed poroelastic behavior associated with the flowing-out and flowing-in water is similar to that of articular cartilage, as detailed in the introduction [114,119–121]. This behavior is also of great interest in biomaterial and biomedical applications as it protects the HA network from damage under large strain conditions and hence increases its lifetime.

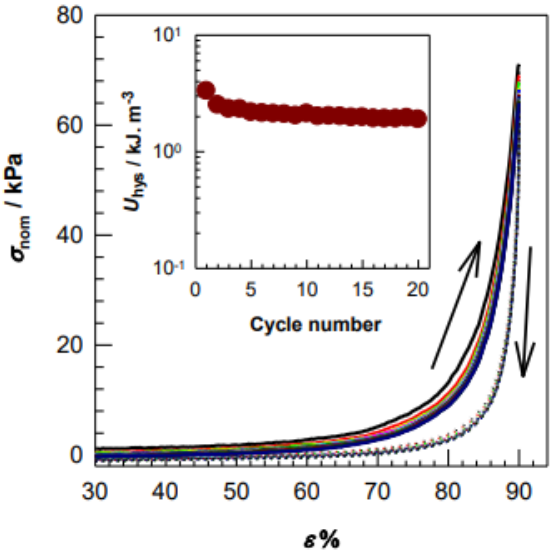

Figure 6.8 : 20 successive loading and unloading cycles conducted on a cryogel specimen prepared at 4% Meth and 0.5 wt % DMA. Strain rate = 1 mm·min^{-1} . The loading and unloading curves are shown by the solid and dotted curves, respectively. The inset shows the hysteresis energy U_{hys}, i.e., the area between the loading and unloading curves plotted against the number of cycles.

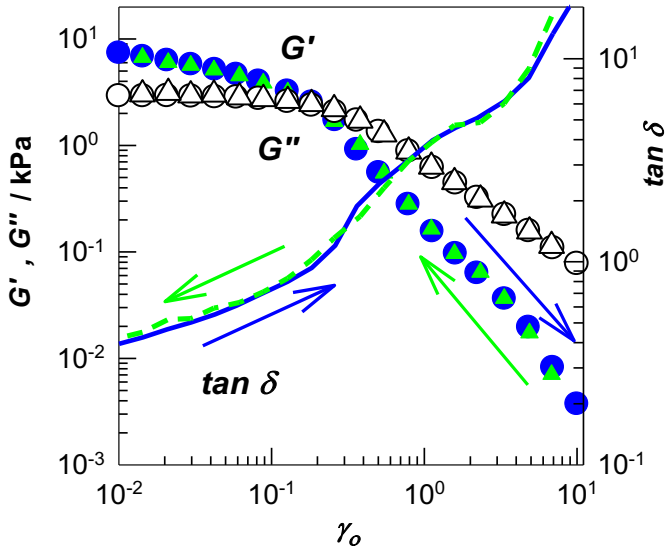

Figure 6.9 : Storage modulus *G'* (filled symbols), loss modulus *G''* (open symbols), and loss factor *tan* δ of a cryogel specimen formed at 5 wt % DMA and 25% Meth as a function of strain γ_o. ω = 6.3 rad·s^{-1}. Dynamic moduli data of up and down strain sweep tests are shown by the circles and triangles, while tan δ data are shown by the solid and dashed lines, respectively. Temperature = 25 °C.

6.2.2 Porous structure and cryoconcentration effect

Because swelling of a cross-linked HA by volume results in the expansion of HA network in water due to the attractive HA–water interactions, while swelling by weight additionally involves pore filling with water and thereby mass increase, one may estimate the total open porosity P from the difference between q_w and q_v by:

$$P\,\% = \left(1 - \frac{q_v}{1 + \left(q_w - 1\right) d_2 / d_1}\right) x10^2 \qquad (6.5)$$

where d_1 and d_2 are densities of water (1.0 g·mL^{-1}) and HA/PDMA (1.8 g·mL^{-1}), respectively [122]. Figure 6.5d showing the Meth-dependence of P reveals that all cryogels have 97- 99% porosities. The lower the DMA content or the methacrylation degree of HA, the higher is the porosity of the cryogels and it becomes 99.5% at 0.5 wt % DMA and 4% Meth (Table 6.1). The porous structure of the cryogels was investigated using destructive SEM and nondestructive μ-CT techniques. SEM provides a higher magnification and thus a greater accuracy in the size determination of the pores than μ-CT. We have to note that all the samples were freeze-dried before subjecting to SEM and μ-CT measurements. Although the cryogels exhibit a high weight-swelling ratio due to the filling of the pores with water, their volume swelling ratios are close to unity, 1.11 ± 0.07 (Table 6.1), revealing that they do not expand or

shrink significantly during swelling or freeze-drying, respectively. Therefore, the change in the porous morphology after freeze-drying is expected to be negligible. Figures 6.10a, b show typical 2D and 3D µ-CT images of the cryogels synthesized at 1 and 5 wt % DMA, respectively, and at a fixed methacrylation degree of 14%. HA cryogel with 1 wt % DMA has a larger pore area (black) as compared to that with 5 wt % DMA, which is in accord with Figure 6.5d. Moreover, no noticeable effect of Meth on the porous structure of the cryogels was observed from 2D and 3D µ-CT images (Figure 6.11). An important requirement for macroporous polymers in many application areas is the presence of interconnecting pores. µ-CT showed the absence of closed pores in all samples and thus, the cryogels have an interconnected open pore structure.

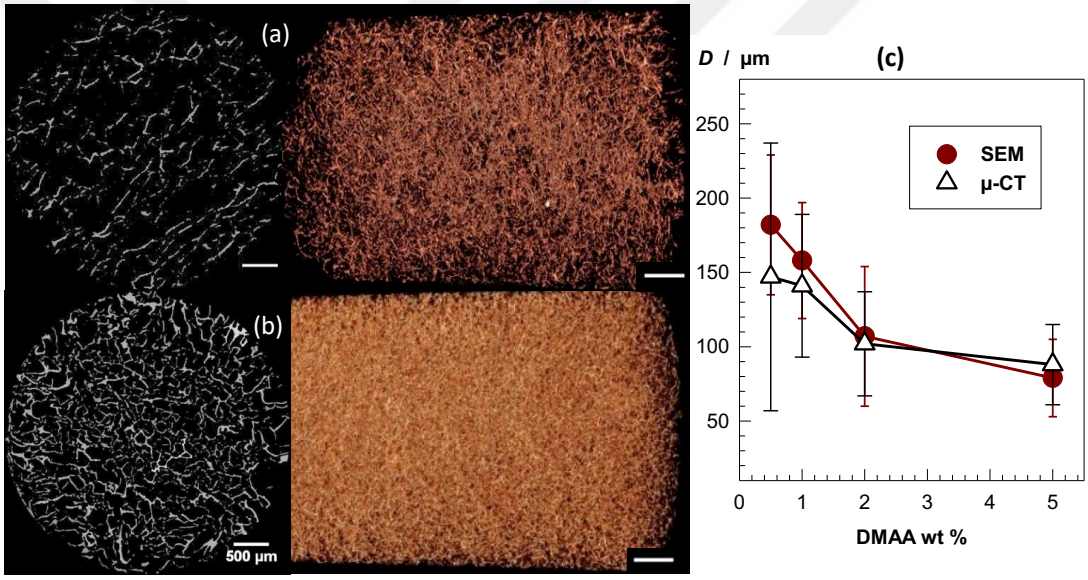

Figure 6.10 : 2D and 3D µ-CT images of cryogels formed at 1 (a) and 5 wt % DMA (b). Scale bars are 0.5 mm. Meth = 14%. **(c):** Pore diameters *D* estimated from µ-CT (open triangles) and SEM (filled circles) of cryogels plotted against DMA wt %. Meth = 4%.

Figure 6.12 presents typical SEM images of HA cryogels prepared at DMA contents between 0.5 and 5 wt % as indicated. Scale bars are 500 and 200 µm in the upper and bottom panel, respectively. The structure consists of µm-sized irregular pores whose sizes decrease while the pore walls become thicker as the DMA content is increased. Similar to µ-CT results, no effect of Meth on the porous structure of the cryogels was observable from the SEM images. Figure 6.10c shows the pore diameters estimated by analyzing µ-CT and SEM images of the cryogels prepared at various DMA contents.

Table 6.1 : Gel fraction W_g, water content H_2O %, weight q_w and volume swelling ratios q_v, total porosity P, fracture stress σ_f, and Young's modulus E of HA cryogels.[a]

Meth %	DMA wt%	W_g	H_2O %	q_w	q_v	P %	σ_f / MPa	E / kPa	σ_f / MPa	E / kPa
							Dry State		Swollen State	
4	0.5	0.99	99	140 (6)	1.25	99.5	0.3	8 (3)	2.6 (0.2)	0.32 (0.07)
14	0.5	0.99	99	117 (4)	1.19	99.4	0.2	15 (5)	2.3 (0.7)	0.39 (0.04)
25	0.5	1.00	99	91 (8)	1.14	99.3	0.17	21	1.5 (0.2)	0.56 (0.2)
4	1	1.00	99	83 (7)	1.14	99.2	0.54	24 (3)	2.5 (0.2)	0.59 (0.2)
14	1	0.98	98	66 (6)	1.08	99.1	0.48	34 (6)	1.9 (0.2)	0.67 (0.2)
25	1	1.00	98	60 (8)	1.04	99.0	0.27	46 (5)	1.8	0.67 (0.02)
4	2	0.99	98	54 (3)	1.15	99,8	1.6 (0.4)	50 (10)	1.1 (0.1)	0.6
14	2	0.97	98	41 (3)	1.12	98.5	1.3	61 (18)	1.0	0.7 (0.1)
25	2	1.00	97	39 (1)	1.09	98.5	0.9 (0.1)	121 (26)	0.6 (0.1)	1.1 (0.2)
4	5	0.98	96	26 (2)	1.03	97.8	3.6 (0.6)	128 (22)	0.5	1.3 (0.3)
14	5	0.94	95	22 (2)	1.04	97.3	2.9 (0.6)	240 (8)	0.3	1.6 (0.8)
25	5	0.87	95	22 (2)	1.06	97.2	2.4 (0.2)	370 (70)	0.2	3.38 (0.1)

[a] Standard deviations are given in parenthesis while for H2O %, Wg, and qv, they are less than 0.2, 5, and 5%, respectively.

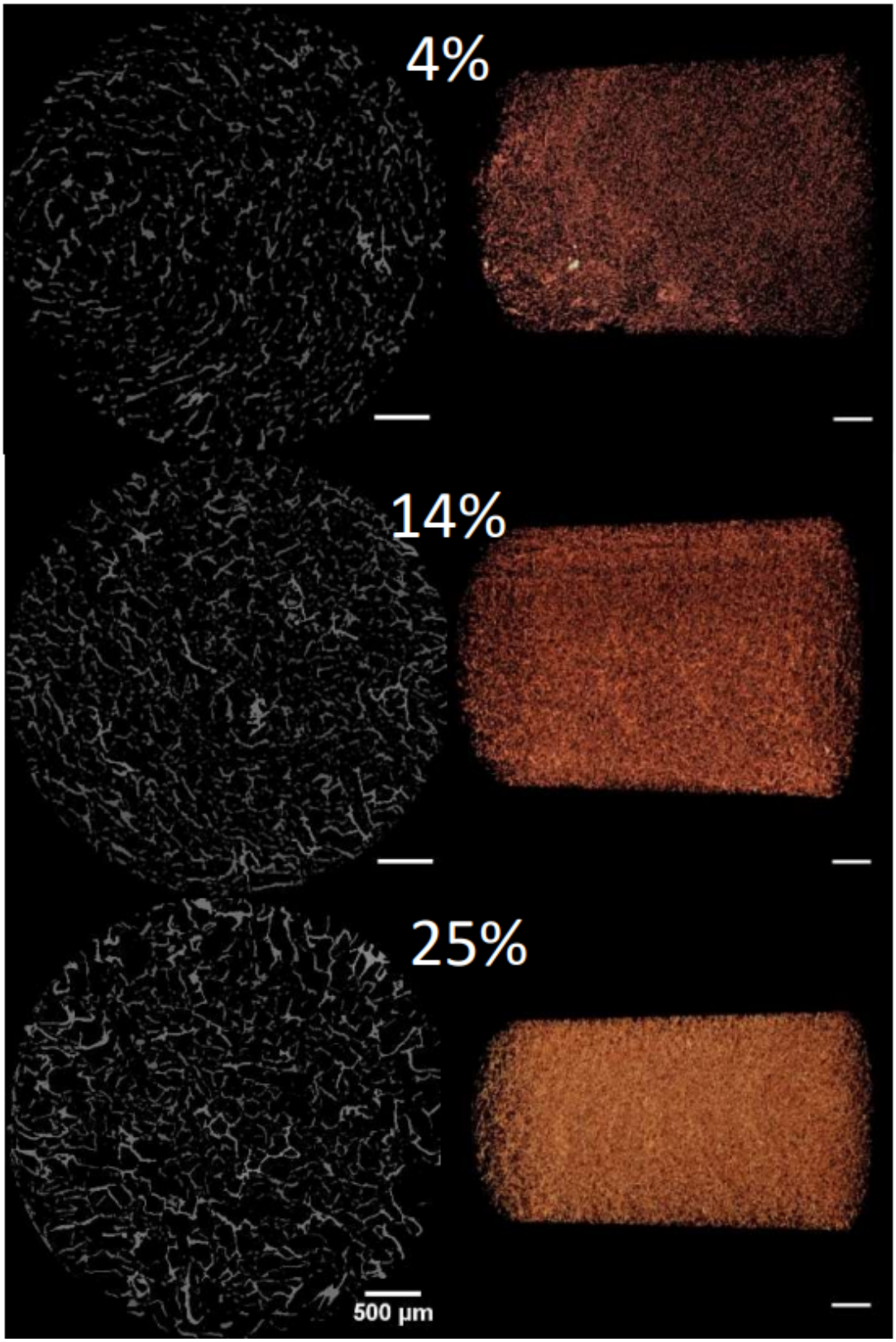

Figure 6.11 : 2D (left) and 3D µ-CT images (right) of cryogels formed 5 wt % DMA and at various Meth of HA as indicated. Scale bars are 0.5 mm.

We have to note that, because the pixel resolution of µ-CT is 8 µm, the precision in estimating the pore diameters using µ-CT is lower than that of SEM. Above 0.5 wt %

DMA, both images give similar diameters *D*, e.g., it decreases from around 150 to 90 µm as DMA content is increased from 0.5 to 5 wt %. Simultaneously, the total porosity decreases from 94 to 88% whereas the thickness of the pore walls increases from 17 to 23 µm. At the lowest DMA content of 0.5 wt %, SEM images show existence of 182 ± 42 µm pores in diameter whereas µ-CT analysis gives polydisperse pores of 147 ± 138 µm in diameter together with large pores of around 0.7 mm forming 11% of the total pore volume. It is likely that some of the pores collapse during drying due to the low polymer content of the cryogels formed at 0.5 wt % DMA.

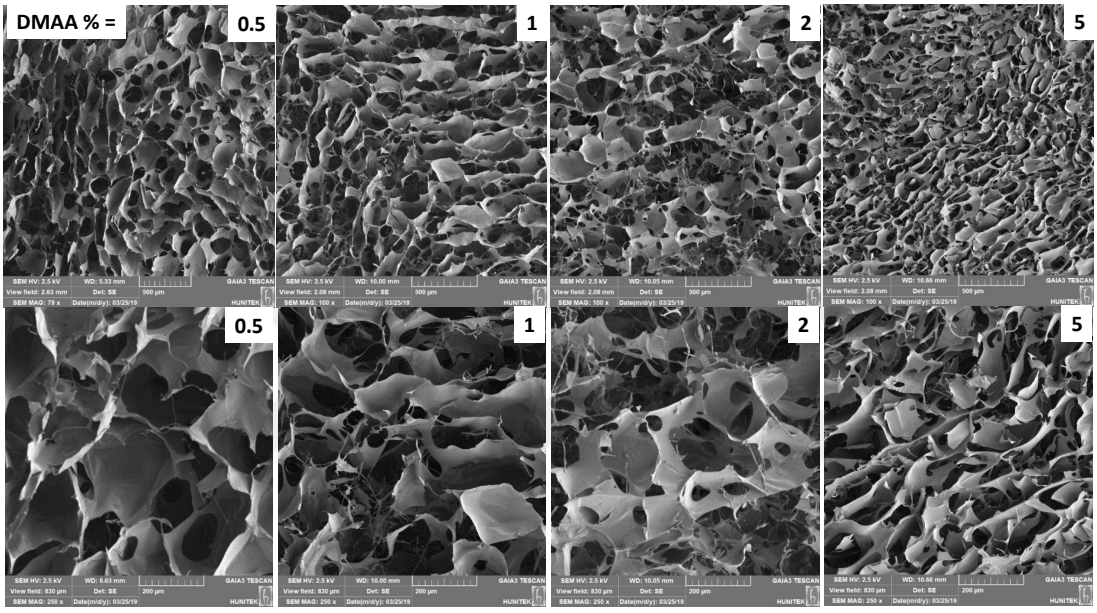

Figure 6.12 : SEM images of HA cryogels prepared at different amounts of DMA. Scaling bars are 500 (top row) and 200 µm (bottom row). Meth = 4 %.

The results thus reveal decreasing porosity and average pore diameter with increasing amount of DMA during cryogelation. The experimental findings can be explained with the actual concentrations of GMHA and DMA in the unfrozen regions as well as the total volume of ice during cryogelation. To determine these parameters, we performed DSC analysis on reaction mixtures which were thermally equilibrated at -18 °C. Figure 6.13a shows DSC scans from -18 to 30 °C of the mixtures containing 1 wt % GMHA and various amounts of DMA. The endothermic melting peak moves to lower temperatures and the peak area becomes smaller with increasing amount of DMA wt %, indicating decreasing the melting temperature T_m and the amount of ice at -18 °C. For instance, T_m calculated from the onset temperature decreases from -1.9 to -8.5 °C as DMA content is increased from 0.5 to 10 wt % DMA. Figure 5b shows the fraction f_{unf} of unfrozen water during cryogelation at -18 °C as a function of DMA wt %. f_{unf} is

around 4% at 0.5 wt % DMA, i.e., 96% of water is frozen during cryogelation and hence, acts as a template, whereas f_{unf} rapidly increases and becomes 17 ± 3 % at 5 wt % DMA. Further increase of DMA content to 10 wt % results in 46 ± 6 % unfrozen water. As mentioned above, no gelation was observed at DMA contents above 5 wt %.

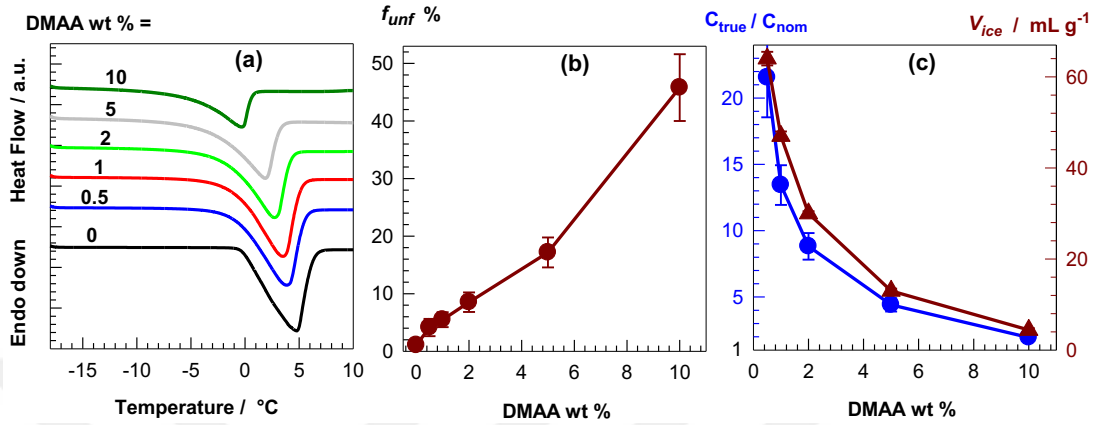

Figure 6.13 : DSC scans of frozen GMHA/DMA solutions at various DMA concentrations as indicated. GMHA = 1 wt %. Heating rate = 1 °C min^{-1}. (b): The fraction f_{unf} of unfrozen water at -18 °C shown as a function of DMA wt %. (c): The concentration ratio C_{true} / C_{nom} (circles) and ice volume V_{ice} (triangles) shown as a function of DMA wt %.

The true concentrations C_{true} of GMHA and DMA in the unfrozen regions, and the ice volume V_{ice} per gram dry cryogel were estimated using the equations:

$$C_{true} = \frac{10^2 C_{nom}}{C_{nom} + (1 - C_{nom}) f_{unf}} \tag{6.6}$$

$$V_{ice} = \frac{(1 - C_{nom})(1 - f_{unf})}{d_1 C_{nom}} \tag{6.7}$$

where d_1 is the ice density at -18 °C (0.995 g mL^{-1}), and C_{nom} is the nominal concentration, which is 1 wt % for GMHA and 0.5 to 10 wt. % for DMA. In Figure 6.13c, the concentration ratio C_{true}/C_{nom} (circles) and the ice volume V_{ice} (triangles) are shown as a function of DMA wt %. It is seen that the lower the DMA concentration, the higher is the C_{true}/C_{nom} ratio, i.e, the extent of cryoconcentration. For instance, at 0.5 wt % DMA, the C_{true}/C_{nom} ratio is around 22 indicating 22-fold increase of DMA concentration under cryogelation condition as compared to the initial concentration. Increasing DMA content decreases the cryoconcentration effect and the C_{true}/C_o ratio reduces to 4.4 and 2 at 5 and 10 wt % DMA, respectively. This means that the true concentration C_{true} approaches to a limiting value of 20 wt % at $C_o \geq 5$ wt % revealing

formation of a saturated GMHA solution that remains unfrozen at -18 °C. The fact that no cryogel could be obtained above 5 wt % DMA can thus be explained with decreasing extent of cryoconcentration. Thus, at high DMA contents, reduced polymerization rates at - 18 °C dominates over the cryoconcentration effect hindering the occurrence of the polymerization reactions of DMA. Figure 6.13c presenting the ice volume V_{ice} in the cryogels reveals continuous decrease of V_{ice} with increasing DMA % which is due to simultaneous decreasing water content and in accord with the experimental results.

6.2.3 Viscoelastic and mechanical properties

Viscoelastic nature of HA cryogels was studied by rheological measurements at a strain γ_0 of 0.01, which is in the linear viscoelastic region for all cryogels. Figures 6.14a shows frequency ω dependences of the storage modulus *G'* and loss factor *tan* δ of HA cryogels prepared at a methacrylation degree of 4% and at various DMA contents as indicated. Both *G'* and *tan* δ are nearly independent of the frequency ω below 1 rad·s^{-1} whereas frequency dependencies appear with increasing ω for high DMA content. The storage modulus increases with increasing DMA wt % or methacrylation degree Meth of HA, reflecting increasing effective cross-link density of the cryogels (Figure 6.14b). For instance, at Meth = 25%, *G'* measured at ω = 0.63 rad·s^{-1} increases from 0.6 to 5.5 kPa with increased DMA content from 0.5 to 5 wt %. Moreover, the loss factor *tan* δ is above 0.1 for all cryogels which is typical for gels with a large extent of energy dissipation under force. This energy dissipation can be attributed to the flowing- out and flowing-in water through the porous network under a pressure gradient due to applied strain, producing frictional resistance and hence frictional energy dissipation, as discussed above (Figure 6.9).

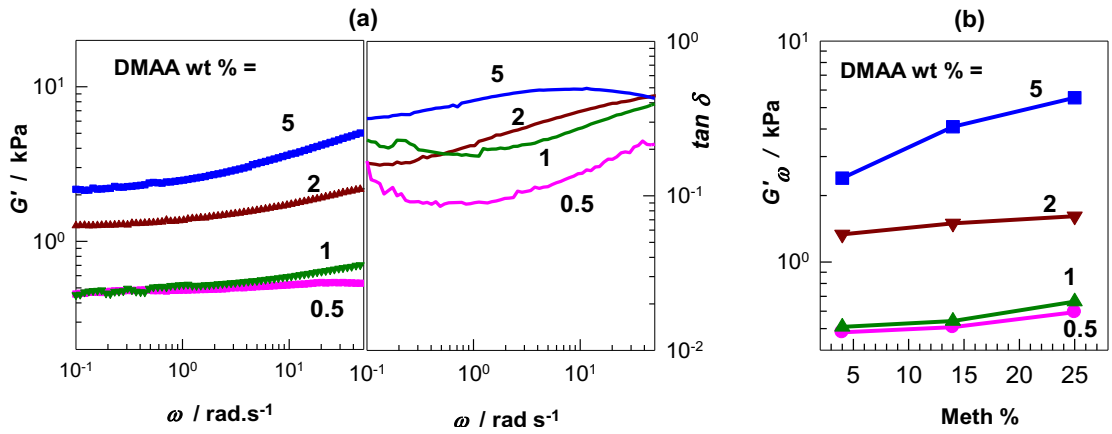

Figure 6.14 : Frequency dependences of the storage modulus *G'* and loss factor *tan* δ (b) of HA cryogels. Meth = 4%. γ_o = 0.01. DMA contents are indicated. (b): Variation of *G'* at ω = 0.63 rad s^{-1} with the methacrylation degree Meth of HA.

Mechanical properties of HA cryogels were investigated by uniaxial compression tests in their freeze- dried and swollen states at 23 ± 2 °C. Figures 6.15a, b show typical stress-strain curves of freeze-dried (a) and swollen cryogels (b) prepared at 4% Meth and various DMA concentrations as indicated in the figures. To highlight the low strain region, the same curves over the whole range of strain are given in the insets in a semi-logarithmic scale. The stress-strain curves of dry cryogels are initially quite linear indicating elastic behavior but then, they exhibit a near-plateau regime where the samples are easily compressed. Finally, a steep increase in stress at strains above 80% is observed. The existence of a plateau regime in the stress-strain curves of dry cryogels indicates disruption of the pore structure in the cryogel networks. Thus, the steep increase in stress in the last region of the stress-strain curves reveals vanishing of the pores and thus, non-porous HA network is compressed in this region. The plateau stress increases with increasing DMA wt % suggesting that the pore walls forming the 3D network structure become mechanically stronger at high DMA contents. For example, it increases by one-order of magnitude with increasing DMA content from 0.5 to 5 w/v %. In contrast, cryogels in swollen state exhibit no plateau region and very low modulus *E*, which is in the same range of that reported before for EGDE-cross-linked cryogels [18,19]. We attribute the disappearance of the plateau regime and the lowering modulus to the squeezability of the cryogels under strain (Figures 6.5c).

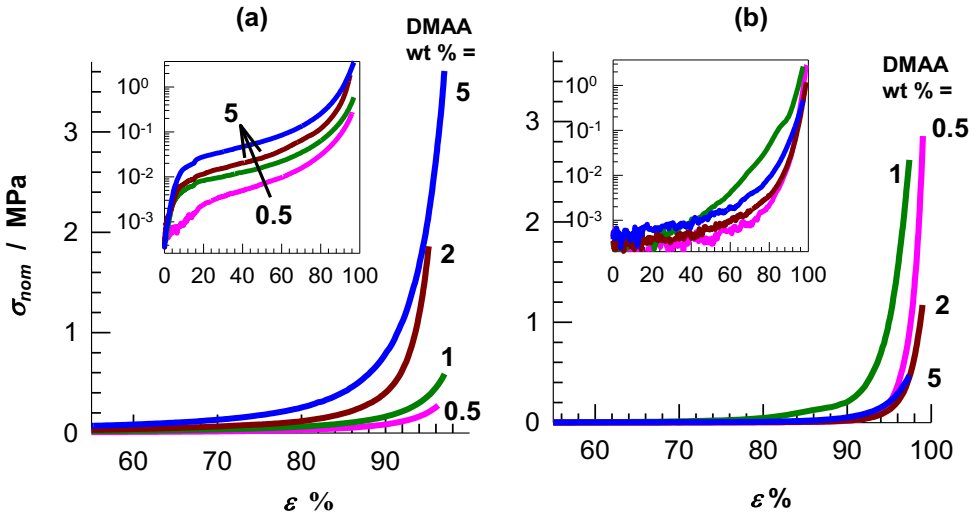

Figure 6.15 : Stress-strain curves (between 55 and 100% strain) of HA cryogels prepared at various DMA contents after freeze-drying (a) and after equilibrium swelling in water (b). Meth = 4%. The insets show semi-logarithmic plots over the whole range of strain.

Moreover, the stress-strain curves of swollen cryogels up to around 80% strain follow a similar path to those reported before for EGDE-cross-linked cryogels [18]. However, the latter cryogels rupture above 80% strain whereas our cryogels sustain up to around 99% strain. The stability of the present cryogels under large strain conditions indicate their high toughness due to the energy dissipation mechanism created in the gel network. For instance, the area under the curve up to the fracture point corresponding to the energy to break (toughness) is calculated as 3.4 $kJ \cdot m^{-3}$ for the EGDE-cross-linked cryogels [18], whereas for the cryogels shown in Figure 6.15B, it is between 17-75 $kJ \cdot m^{-3}$, i.e., 5 to 22 times higher than that of the former cryogels. Figure 6.16a showing Young's modulus E of the cryogels reveals that E increases with increasing DMA content or methacrylation degree of HA. At Meth = 25% and 5 wt % DMA, the modulus E of freeze-dried cryogels becomes 370 ± 70 kPa which is around 50-fold higher than E of dry cryogel formed at 4% Meth and 0.5 wt % DMA (8 ± 3 kPa, Table 6.1). Figure 6.15 also shows 94 to 97% compressibility of all cryogels in dry or wet states without any damage. An interesting feature is that the fracture stress σ_f of freeze-dried cryogels increases with increasing DMA content (left panel in Figure 6.16b), whereas a reverse behavior appears for swollen cryogels (right panel). For instance, the maximum fracture stresses σ_f for freeze-dried and swollen cryogels are 3.6 and 2.6 MPa recorded at 5 and 0.5 wt % DMA, respectively (Figure 6.16b, Table 6.1).

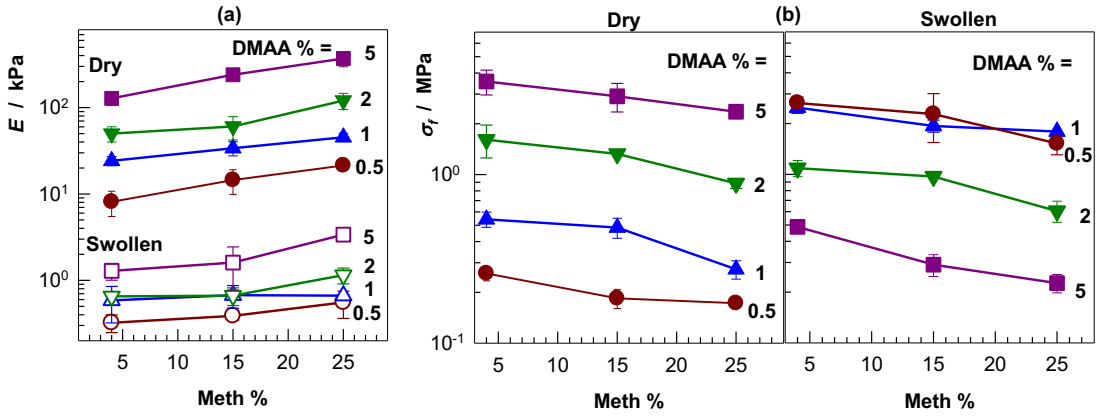

Figure 6.16 : Young's modulus E of freeze-dried (filled symbols) and swollen HA cryogels (open symbols) plotted against Meth %. **(b):** Meth-dependence of the compressive fracture stress σ_f of freeze-dried (left panel) and swollen cryogels (right panel). DMA contents are indicated.

Another characteristic feature is that swollen cryogels with less than 2 wt % DMA are mechanically stronger than in their dried states. To highlight this behavior, Figures 6.17 and 18 compare stress-strain curves of freeze-dried (solid line) and swollen cryogels (dashed curves) below and above 2 wt % DMA. At 1 wt % DMA, cryogels in swollen state are around 5-fold stronger than in their dried states, i.e**.,** σ_f = 2.5 vs 0.54 MPa, respectively (Table 6.1). At 5 wt % DMA, however, the expected behavior appears in that freeze-dried cryogels are stronger than swollen ones, i.e., σ_f = 3.6 vs 0.49 MPa, respectively. How is it possible that easily squeezable swollen cryogels exhibit higher compressive fracture stress and strain than in their dried states? To explain this observation, we calculated the water content of swollen cryogels depending on the applied strain. At 5 wt % DMA, water content h_w of hydrated cryogel under 99% compression was 0.18 ± 0.02 whereas at 1 wt % DMA, h_w under the same compression increased to 0.41 ± 0.03. Previous work shows that at $h_w \leq 0.17$, only bound water exists in hydrated HA and hence, there is no free water molecules acting as plasticizer [123]. Thus, higher mechanical strength of swollen HA cryogels formed at a low DMA content is likely due to the plasticizer effect of free, unbound water improving their large strain properties, which is absent at high DMA contents.

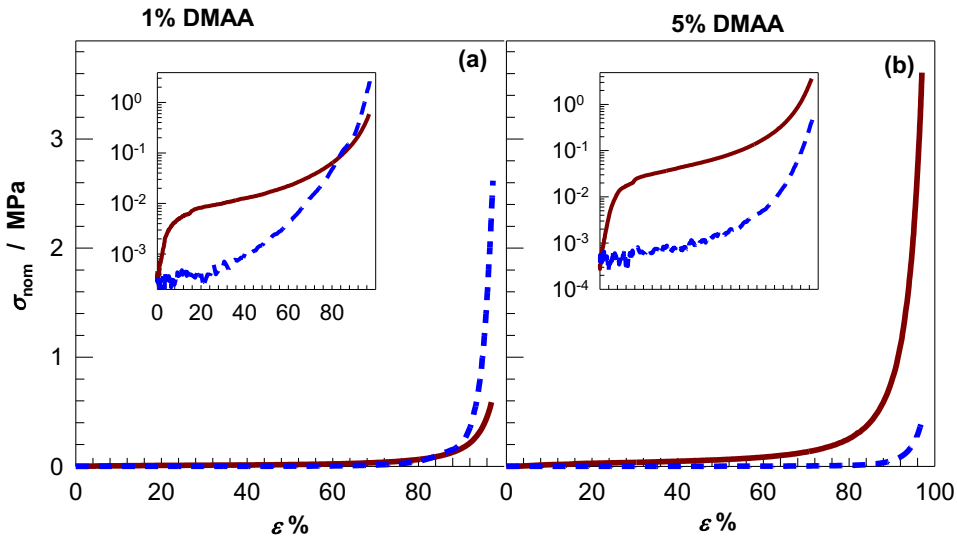

Figure 6.17 : Stress-strain curves of freeze-dried (solid curve) and swollen cryogels (dashed curve) formed at 1 (a) and 5 wt % DMA (b). Meth = 4%.

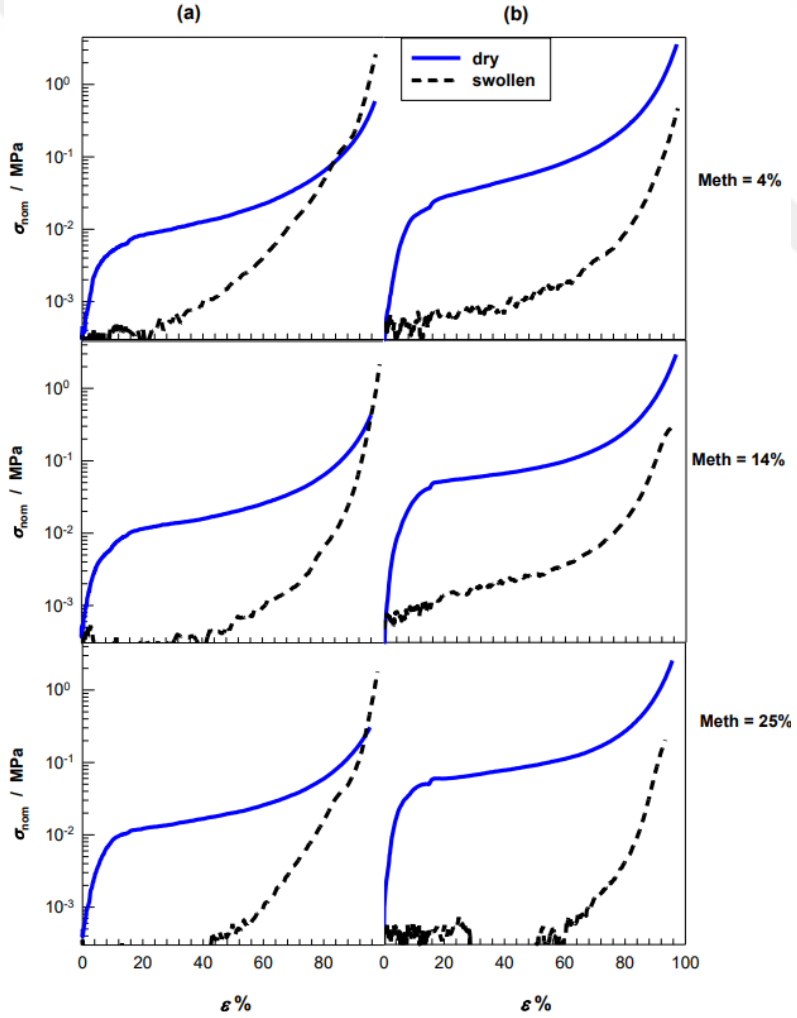

Figure 6.18 : Stress-strain curves of freeze-dried (solid blue curves) and swollen HA cryogels (dashed black curves) formed at 1 (a) and 5 wt % DMA (b). Meth of HA indicated.

6.2.4 Conclusions

We presented a new cryogelation approach for the fabrication of macroporous HA cryogels with a variety of properties, flow-dependent viscoelasticity, complete squeezability, and a high mechanical strength. HA cryogels were synthesized from 1 wt % methacrylated HA of various methacrylation degrees in aqueous solutions at -18 °C by free-radical mechanism using in situ prepared PDMA chains as a spacer between 0.5 and 5 wt %. The porous structure of the cryogels investigated by SEM and μ- CT reveals consists of an interconnected open pore structure. It was found that the total open porosity and the average pore diameter decrease from 99 to 90% and from 150 to 90 μm, respectively, with increasing amount of PDMA. These findings could be explained with the actual concentrations of HA and DMA as well as the volume of ice during cryogelation. HA cryogels in swollen state sustain up to 2.6 ± 0.2 MPa compressive stress, which is around 2 orders of magnitude higher than those obtained by chemical cross-linking of native HA. This high compressive stiffness originates from the flow of pore water out of the cryogel phase under compression. HA cryogels confined between parallel plates also exhibit reversible strain-dependent apparent gel-to-sol transition behavior due to the flowing-out and flowing-in water through the pores, similar to water squeezing out of a sponge. This flow-dependent viscoelasticity of HA cryogels is similar to that observed with articular cartilage, and produces frictional resistance and hence frictional energy dissipation mechanism in HA cryogels. Such an apparent gel-to- sol transition behavior of HA cryogels is also of great interest in biomaterial and biomedical applications as it protects HA network from damage under large strain conditions and hence act as a self-defense mechanism. It was also found that swollen HA cryogels prepared at a low PDMA content are mechanically stronger than in their freeze-dried states, which we attribute to the plasticizer effect of free, unbound water improving their large strain properties.

7. CONCLUSIONS

In the current thesis, we focused on synthesizing and improving the mechanical performances of HA-based hydrogels. Firstly, DN hydrogels are prepared starting from native HA and DMA as the first and second network components, respectively. After successful methacrylation of HA with glycidyl methacrylate, HA/PDMA/PDMA triple-network hydrogels could also be prepared. By taking the advantage of GMHA as being a multi-functional cross-linker, one-pot synthesis method of HA hydrogels was introduced. DMA or MAAc, and DMA and SF were incorporated separately into a reaction solution containing GMHA and then polymerized to produce HA hydrogels. Lastly, robust macroporous HA cryogels were successfully obtained starting from GMHA in the presence of a small amount of DMA as a spacer by using the cryogelation technique conducted at sub-zero temperatures. The thesis presented here produced five publications, mainly based on fabricating mechanically strong HA hydrogels, which are summarized in five sections as given below. They are classified according to their synthesis methods and named in agreement with IUPAC nomenclature recommendation [124]. Synthesis parameters of the hydrogels with the highest mechanical strength were given in each section.

Sequential polymerization (DN and TN):

1) (*net*-HA)-*ipn*-[(*net*-(poly(DMA)]

SN hydrogels: C_1 = 0.08 g.mL^{-1} HA ; 7.1 w/v% EDGE.

DN hydrogels: C_2 = 0.,30 g.mL^{-1} ; %0.05 BAAm by mole; w_{21} = 49.

2) (*net*-HA)-*ipn*-[(*net*-(poly(DMA)] -*ipn*-[(*net*-(poly(DMA)]

SN hydrogels: C_1 = 0.01 g.mL^{-1} GMHA; DM = %4.

DN hydrogels: C_2 = 0.30 g.mL^{-1} ; %0.05 BAAm by mole ; w_{21} = 29.

TN hydrogels: C_3 = 0.30 g.mL^{-1} ; %0.05 BAAm by mole; w_{321} = 106.

One-pot synthesis:

3) (*net*-HA)-*ipn*-[(*net*-(poly(DMA)]

1st component: C_1 = 0.01 g.mL^{-1} GMHA ; DM = %8

2nd component: C_2 = 0.30 g.mL^{-1} MAAc.

4) (*net*-HA)-*ipn*-(*net*-SF)-*ipn*-[(*net*-(poly(DMA)]

1st component: C_1 = 0.01 g.mL^{-1} GMHA ; DM = %4

2nd component: C_2 = 0.025 g.mL^{-1} SF.

3rd component: C_3 = 0.05 g.mL^{-1} DMA

Cryogelation:

5) (*net*-HA)-*ipn*-[(*net*-(poly(DMA)]

1st component: C_1 = 0.01 g.mL^{-1} GMHA ; DM = %4

2nd comp.: C_2 = 0.05 and 0.005 g.mL^{-1} DMA for dry and swollen state, respectively.

In the first part of the thesis, DN hydrogels based on HA and PDMA were prepared by utilizing a two-step process. Primarily, HA was chemically cross-linked in aqueous solutions using ethylene glycol diglycidyl ether (EDGE) and the gelation reactions were monitored by rheological measurements. First-network hydrogels containing 97-99% water were fragile and ruptured when compressed to 25-51% strain under 0.02-0.15 MPa stresses. By applying the double-network approach in the second step, DN hydrogels bearing high strength and containing 84-94% water were generated. Adjusting the first and second network components ratio resulted in hydrogels that exhibit a compressive modulus of 0.9 MPa that sustain 19.4 MPa compressive stresses. It was proven that internal fracture of the HA first network under a low strain together with the high mass ratio of the second to the first-network components are responsible for the high mechanical properties. Cyclic mechanical tests also exhibited irreversible stress-strain curves with a large hysteresis, indicating that elastically effective cross-links of HA first-network are irreversibly destroyed under load by dissipating energy.

In the second part of the thesis, DN and TN hydrogels based on GMHA and DMA were prepared by sequential free radical photopolymerizations. GMHA macromers were prepared by methacrylation of HA using different ratios of glycidyl methacrylate, and the methacrylation degrees of the products were characterized by the ^{1}H-NMR

technique. GMHA macromers of various methacrylation degrees were photopolymerized to obtain SN hydrogels. SN hydrogels can sustain up to 40% compression and break at a stress of 0.02 – 0.05 MPa. By tuning the methacrylation degree of HA, DN hydrogels with fracture stress above 10 MPa and a fracture strain of 96% were obtained. Triple-networking of DN hydrogels further increases the ratio of ductile/brittle components, and thus produces mechanically strong HA/PDMA/PDMA TN hydrogels. TN hydrogels contain 81-91% water and sustain compressive stresses above 20 MPa and Young's modulus of up to 1 MPa. Cyclic mechanical tests showed that, although TN hydrogels internally fracture even under small strain, the ductile components hinder macroscopic crack propagation by keeping the macroscopic gel samples together.

In the third part of the study, a simple one-pot synthesis of HA hydrogels via free-radical copolymerization of GMHA and DMA in aqueous solutions were introduced. Gelation profiles of the reaction systems were obtained by rheometry using oscillatory deformation tests. It was found that GMHA acts as a multifunctional cross-linker during its copolymerization with DMA. Moreover, the effective functionality of GMHA increased both with the methacrylation degree of HA, and DMA concentration. Hydrogels prepared at 30 w/v % DMA sustain above 600% elongation ratios, and exhibit a tensile strength and compressive stress up to 111 kPa and 11 MPa, respectively. A significant improvement in the mechanical performance of the hydrogels was observed when DMA is replaced with methacrylic acid (MAAc) monomer. When MAAc is used in the gel preparation, hydrogels with a Young's modulus of around 200 kPa could be prepared that sustain up to 20 MPa stresses at 96% compression.

In the fourth part, mechanically robust and stretchable SF/HA hydrogels were prepared from GMHA, SF and DMA in aqueous solutions in the presence of a radical initiator. It was found that DMA acts as a spacer to connect GMHA's through their pendant vinyl groups. Rheological measurements showed that SF/HA hydrogels form in two steps: In the first step, copolymerization reactions between GMHA and DMA lead to the formation of a loosely cross-linked network. In the second step, fibroin gelation takes place due to the conformational transition in SF from random coil to β-sheet structures. XRD measurements confirmed the formation of β-sheet structure leading to a significant enhancement in the mechanical strengths of HA hydrogels. After

incorporating SF into the gel network, Young's modulus and fracture stress of the as-prepared hydrogels increased markedly from 5 to 54 kPa and from 0.6 to 4.9 MPa, respectively. Despite the fact that SF hydrogels are generally brittle in tension, the materials prepared in this part of the thesis could sustain up to 400% stretch ratio under a stress of 80 kPa. This finding demonstartes GMHA's contribution to the stretchability of the composite hydrogels. Cyclic mechanical tests revealed that the damage in SF network under strain leads to a significant energy dissipation, which is responsible for the improved mechanical properties of SF/HA hydrogels.

In the last part of the study, HA cryogels were prepared via free-radical copolymerization of GMHA and DMA in aqueous solutions at -18 ^{o}C. HA cryogels could sustain up to 2.6 and 3.6 MPa compressive stresses in swollen and freeze-dried states, respectively. Moreover, they are squeezable and no crack propagation occurred when compressed up to 97% strain. This high compressive stiffness originates from the flow of pore water out of the cryogel phase under compression. Cyclic strain-sweep tests verified the effect of flowing-out and flowing-in water on the viscoelastic response of the cryogels. HA cryogels have an interconnected pore structure with pores of >90 μm in diameter and exhibit a high porosity (>97%), as observed by SEM and μ-CT analysis. It was also found that water-swollen HA cryogels prepared at a low PDMA content are mechanically stronger than in their freeze-dried states, which we attribute to the plasticizer effect of free, unbound water, improving their large strain properties.

In conclusion, HA hydrogels with excellent mechanical properties were successfully synthesized by using various synthesis methods. Most of the mechanical properties achieved in the present thesis are the highest reported so far in the literature. Further investigations will be held for these materials for in vivo studies. Highly tough HA hydrogels and cryogels developed in this thesis have many potential application areas such as controlled drug delivery systems, wound dressings, cell therapy, artificial organs, soft machines, and scaffolds for tissue engineering as 3D printed natural biopolymers that are attracting attention nowadays.

REFERENCES

[1] **Fraser, J. R. E., Laurent, T. C., & Laurent, U. B. G.** (1997). Hyaluronan: Its nature, distribution, functions and turnover. *J. Intern. Med.*, *242*, 27–33.

[2] **Chen, W. Y. J., & Abatangelo, G.** (1999). Functions of hyaluronan in wound repair. *Wound Repair Regen.*, *7*, 79–89.

[3] **Lapčík Jr., L., Lapčík, L., De Smedt, S., Demeester, J., & Chabreček, P.** (1998). Hyaluronan: Preparation, structure, properties, and applications. *Chem. Rev.*, *98*, 2663–2684.

[4] **Kogan, G., Šoltés, L., Stern, R., & Gemeiner, P.** (2007). Hyaluronic acid: A natural biopolymer with a broad range of biomedical and industrial applications. *Biotechnol. Lett.*, *29*, 17–25.

[5] **Necas, J., Bartosikova, L., Brauner, P., & Kolar, J.** (2008). Hyaluronic acid (hyaluronan): A review. *Vet. Med. (Praha).*, *53*, 397–411.

[6] **Neovius, E., Lemberger, M., Docherty Skogh, A., Hilborn, J., & Engstrand, T.** (2013). Alveolar bone healing accompanied by severe swelling in cleft children treated with bone morphogenetic protein-2 delivered by hydrogel. *J. Plast. Reconstr. Aesthetic Surg.*, *66*, 37–42.

[7] **Xu, X., Jha, A. K., Harrington, D. A., Farach-Carson, M. C., & Jia, X.** (2012). Hyaluronic acid-based hydrogels: From a natural polysaccharide to complex networks. *Soft Matter*, *8*, 3280–3294.

[8] **Luan, T., Wu, L., Zhang, H., & Wang, Y.** (2012). A study on the nature of intermolecular links in the cryotropic weak gels of hyaluronan. *Carbohydr. Polym.*, *87*, 2076–2085.

[9] **Collins, M. N., & Birkinshaw, C.** (2007). Comparison of the effectiveness of four different crosslinking agents with hyaluronic acid hydrogel films for tissue-culture applications. *J. Appl. Polym. Sci.*, *104*, 3183–3191.

[10] **Collins, M. N., & Birkinshaw, C.** (2013). Hyaluronic acid based scaffolds for tissue engineering - A review. *Carbohydr. Polym.*, *92*, 1262–1279.

[11] **Horkay, F., Hecht, A. M., & Geissler, E.** (2006). Similarities between polyelectrolyte gels and biopolymer solutions. *J. Polym. Sci. Part B Polym. Phys.*, *44*, 3679–3686.

[12] **Tomihata, K., & Ikada, Y.** (1997). Preparation of cross-linked hyaluronic acid films of low water content. *Biomaterials*, *18*, 189–195.

[13] **Segura, T., Anderson, B. C., Chung, P. H., Webber, R. E., Shull, K. R., & Shea, L. D.** (2005). Crosslinked hyaluronic acid hydrogels: A strategy to functionalize and pattern. *Biomaterials*, *26*, 359–371.

[14] **Hwang, H. D., Cho, H. J., Balakrishnan, P., Chung, C. W., Yoon, I. S., Oh, Y. K., Byun, Y., & Kim, D. D.** (2012). Cross-linked hyaluronic acid-based flexible cell delivery system: Application for chondrogenic differentiation. *Colloids Surfaces B Biointerfaces*, *91*, 106–113.

[15] **Kim, H. J., Kim, K. K., Park, I. K., Choi, B. S., Kim, J. H., & Kim, M. S.** (2012). Hybrid scaffolds composed of hyaluronic acid and collagen for cartilage regeneration. *Tissue Eng. Regen. Med.*, *9*, 57–62.

[16] **Brown, H. R.** (2007). A model of the fracture of double network gels. *Macromolecules*, *40*, 3815–3818.

[17] **Abdurrahmanoglu, S., Can, V., & Okay, O.** (2009). Design of high-toughness polyacrylamide hydrogels by hydrophobic modification. *Polymer*, *50*, 5449–5455.

[18] **Ström, A., Larsson, A., & Okay, O.** (2015). Preparation and physical properties of hyaluronic acid-based cryogels. *J. Appl. Polym. Sci.*, *132*.

[19] **Oelschlaeger, C., Bossler, F., & Willenbacher, N.** (2016). Synthesis, Structural and Micromechanical Properties of 3D Hyaluronic Acid-Based Cryogel Scaffolds. *Biomacromolecules*, *17*, 580–589.

[20] **Okay, O., & Lozinsky, V. I.** (2014). Synthesis and structure–property relationships of cryogels. *Adv. Polym. Sci.*, *263*, 103–157.

[21] **Leach, J. B., Bivens, K. A., Patrick, C. W., & Schmidt, C. E.** (2003). Photocrosslinked hyaluronic acid hydrogels: Natural, biodegradable tissue engineering scaffolds. *Biotechnol. Bioeng.*, *82*, 578–589.

[22] **Prado, S. S., Weaver, J. M., & Love, B. J.** (2011). Gelation of photopolymerized hyaluronic acid grafted with glycidyl methacrylate. *Mater. Sci. Eng. C*, *31*, 1767–1771.

[23] **Ibrahim, S., Kothapalli, C. R., Kang, Q. K., & Ramamurthi, A.** (2011). Characterization of glycidyl methacrylate - Crosslinked hyaluronan hydrogel scaffolds incorporating elastogenic hyaluronan oligomers. *Acta Biomater.*, *7*, 653–665.

[24] **Shu, X. Z., Liu, Y., Luo, Y., Roberts, M. C., & Prestwich, G. D.** (2002). Disulfide cross-linked hyaluronan hydrogels. *Biomacromolecules*, *3*, 1304–1311.

[25] **Ghosh, K., Shu, X. Z., Mou, R., Lombardi, J., Prestwich, G. D., Rafailovich, M. H., & Clark, R. A. F.** (2005). Rheological characterization of in situ cross-linkable hysluronan hydrogels. *Biomacromolecules*, *6*, 2857–2865.

[26] **Jeffery, A. F., Churchward, M. A., Mushahwar, V. K., Todd, K. G., & Elias, A. L.** (2014). Hyaluronic acid-based 3D culture model for in vitro testing of electrode biocompatibility. *Biomacromolecules*, *15*, 2157–2165.

[27] **Jia, X., Burdick, J. A., Kobler, J., Clifton, R. J., Rosowski, J. J., Zeitels, S. M., & Langer, R.** (2004). Synthesis and characterization of in situ cross-linkable hyaluronic acid-based hydrogels with potential application for vocal fold regeneration. *Macromolecules*, *37*, 3239–3248.

[28] **Elia, R., Newhide, D. R., Pedevillano, P. D., Reiss, G. R., Firpo, M. A., Hsu, E. W., Kaplan, D. L., Prestwich, G. D., & Peattie, R. A.** (2013). Silk-hyaluronan-based composite hydrogels: A novel, securable vehicle for drug delivery. *J. Biomater. Appl.*, *27*, 749–762.

[29] **Chang, K. H., Liao, H. T., & Chen, J. P.** (2013). Preparation and characterization of gelatin/hyaluronic acid cryogels for adipose tissue engineering: In vitro and in vivo studies. *Acta Biomater.*, *9*, 9012–9026.

[30] **Foss, C., Merzari, E., Migliaresi, C., & Motta, A.** (2013). Silk fibroin/hyaluronic acid 3D matrices for cartilage tissue engineering. *Biomacromolecules*, *14*, 38–47.

[31] **Weng, L., Gouldstone, A., Wu, Y., & Chen, W.** (2008). Mechanically strong double network photocrosslinked hydrogels from N,N-dimethylacrylamide and glycidyl methacrylated hyaluronan. *Biomaterials*, *29*, 2153–2163.

[32] **Tavsanli, B., Can, V., & Okay, O.** (2015). Mechanically strong triple network hydrogels based on hyaluronan and poly(N,N-dimethylacrylamide). *Soft Matter*, *11*, 8517–8524.

[33] **Gong, J. P., Katsuyama, Y., Kurokawa, T., & Osada, Y.** (2003). Double-network hydrogels with extremely high mechanical strength. *Adv. Mater.*, *15*, 1155–1158.

[34] **Tanaka, Y., Gong, J. P., & Osada, Y.** (2005). Novel hydrogels with excellent mechanical performance. *Prog. Polym. Sci.*, *30*, 1–9.

[35] **Haque, M. A., Kurokawa, T., & Gong, J. P.** (2012). Super tough double network hydrogels and their application as biomaterials. *Polymer*, *53*, 1805–1822.

[36] **Webber, R. E., Creton, C., Brown, H. R., & Gong, J. P.** (2007). Large strain hysteresis and mullins effect of tough double-network hydrogels. *Macromolecules*, *40*, 2919–2927.

[37] **Nakajima, T., Kurokawa, T., Ahmed, S., Wu, W. L., & Gong, J. P.** (2013). Characterization of internal fracture process of double network hydrogels under uniaxial elongation. *Soft Matter*, *9*, 1955–1966.

[38] **Lu, X., Xu, Y., Zheng, C., Zhang, G., & Su, Z.** (2006). Ethylene glycol diglycidyl ether as a protein cross-linker: A case study for cross-linking of hemoglobin. *J. Chem. Technol. Biotechnol.*, *81*, 767–775.

[39] **Topuz, F., & Okay, O.** (2008). Rheological behavior of responsive DNA hydrogels. *Macromolecules*, *41*, 8847–8854.

[40] **Karakutuk, I., Ak, F., & Okay, O.** (2012). Diepoxide-triggered conformational transition of silk fibroin: Formation of hydrogels. *Biomacromolecules*, *13*, 1122–1128.

[41] **Gatej, I., Popa, M., & Rinaudo, M.** (2005). Role of the pH on hyaluronan behavior in aqueous solution. *Biomacromolecules*, *6*, 61–67.

[42] **Calvet, D., Wong, J. Y., & Giasson, S.** (2004). Rheological monitoring of polyacrylamide gelation: Importance of cross-link density and temperature. *Macromolecules*, *37*, 7762–7771.

[43] **Giraldo, J., Vivas, N. M., Vila, E., & Badia, A.** (2002). Assessing the (a)symmetry of concentration-effect curves: Empirical versus mechanistic models. *Pharmacol. Ther.*, *95*, 21–45.

[44] **Okay, O., & Oppermann, W.** (2007). Polyacrylamide-clay nanocomposite hydrogels: Rheological and light scattering characterization. *Macromolecules*, *40*, 3378–3387.

[45] **Clark, A. H., & Ross-Murphy, S. B.** (1987). Structural and mechanical properties of biopolymer gels. *Adv. Polym. Sci.*, 57–192.

[46] **Teodorescu, M., Andrei, M., Turturicə, G., Stənescu, P. O., Zaharia, A., & Sârbu, A.** (2015). Novel Thermoreversible Injectable Hydrogel Formulations Based on Sodium Alginate and Poly(N-Isopropylacrylamide). *Int. J. Polym. Mater. Polym. Biomater.*, *64*, 763–771.

[47] **D'Este, M., Alini, M., & Eglin, D.** (2012). Single step synthesis and characterization of thermoresponsive hyaluronan hydrogels. *Carbohydr. Polym.*, *90*, 1378–1385.

[48] **Kundu, M., Mallapragada, S., Larock, R. C., & Kundu, P. P.** (2010). Rheological properties of methylcellulose aqueous gels under dynamic compression: Frequency sweep and validity of scaling law. *J. Appl. Polym. Sci.*, *117*, 2436–2443.

[49] **Treloar, L. R. G.** (1975). *The Physics of Rubber Elasticity*, University Press, Oxford.

[50] **Flory, P. J.** (1953). *Principles of Polymer Chemistry*, Cornell University Press, Ithaca, NY.

[51] **Calvert, P.** (2009). Hydrogels for soft machines. *Adv. Mater.*, *21*, 743–756.

[52] **Argun, A., Can, V., Altun, U., & Okay, O.** (2014). Nonionic double and triple network hydrogels of high mechanical strength. *Macromolecules*, *47*, 6430–6440.

[53] **Kayaman, N., Okay, O., & Baysal, B. M.** (1997). Swelling of polyacrylamide gels in aqueous solutions of ethylene glycol oligomers. *Polym. Gels Networks*, *5*, 339–356.

[54] **Nakajima, T., Furukawa, H., Tanaka, Y., Kurokawa, T., Osada, Y., & Gong, J. P.** (2009). True chemical structure of double network hydrogels. *Macromolecules*, *42*, 2184–2189.

[55] **Lake, G. J., & Thomas, A. G.** (1967). The strength of highly elastic materials. *Proc. R. Soc. London. Ser. A. Math. Phys. Sci.*, *300*, 108–119.

[56] **Balazs, E. A., & Band, P. A.** (2008). Therapeutic use of Hyaluronan-Based Products. In *Carbohydr. Chem. Biol. Med. Appl.* (pp. 311–332).

[57] **Ahagon, A., & Gent, A. N.** (1975). Threshold fracture energies for elastomers. *J. Polym. Sci. Polym. Phys. Ed.*, *13*, 1903–1911.

[58] **Chen, Q., Chen, H., Zhu, L., & Zheng, J.** (2015). Fundamentals of double network hydrogels. *J. Mater. Chem. B*, *3*, 3654–3676.

[59] **Ahmed, S., Nakajima, T., Kurokawa, T., Anamul Haque, M., & Gong, J. P.** (2014). Brittle-ductile transition of double network hydrogels: Mechanical balance of two networks as the key factor. *Polymer*, *55*, 914–923.

[60] **Nakajima, T., Fukuda, Y., Kurokawa, T., Sakai, T., Chung, U. Il, & Gong, J. P.** (2013). Synthesis and fracture process analysis of double network hydrogels with a well-defined first network. *ACS Macro Lett.*, *2*, 518–521.

[61] **Funke, W., Okay, O., & Joos-Müller, B.** (1998). Microgels - Intramolecularly Crosslinked Macromolecules with a Globular Structure. *Adv. Polym. Sci.*, *136*, 138–234.

[62] **Hardingham, T.** (2004). Solution Properties of Hyaluronan. In *Chem. Biol. Hyaluronan* (pp. 1–19). Amsterdam: Elsevier.

[63] **Finelli, I., Chiessi, E., Galesso, D., Renier, D., & Paradossi, G.** (2009). Gel-like structure of a hexadecyl derivative of hyaluronic acid for the treatment of osteoarthritis. *Macromol. Biosci.*, *9*, 646–653.

[64] **Khanlari, A., Schulteis, J. E., Suekama, T. C., Detamore, M. S., & Gehrke, S. H.** (2015). Designing crosslinked hyaluronic acid hydrogels with tunable mechanical properties for biomedical applications. *J. Appl. Polym. Sci.*, *132*, 42009.

[65] **Tavsanli, B., & Okay, O.** (2016). Preparation and fracture process of high strength hyaluronic acid hydrogels cross-linked by ethylene glycol diglycidyl ether. *React. Funct. Polym.*, *109*, 42–51.

[66] **Lozinsky, V. I., & Okay, O.** (2014). Basic Principles of Cryotropic Gelation. *Adv. Polym. Sci.*, *263*, 49–101.

[67] **Uemura, Y., McNulty, J., & Macdonald, P. M.** (1995). Associative Behavior and Diffusion Coefficients of Hydrophobically Modified Poly(N,N-dimethylacrylamides). *Macromolecules*, *28*, 4150–4158.

[68] **Peppas, N. A.** (1987). *Hydrogels in medicine and pharmacy* (Vol. 10). New York: Wiley.

[69] **Relógio, P., Martinho, J. M. G., & Farinha, J. P. S.** (2005). Effect of surfactant on the intra- and intermolecular association of hydrophobically modified poly(N,N-dimethylacrylamide). *Macromolecules*, *38*, 10799–10811.

[70] **Cipriano, B. H., Banik, S. J., Sharma, R., Rumore, D., Hwang, W., Briber, R. M., & Raghavan, S. R.** (2014). Superabsorbent hydrogels that are robust and highly stretchable. *Macromolecules*, *47*, 4445–4452.

[71] **Orakdogen, N., & Okay, O.** (2007). Influence of the initiator system on the spatial inhomogeneity in acrylamide-based hydrogels. *J. Appl. Polym. Sci.*, *103*, 3228–3237.

[72] **Okay, O., Kurz, M., Lutz, K., & Funke, W.** (1995). Cyclization and Reduced Pendant Vinyl Group Reactivity during the Free-Radical Cross-Linking Polymerization of 1,4-Divinylbenzene. *Macromolecules*, *28*, 2728–2737.

[73] **Hu, X., Vatankhah-Varnoosfaderani, M., Zhou, J., Li, Q., & Sheiko, S. S.** (2015). Weak Hydrogen Bonding Enables Hard, Strong, Tough, and Elastic Hydrogels. *Adv. Mater.*, *27*, 6899–6905.

[74] **Burdick, J. A., & Prestwich, G. D.** (2011). Hyaluronic acid hydrogels for biomedical applications. *Adv. Mater.*, *23*, 41–56.

[75] **Hardy, J. G., Römer, L. M., & Scheibel, T. R.** (2008). Polymeric materials based on silk proteins. *Polymer*, *49*, 4309–4327.

[76] **Highley, C. B., Prestwich, G. D., & Burdick, J. A.** (2016). Recent advances in hyaluronic acid hydrogels for biomedical applications. *Curr. Opin. Biotechnol.*, *40*, 35–40.

[77] **Kim, U. J., Park, J., Joo Kim, H., Wada, M., & Kaplan, D. L.** (2005). Three-dimensional aqueous-derived biomaterial scaffolds from silk fibroin. *Biomaterials*, *26*, 2775–2785.

[78] **Melke, J., Midha, S., Ghosh, S., Ito, K., & Hofmann, S.** (2016). Silk fibroin as biomaterial for bone tissue engineering. *Acta Biomater.*, *31*, 1–16.

[79] **Sasaki, T., & Noda, H.** (1974). Studies on silk fibroin of Bombyx mori directly extracted from the silk gland: III. n-terminal analysis and degradation in a slightly alkaline solution. *J. Biochem.*, *76*, 493–502.

[80] **Iizuka, E.** (1969). Conformation of silk sericine in solution, Bombyx mori L. *BBA - Protein Struct.*, *181*, 477–479.

[81] **Jin, H. J., & Kaplan, D. L.** (2003). Mechanism of silk processing in insects and spiders. *Nature*, *424*, 1057–1061.

[82] **Zhou, C. Z., Confalonieri, F., Medina, N., Zivanovic, Y., Esnault, C., Yang, T., Jacquet, M., Janin, J., Duguet, M., Perasso, R., & Li, Z. G.** (2000). Fine organization of Bombyx mori fibroin heavy chain gene. *Nucleic Acids Res.*, *28*, 2413–2419.

[83] **Zamboni, F., Vieira, S., Reis, R. L., Miguel Oliveira, J., & Collins, M. N.** (2018). The potential of hyaluronic acid in immunoprotection and immunomodulation: Chemistry, processing and function. *Prog. Mater. Sci.*, *97*, 97–122.

[84] **Valachová, K., Topol'ská, D., Mendichi, R., Collins, M. N., Sasinková, V., & Šoltés, L.** (2016). Hydrogen peroxide generation by the Weissberger biogenic oxidative system during hyaluronan degradation. *Carbohydr. Polym.*, *148*, 189–193.

[85] **Collins, M. N., & Birkinshaw, C.** (2008). Physical properties of crosslinked hyaluronic acid hydrogels. *J. Mater. Sci. Mater. Med.*, *19*, 3335–3343.

[86] **Hu, X., Lu, Q., Sun, L., Cebe, P., Wang, X., Zhang, X., & Kaplan, D. L.** (2010). Biomaterials from ultrasonication-induced silk fibroin-hyaluronic acid hydrogels. *Biomacromolecules*, *11*, 3178–3188.

[87] **Park, S. H., Cho, H., Gil, E. S., Mandal, B. B., Min, B. H., & Kaplan, D. L.** (2011). Silk-fibrin/hyaluronic acid composite gels for nucleus pulposus tissue regeneration. *Tissue Eng. - Part A*, *17*, 2999–3009.

[88] **Raia, N. R., Partlow, B. P., McGill, M., Kimmerling, E. P., Ghezzi, C. E., & Kaplan, D. L.** (2017). Enzymatically crosslinked silk-hyaluronic acid hydrogels. *Biomaterials*, *131*, 58–67.

[89] **Chi, N. H., Yang, M. C., Chung, T. W., Chen, J. Y., Chou, N. K., & Wang, S. S.** (2012). Cardiac repair achieved by bone marrow mesenchymal stem cells/silk fibroin/hyaluronic acid patches in a rat of myocardial infarction model. *Biomaterials*, *33*, 5541–5551.

[90] **Ren, Y.-J., Zhou, Z.-Y., Liu, B.-F., Xu, Q.-Y., & Cui, F.-Z.** (2009). Preparation and characterization of fibroin/hyaluronic acid composite scaffold. *Int. J. Biol. Macromol.*, *44*, 372–378.

[91] **Yan, S., Wang, Q., Tariq, Z., You, R., Li, X., Li, M., & Zhang, Q.** (2018). Facile preparation of bioactive silk fibroin/hyaluronic acid hydrogels. *Int. J. Biol. Macromol.*, *118*, 775–782.

[92] **Yang, X., Wang, X., Yu, F., Ma, L., Pan, X., Luo, G., Lin, S., Mo, X., He, C., & Wang, H.** (2016). Hyaluronic acid/EDC/NHS-crosslinked green electrospun silk fibroin nanofibrous scaffolds for tissue engineering. *RSC Adv.*, *6*, 99720–99728.

[93] **Zhou, J., Zhang, B., Liu, X., Shi, L., Zhu, J., Wei, D., Zhong, J., Sun, G., & He, D.** (2016). Facile method to prepare silk fibroin/hyaluronic acid films for vascular endothelial growth factor release. *Carbohydr. Polym.*, *143*, 301–309.

[94] **Garcia-Fuentes, M., Giger, E., Meinel, L., & Merkle, H. P.** (2008). The effect of hyaluronic acid on silk fibroin conformation. *Biomaterials*, *29*, 633–642.

[95] **Tavsanli, B., & Okay, O.** (2017). Mechanically strong hyaluronic acid hydrogels with an interpenetrating network structure. *Eur. Polym. J.*, *94*, 185–195.

[96] **Kim, U. J., Park, J., Li, C., Jin, H. J., Valluzzi, R., & Kaplan, D. L.** (2004). Structure and properties of silk hydrogels. *Biomacromolecules*, *5*, 786–792.

[97] **Vepari, C., & Kaplan, D. L.** (2007). Silk as a biomaterial. *Prog. Polym. Sci.*, *32*, 991–1007.

[98] **Vollrath, F., & Porter, D.** (2009). Silks as ancient models for modern polymers. *Polymer*, *50*, 5623–5632.

[99] **Chen, X., Knight, D. P., Shao, Z., & Vollrath, F.** (2002). Conformation Transition in Silk Protein Films Monitored by Time-Resolved Fourier Transform Infrared Spectroscopy: Effect of Potassium Ions on Nephila Spidroin Films. *Biochemistry*, *41*, 14944–14950.

[100] **Ayub, Z. H., Arai, M., & Hirabayashi, K.** (1993). Mechanism of the Gelation of Fibroin Solution. *Biosci. Biotechnol. Biochem.*, *57*, 1910–1912.

[101] **Creton, C.** (2017). 50th Anniversary Perspective: Networks and Gels: Soft but Dynamic and Tough. *Macromolecules*, *50*, 8297–8316.

[102] **Uzumcu, A. T., Guney, O., & Okay, O.** (2018). Highly Stretchable DNA/Clay Hydrogels with Self-Healing Ability. *ACS Appl. Mater. Interfaces*, *10*, 8296–8306.

[103] **Tavsanli, B., & Okay, O.** (2019). Mechanically robust and stretchable silk/hyaluronic acid hydrogels. *Carbohydr. Polym.*, *208*.

[104] **Babič, M., Horák, D., Jendelová, P., Glogarová, K., Herynek, V., Trchová, M., Likavčanová, K., Lesný, P., Pollert, E., Hájek, M., & Syková, E.** (2009). Poly(N,N-dimethylacrylamide)-coated maghemite nanoparticles for stem cell labeling. *Bioconjug. Chem.*, *20*, 283–294.

[105] **Li, W., Li, J., Gao, J., Li, B., Xia, Y., Meng, Y., Yu, Y., Chen, H., Dai, J., Wang, H., & Guo, Y.** (2011). The fine-tuning of thermosensitive and degradable polymer micelles for enhancing intracellular uptake and drug release in tumors. *Biomaterials*, *32*, 3832–3844.

[106] **Wang, F., Yong, X., Deng, J., & Wu, Y.** (2018). Poly(N, N - dimethylacrylamide-octadecyl acrylate)-clay hydrogels with high mechanical properties and shape memory ability. *RSC Adv.*, *8*, 16773–16780.

[107] **de Queiroz, A. A. A., Castro, S. C., & Higa, O. Z.** (1997). Adsorption of plasma proteins to DMAA hydrogels obtained by ionizing radiation and its relationship with blood compatibility. *J. Biomater. Sci. Polym. Ed.*, *8*, 335–347.

[108] **Abraham, G. A., De Queiroz, A. A. A., & Román, J. S.** (2001). Hydrophilic hybrid IPNs of segmented polyurethanes and copolymers of vinylpyrrolidone for applications in medicine. *Biomaterials*, *22*, 1971–1985.

[109] **Lozinsky, V. I.** (2002). Cryogels on the basis of natural and synthetic polymers: Preparation, properties and application. *Russ. Chem. Rev.*, *71*, 489–511.

[110] **Cai, Z., Zhang, F., Wei, Y., & Zhang, H.** (2017). Freeze-Thaw-Induced Gelation of Hyaluronan: Physical Cryostructuration Correlated with Intermolecular Associations and Molecular Conformation. *Macromolecules*, *50*, 6647–6658.

[111] **Hu, Y., & Suo, Z.** (2012). Viscoelasticity and poroelasticity in elastomeric gels. *Acta Mech. Solida Sin.*, *25*, 441–458.

[112] **Noselli, G., Lucantonio, A., McMeeking, R. M., & DeSimone, A.** (2016). Poroelastic toughening in polymer gels: A theoretical and numerical study. *J. Mech. Phys. Solids*, *94*, 33–46.

[113] **Oyen, M. L.** (2014). Mechanical characterisation of hydrogel materials. *Int. Mater. Rev.*, *59*, 44–59.

[114] **Lu, X. L., & Mow, V. C.** (2008). Biomechanics of articular cartilage and determination of material properties. *Med. Sci. Sports Exerc.*, *40*, 193–199.

[115] **Su, E., & Okay, O.** (2019). Cryogenic formation-structure-property relationships of poly(2-acrylamido-2-methyl-1-propanesulfonic acid) cryogels. *Polymer*, *178*, 121603.

[116] **Zaborina, O. E., Gasanov, R. G., Peregudov, A. S., & Lozinsky, V. I.** (2014). Cryostructuring of polymeric systems. 38. the causes of the covalently-crosslinked cryogels formation upon the homopolymerization of N,N-dimethylacrylamide in moderately-frozen aqueous media. *Eur. Polym. J.*, *61*, 226–239.

[117] **Tuncaboylu, D. C., Sahin, M., Argun, A., Oppermann, W., & Okay, O.** (2012). Dynamics and large strain behavior of self-healing hydrogels with and without surfactants. *Macromolecules*, *45*, 1991–2000.

[118] **Yetiskin, B., & Okay, O.** (2019). High-strength and self-recoverable silk fibroin cryogels with anisotropic swelling and mechanical properties. *Int. J. Biol. Macromol.*, *122*, 1279–1289.

[119] **Malandrino, A., & Moeendarbary, E.** (2019). Poroelasticity of living tissues. In *Encycl. Biomed. Eng.* (Vol. 1–3, pp. 238–245). Amsterdam: Elsevier.

[120] **Mow, V. C., Kuei, S. C., Lai, W. M., & Armstrong, C. G.** (1980). Biphasic creep and stress relaxation of articular cartilage in compression: Theory and experiments. *J. Biomech. Eng.*, *102*, 73–84.

[121] **Soltz, M. A., & Ateshian, G. A.** (1998). Experimental verification and theoretical prediction of cartilage interstitial fluid pressurization at an impermeable contact interface in confined compression. In *J. Biomech.* (Vol. 31, pp. 927–934).

[122] **Okay, O.** (2000). Macroporous copolymer networks. *Prog. Polym. Sci.*, *25*, 711–779.

[123] **Panagopoulou, A., Molina, J. V., Kyritsis, A., Pradas, M. M., Lluch, A. V., Ferrer, G. G., & Pissis, P.** (2013). Glass Transition and Water Dynamics in Hyaluronic Acid Hydrogels. *Food Biophys.*, *8*, 192–202.

[124] **Kahovec, J., Kratochvíl, P., Jenkins, A. D., Mita, I., Papisov, I. M., Sperling, L. H., & Stepto, R. F. T.** (1997). Source-based nomenclature for non-linear macromolecules and macromolecular assemblies (IUPAC Recommendations 1997). *Pure Appl. Chem.*, *69*, 2512–2521.

CURRICULUM VITAE

Name Surname **:** Burak TAVŞANLI

Place and Date of Birth **:**

EDUCATION **:**

- **B.Sc.** **:** 2011, Hacettepe University, Faculty of Science, Chemistry
- **M.Sc.** **:** 2014, Hacettepe University, Graduate School of Science and Engineering, Chemistry
- **Ph.D.** **:** 2021, Istanbul Technical University, Graduate School, Chemistry

PROFESSIONAL EXPERIENCE:

- Research Assistant, Chemistry, Istanbul Technical University (2014-2020)

PUBLICATIONS ON THE THESIS:

- **Tavsanli, B.** and Okay, O. (2016). Preparation and fracture process of high strength hyaluronic acid hydrogels cross-linked by ethylene glycol diglycidyl ether. *Reactive and Functional Polymers*, 109, 42-51.
- **Tavsanli, B.** Can, V. Okay, O. (2015). Mechanically strong triple network hydrogels based on hyaluronan and poly(N,N-dimethylacrylamide). *Soft Matter*, 11, 8517-8524.
- **Tavsanli, B.** and Okay, O. (2017). Mechanically strong hyaluronic acid hydrogels with an interpenetrating network structure. *European Polymer Journal*, 90, 185-195.
- **Tavsanli, B.** and Okay, O. (2019). Mechanically robust and stretchable silk/hyaluronic acid hydrogels. *Carbohydrate Polymers*, 208, 413-420.

- **Tavsanli, B.** and Okay, O. (2020). Macroporous methacrylated hyaluronic acid cryogels of high mechanical strength and flow-dependent viscoelasticity. *Carbohydrate Polymers*, 229, 115458.